

**Cannabinoid type 2 receptor-mediated cell type-
specific self-inhibition in hippocampal and
cortical neurons**

Inaugural-Dissertation

to obtain the academic degree

Doctor rerum naturalium (Dr. rer. nat.)

submitted to the Department of Biology, Chemistry and Pharmacy
of Freie Universität Berlin

by

ALEXANDER STUMPF

2019

The experimental work of this thesis was completed from October 2014 to August 2018 under the supervision of Prof. Dr. Dietmar Schmitz at the Neuroscience Research Centre (NWFZ) of the Charité Universitätsmedizin Berlin, Germany.

1st reviewer: Prof. Dr. Dietmar Schmitz

2nd reviewer: Prof. Dr. Stephan Sigrist

Date of disputation: 1st July 2019

Acknowledgements

Firstly, I would like to express my sincere gratitude to my doctoral supervisor Prof. *Dietmar Schmitz* for the continuous support of my doctoral study, for his patience, his generosity and motivation. Thank you for guiding me into the fields of research that I was interested in and for giving me the opportunity to work independently and to be part in several research cooperations to broaden my scientific understanding. I could not have imagined having a better supervisor for my doctoral thesis.

Thanks to Prof. *Stephan Sigrist* who agreed to be my second reviewer.

I would like to express special thanks to my co-supervisors *Benjamin R. Rost* and *Jörg M. Breustedt* for the constant support and help in experimental design, data visualization and discussions as well as for proof reading of the manuscript.

Thank you to *A. Vanessa Stempel* for introducing me into the cannabinoid field, for teaching me the proper way to perform scientific experiments and for the valuable inputs and help in this project.

Special thanks to *Daniel Parthier*, *Rosanna Sammons* and *Ulrike Pannasch* for helping me with some of the recordings for this project, that turned out to be demanding and time-consuming.

I thank all present and former members of the Schmitzlab for the stimulating discussions, the great working atmosphere, the support and help while working together on several projects and for all the fun we had: *Laura Moreno Velasques*, *Aarti Swaminathan*, *Constance Holman*, *Silvia Oldani*, *Anne-Kathrin Theis*, *Roberto de Fillipo*, *Noam Nitzan*, *Hung Lo*, *Prateep Beed*, *John Tukker*, *Marta Orlando*, *Barbara Imbrosci*, *Friedrich Jochenning* and *Nikolaus Maier*. I appreciated all the feedback and suggestions about the project and the lively discussions. It was a great pleasure working with all of you and I feel very happy that I could spend the last four years together with you.

Thanks to *Anke Schönherr* and *Susanne Rieckmann* for being the backbone of the laboratory and for their reliable and skilled technical assistance.

I would like to thank the *Collaborative Research Center 958* of the DFG (Scaffolding of Membranes – Molecular Mechanisms and Cellular Functions) for its generous financial support.

Last but not least I would like to express a special thanks to my family: To my wife *Laura* and my children *Clea* and *Caspar* who were always there for me, supported me and were calming compensation when the work was stressful; To my parents and my sister for supporting me my whole life; To my parents-in-law for all the support and motivation and for always believing in me. I am very indebted to you and I could not have achieved to finish my doctor degree without your help.

Synopsis

Endogenous cannabinoids are lipid-based ligands of the main cannabinoid receptors type 1 and 2 (CB₁R and CB₂R). In contrast to the well-studied effects of CB₁Rs, much less is known about the physiological role of CB₂Rs in the central nervous system (CNS). In fact, CB₂Rs were considered as peripheral cannabinoid receptors representing the complementary cannabinoid receptor to the CB₁R in the CNS. However recent pharmacological, behavioral and genetic studies have determined the presence of functional CB₂Rs in the brain and their involvement in various physiological and pathological conditions. Endocannabinoids are produced in an activity-dependent manner. Next to their well-described role as retrograde modulators of synaptic transmission, endocannabinoids also mediate a cell-autonomous slow self-inhibition (SSI). Action potential-driven endocannabinoid production followed by binding to cannabinoid receptors induces a long-lasting hyperpolarization of the membrane potential, rendering the cell less excitable. Several studies described different endocannabinoid receptors and cellular mechanisms by which SSI is implemented in different cell types and brain areas: While pyramidal cells and interneurons in the somatosensory cortex were reported to mediate SSI via CB₁Rs and G protein-coupled inward rectifying K⁺ (GIRK) channels, hippocampal principal cells were shown to mediate SSI in a CB₂R mediated and input-resistance-independent manner. However, the molecular mechanism by which the long-lasting hyperpolarization is implemented was not clear. During my thesis I was part of a team that demonstrated that hippocampal SSI is mediated via activation of the Na⁺/bicarbonate cotransporter. In order to get further insight in the occurrence of SSI in different classes of neurons, we analyzed the presence of SSI in one type of hippocampal interneuron and showed that oriens-lacunosum moleculare (OLM) interneurons do not express SSI. Further, we investigate SSI in different neuron types of layer 2/3 in the primary somatosensory cortex and show that regular firing cells express SSI in contrast to fast-spiking interneurons. Trains of action potentials induced a long-lasting hyperpolarization that was accompanied by a change in input resistance due to GIRK channel activation. By using cannabinoid receptor-specific pharmacology as well as transgenic mice lacking either CB₁Rs or CB₂Rs, we demonstrate that this effect is mediated by CB₂R activation.

Taken together, hippocampal and cortical SSI both represent a CB₂R-dependent mechanism; however the underlying mechanism by which the hyperpolarization is implemented differs between the different brain regions. By describing an additional cellular mechanism for SSI induction, these findings add further insights on the physiological role of CB₂Rs and expand our knowledge about cell type-specific differential cannabinoid signaling. Moreover, these findings suggest CB₂Rs as a promising target for therapeutic approaches.

Zusammenfassung

Endogene Cannabinoide sind bioaktive Lipide, die an die Cannabinoid Rezeptoren Typ 1 und 2 (CB₁R und CB₂R) binden. Im Gegensatz zum CB₁R, ist weitaus weniger über die physiologische Rolle der CB₂R im zentralen Nervensystem (ZNS) bekannt. CB₂R wurden auch als Cannabinoid Rezeptoren der peripheren Region angesehen, komplementär zu den CB₁R im ZNS. Jedoch haben zahlreiche pharmakologische, genetische und Verhaltensstudien in den letzten Jahren immer mehr Hinweise geliefert, die das Vorkommen von funktionalen CB₂R auch im Gehirn zeigen und ihre Funktion in physiologischen und pathologischen Prozessen belegen.

Endocannabinoide werden aktivitätsabhängig gebildet. Die meisten bisher untersuchten neuronalen Endocannabinoid vermittelten Effekte beschreiben deren Aktivität als retrograde Signalmoleküle, die die synaptische Transmission modulieren. Zusätzlich wurde gezeigt, dass einige Zellen eine zellautonome Form der Selbstinhibierung (*slow self-inhibition*, SSI) aufweisen, bei der Endocannabinoide eine tragende Rolle spielen. Diese Zellen zeigen eine Aktionspotential getriebene Produktion von Endocannabinoiden, welche anschließend Cannabinoidrezeptoren an derselben Zelle aktivieren und dadurch eine Hyperpolarisierung des Membranpotentials zur Folge haben. Dabei wurden unterschiedliche zelluläre Mechanismen, aber auch unterschiedliche Cannabinoidrezeptoren beschrieben, die diesen Effekt hervorrufen. Während in Pyramidenzellen und Interneuronen des somatosensorischen Cortexes eine Aktivierung von CB₁R K⁺-Kanäle (GIRK) erregen, ist in Pyramidenzellen des Hippocampus eine Aktivierung von CB₂R erforderlich, um SSI zu induzieren, die keine Änderung des Eingangswiderstandes zur Folge hat. Allerdings war der zelluläre Mechanismus, mit welchem die Hyperpolarisierung im Hippocampus implementiert wird, noch unbekannt. In dieser Arbeit zeigen wir, dass SSI in Pyramidenzellen des Hippocampus durch Aktivierung des Na⁺-Bikarbonat Transporters hervorgerufen wird und dass dieser Effekt in einer Gruppe von hippocampalen Interneuronen nicht vorhanden ist.

Desweiteren untersuchen wir SSI in verschiedenen Zelltypen der Schicht 2/3 des somatosensorischen Cortexes und konnten zeigen, dass die langanhaltende Hyperpolarisierung in regulär feuernenden Zellen auslösbar ist während schnell feuernende Interneurone kein SSI aufweisen. Wiederholtes Auslösen von Aktionspotentialen führt zu einer langanhaltenden Hyperpolarisierung des Membranpotentials, die mit einer Änderung des Eingangswiderstandes einhergeht. Diese wird durch Aktivierung von GIRK-Kanälen hervorgerufen. Mithilfe von pharmakologischen Interventionen und transgenen Knockout-Mäusen, die kein CB₁R oder CB₂R exprimieren, zeigen, dass dieser Effekt durch CB₂R Aktivierung initiiert wird.

Zusammenfassend zeigt diese Arbeit, dass SSI im Hippocampus sowie im Cortex durch CB₂R Aktivierung ausgelöst wird. Die zellulären Mechanismen, die für die Hyperpolarisierung eine Rolle spielen unterscheiden sich jedoch in den beiden Gehirnregionen. Dies beschreibt einen weiteren CB₂R vermittelten Effekt und erweitert das Verständnis der physiologischen Bedeutung von CB₂R im ZNS zu erweitern. Zusätzlich heben diese Befunde die Bedeutung von CB₂R und das Potential ihrer Manipulation als Grundlage für therapeutische Behandlungen hervor.

Table of contents

1. INTRODUCTION	1
1.1 History of cannabinoids	1
1.2 Endocannabinoid system	3
1.2.1 Cannabinoid receptors	3
1.2.1.1 CB ₁ R	3
1.2.1.2 CB ₂ R	7
1.2.1.3 Other targets of endocannabinoids	9
1.2.2 Endocannabinoids	10
1.2.2.1 AEA	11
1.2.2.2 2-AG	12
1.2.2.3 Noladin Ether	14
1.2.2.4 NADA	14
1.2.2.5 Virodhamine	14
1.2.2.6 Mobilization of endocannabinoids	15
1.2.3 Role of cannabinoid system in behavior and diseases	16
1.2.3.1 Anxiety and depression	17
1.2.3.2 Learning and memory	18
1.2.3.3 Neuroprotective effects of endocannabinoids	19
1.2.3.4 Therapeutic use of cannabinoids	20
1.2.3.5 Endocannabinoid system as target for drug-discovery research	20
1.2.4 Physiological effects of cannabinoids on synaptic transmission	21
1.2.4.1 Short-term plasticity	22
1.2.4.2 Spread of endocannabinoids	23
1.2.4.3 Termination of endocannabinoid signaling	24
1.2.4.4 Long-term plasticity	25
1.2.4.5 Involvement of glial cells in cannabinoid mediated synaptic modulation	26
1.2.5 Cell-autonomous action of endocannabinoids	27
1.3 Aim of this study	29
2. MATERIALS AND METHODS	30
2.1 Materials	30
2.1.1 Technical Equipment	30
2.1.2 Software	31
2.2 Experimental preparations	31
2.2.1 Ethical Statement and Animal Handling	31
2.2.2 Transgenic animals	32
2.2.3 Preparation of brain slices	32
2.2.4 Electrophysiology	33
2.2.4.1 General setup	33
2.2.4.2 Whole-cell patch clamp recordings	34
2.2.4.3 Substitution experiments	35
2.2.4.4 Pharmacological agents	36
2.2.4.5 Action potential protocols	36

2.2.4.6 Data analysis	37
2.2.5 Immunohistochemistry and morphological reconstruction	38
3. RESULTS	39
3.1 Hippocampal SSI	39
3.1.1 Mechanism underlying SSI in hippocampal PCs	39
3.1.2 SSI in OLM cells	44
3.2 Cortical SSI	46
3.2.1 Cell type-specific expression of SSI in cortical neurons	46
3.2.2 Mechanism underlying cortical SSI in RSNPCs	52
3.2.3 Pharmacological investigation of the cannabinoid receptor involved in SSI of RSNPCs	54
3.2.5 Identity of RSNPCs	61
4. DISCUSSION	63
4.1 Hippocampal SSI	63
4.1.1 Mechanism of hippocampal SSI	63
4.1.2 Cell type-specific expression of SSI	66
4.2 Cortical SSI	67
4.2.1 Responding and non-responding cells	67
4.2.2 CB ₂ Rs are mediating SSI	69
4.2.3 Mechanism of cortical SSI	70
4.2.4 Physiological relevance	71
4.2.4.1 Activation pattern	71
4.2.4.2 Network effects	71
4.3 Neuroprotective role of CB₂Rs	75
5. REFERENCES	78
6. APPENDIX	98
6.1. Glossary	98
6.2. Statement of contributions	100
6.3. List of Publications	101
6.3.1 Related to this dissertation	101
6.3.2. Non-related to this dissertation	101
6.3.3. In revision or preparation	102
6.4. Presentations	102
6.5. Erklarung an Eides statt	103

1. Introduction

1.1 History of cannabinoids

Cannabinoids represent a class of chemical compounds that act on cannabinoid receptors. These substances were initially found in *Cannabis Sativa*, a plant that has been cultivated throughout recorded history (Clarke and Merlin, 2017). Cannabis originated in South and Central Asia and was cultivated for fiber, seed and resin production. Subsequently, cannabis was traded to different cultures to reach cosmopolitan distribution while diverse species of cannabis evolved since different parts of the plants were traditionally used for particular purposes: While European and East Asian societies mainly used cannabis for its strong fibers and nutritious seeds, African, Middle Eastern and South Asian cultures used it to a higher extent for its psychoactive properties. The latter caused recreational, religious and medical use of cannabis (Pain 2015). The earliest traceable use of cannabis as medicine is attributed to the Chinese Emperor Shen-Nung at around 2700 BC, where it was used as a treatment for different maladies including rheumatic pain, intestinal constipation and malaria (Zuardi, 2006). Around 1000 BC, cannabis was widely used in India for religious and medical purposes: It was used inter alia as analgesic, anticonvulsant, hypnotic, tranquilizer, anesthetic, antibiotic and appetite stimulant (Zuardi, 2006). In the Assyrian Empire (800 BC), cannabis fumes were prescribed as a treatment for symptoms of depression and arthritis (Mechoulam and Hanus, 2001). A Greek physician, Padacius Discodires, described in the first century AD the benefits of Cannabis seed's juice in the treatment of earache in *De Materia Medica*, an encyclopedia about herbal medicine (Figure 1A).

The introduction of cannabis in the Western medicine occurred in the 19th century and numerous scientific articles describing its effects were published in this time. William B. O'Shaugnessy described in his book '*On the preparation of the Indian hemp, or gunjah*' several human experiments for treatment of rheumatism, convulsions, migraines, inflammation, cholera and muscular spasms of tetanus and rabies (Mechoulam and Hanus, 2001; Zuardi, 2006). Jacques-Joseph Moreau de Tours was rather interested in the psychoactive effects of cannabis (Moreau de Tours, 1845). He tested different cannabis preparations for the treatment for depression and anxiety and proposed its use in melancholia. His idea of the potential in psychoactive substances for treating mental illnesses is seen as the origin of experimental psychiatry and psychopharmacology (Fankhauser, 2008; Pacher and Mechoulam, 2011). In the late 19th century, cannabis extracts or tinctures were produced and marketed by several companies (Figure 1B). The medical indication of cannabis by that time was summarized in *Sajou's Analytic Cyclopedia of Practical Medicine* (1924) as 1) sedative or hypnotic, 2)

analgesic and 3) other uses (including: Improve appetite and digestion, diarrhea, cholera, diabetis mellitus).

In 1895, Wood and his colleagues were able to identify and isolate the first cannabinoid: Cannabinol (CBN; Wood et al., 1896), whose structure was identified 40 years later (Cahn, 1933). Shortly after, a second phyto-cannabinoid, cannabidiol was independently isolated and identified by the laboratories of Adams and Todd (Adams et al., 1940; Jacob and Todd, 1940) and its chemical structure was fully established by Raphael Mechoulam (Mechoulam and Shvo, 1963). It was also Raphael Mechoulam, who isolated and identified the structure of tetrahydrocannabinol (THC; chemical name $(-)$ -*trans*- Δ^9 -tetrahydrocannabinol), the major psychoactive compound of cannabis (Gaoni and Mechoulam, 1964), which initiated the start of modern cannabinoid research. From now on, it was possible to investigate the effects of individual cannabinoids by direct administration, instead of using infusions or extracts of cannabis plants, which often varied in their cannabinoid compositions and content. In the following years various publications demonstrated the potential of cannabinoids, especially of THC, as a therapeutic agent for several conditions. These finding led to the discovery of the endocannabinoid system (see chapter 1.2). Until today almost 150 different phytocannabinoids have been described, exhibiting varied effects (Hanus et al., 2016). In addition, a plethora of synthetic cannabinoids were developed that show diverse properties including increased potency or selectivity towards specific cannabinoid receptors. This enabled more detailed research on the role of the cannabinoid system in physiology and disease.



Figure 1: Cannabis Sativa.

A: Illustration from the *Vienna Dioscorides*, 512 AD, illustrated manuscript of *De Materia Medica* by Dioscorides. **B:** Advertisement by the company E. Merck (Darmstadt, Germany) around 1885; Adapted from Russo and Grotenhermen, 2013.

1.2 Endocannabinoid system

The endocannabinoid system consists of the endogenously produced lipid-based signaling molecules known as endocannabinoids, the enzymes required for synthesis and degradation of the endocannabinoids, as well as the endocannabinoid receptors. It represents one of the main modulatory systems and is expressed in vertebrates and various clades of invertebrates including nematodes, mussels, leeches, crustaceans and even in the most primitive animal with a nervous system, the Hydra (McPartland et al., 2006). Due to a secondary loss during evolution, cannabinoid receptors are absent in insects (McPartland et al., 2001).

The discovery and characterization of cannabinoid receptor type 1 (CB₁R) marked the beginning of the identification of the endocannabinoid system. A radiolabeled synthetic cannabinoid was found to bind cell membranes from the rat brain in a specific and selective manner exhibiting characteristic features of receptor binding (Devane et al., 1988). Shortly after this discovery, the CB₁R was cloned from rat and human brain (Gerard et al., 1990; Matsuda et al., 1990). It has been proposed that CB₁R expression is mainly limited to the CNS (Herkenham et al., 1990) and it was not clear how the non-psychoactive effects of cannabis were mediated, until the CB₂R was identified and cloned (Munro et al., 1993). By this time it was proposed that CB₂Rs are only expressed in the periphery and not in the CNS (Buckley et al., 2000; Munro et al., 1993). Meanwhile, endogenously produced ligands of cannabinoid receptors were identified: Anandamide (AEA, chemical name: N-Arachidonyl ethanolamide; Devane et al., 1992) and 2-arachnidonyl glycerol (2-AG; Mechoulam et al., 1995; Sugiura et al. 1995). These two ligands are regarded as the two major endocannabinoids.

1.2.1 Cannabinoid receptors

1.2.1.1 CB₁R

CB₁Rs are among the most widely expressed G protein-coupled receptors (GPCRs) in the brain (Figure 3C). As characteristic for GPCRs, CB₁Rs possess seven transmembrane domains with extracellular N-terminus and intracellular C-terminus. Extracellular ligand binding leads to activation of the GPCR associated with conformational change of the receptor. This causes the exchange of Guanosine diphosphate (GDP) to Guanine triphosphate (GTP) at the G α -subunit of the G protein. This exchange triggers dissociation of the G α -subunit and the G $\beta\gamma$ -subunit from the receptor. Both G α and G $\beta\gamma$ act as second messengers and activate different transduction pathways while the receptor is able to activate the next G protein. G protein signaling is terminated by the hydrolysis of GTP by the G α -subunit and reassociation of G α and GPCR to G $\beta\gamma$ (Wettschureck and Offermanns, 2005).

Different types of G α -subunits were categorized based on their downstream transduction target: G α_s , G $\alpha_{i/o}$, G $\alpha_{q/11}$ and G $\alpha_{12/13}$. G α_s and G $\alpha_{i/o}$ subunits influence the cyclic adenosine monophosphate (cAMP)-dependent transduction pathway by stimulating or inhibiting the cAMP-producing enzyme adenylate cyclase (AC), respectively. Increased cAMP can activate cyclic nucleotide-gated ion channels and protein kinase A (PKA), which in turn phosphorylates a number of other proteins including transcription factors. Further, activation of G $\alpha_{i/o}$ can activate the mitogen-activated protein kinase (MAPK) pathway generating diverse responses including cell proliferation, differentiation, migration and apoptosis. G $\alpha_{q/11}$ activates the phospholipase C β (PLC β) pathway resulting in an increase of the second messengers inositol (1,4,5) triphosphate (IP $_3$) and diacylglycerol (DAG). IP $_3$ acts on IP $_3$ receptors in the endoplasmic reticulum (ER) resulting in an intracellular Ca $^{2+}$ increase from ER-stores. While IP $_3$ diffuses into the cytosol, DAG remains in the plasmamembrane acting as a physiological activator of protein kinase C (PKC) that is involved in regulation of a variety of enzymes. DAG further serves as a precursor of the endocannabinoid 2-AG. The effectors of the G $\alpha_{12/13}$ pathway are RhoGEF (Rho-guanine nucleotide exchange factors) which in turn can activate various proteins responsible for regulation of the cytoskeleton (for more information on G protein-signaling please see the reviews by: Hilger et al., 2018, Gurevich and Gurevich, 2017, Wettschureck and Offermanns, 2005).

The interaction with various intracellular signaling proteins does not only affect the cell-specific signaling cascade after activation of GPCRs, but may also influences receptor confirmation, which can lead to modified agonist binding properties (DeVree et al., 2016). On the other hand, the structure of the agonist influences binding kinetics and activation degree of the receptor, meaning that different agonists can give rise to different cellular responses in the same tissue due to different binding kinetics and stabilization of different receptor confirmations (Ibsen et al., 2017). This concept is called functional selectivity or biased signaling (Figure 2).

Agonist binding to CB $_1$ Rs induces activation of several second messenger cascades primarily via pertussis toxin sensitive activation of G $\alpha_{i/o}$ protein signaling. However, coupling to G α_s was also reported under certain conditions. Additionally, ligand binding to CB $_1$ Rs was shown to evoke Ca $^{2+}$ transients that were PLC dependent and mediated by G $\alpha_{i/o}$ or G $\alpha_{q/11}$ proteins (Sugiura et al., 1997). Further, CB $_1$ R activation modulates various types of ion channels by direct interaction of the G $\beta\gamma$ subunit: Activation of A-type K $^+$ channels and G protein coupled inward rectifying K $^+$ (GIRK) channels; inhibition of N- and P/Q-type Ca $^{2+}$ channels, D- and M-type K $^+$ channels (Kano et al., 2009).

Next to G protein-mediated signaling, another form of GPCR-signaling is the arrestin mediated pathway that is activated by binding of arrestin to the phosphorylated receptor. In order to prevent excessive signaling or to adapt to persistent stimulation, GPCR to G protein coupling can be inhibited by arrestins in a process called desensitization (Smith and Rajagopal, 2016). Besides receptor desensitization, arrestin promotes regulation of signal transduction, receptor trafficking and arrestin-mediated signaling. After binding arrestin acts as a scaffolding protein for different signaling pathways including extracellular signal-regulated kinases (ERK). CB₁R activation can lead to a direct recruitment of β -arrestin which induces endocytosis of the receptor leading to CB₁R removal from the plasma membrane (Ibsen et al., 2017). In addition, several CB₁R agonists display biased agonism: WIN55,212,2, CP55,940, THC, 2-AG and N-arachnidonoyl dopamine (NADA). Remarkably, the endocannabinoid NADA represents a highly biased CB₁R agonist that is able to induce Ca²⁺ influx from intracellular Ca²⁺ stores and slow internalization of CB₁Rs but has no effect on AC activity, GIRK channels or phosphorylation of ERK (Ibsen et al., 2017).

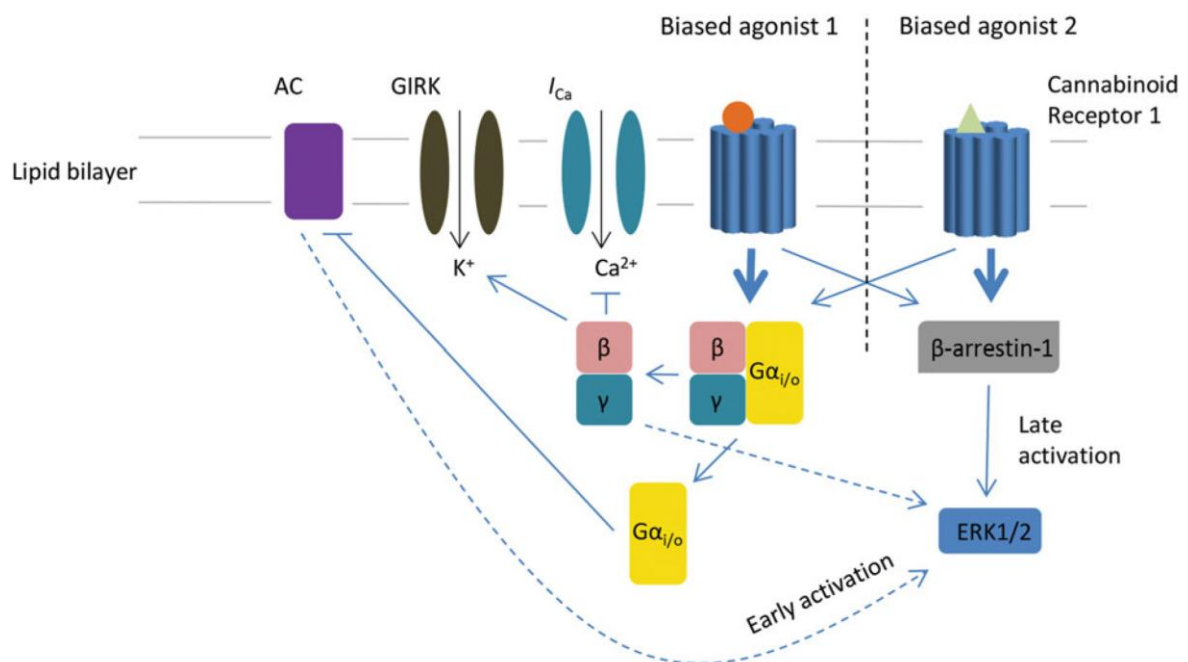


Figure 2: Schematic illustration of characteristic CB₁Rs signaling.

CB₁R typically signal via the Gα_{i/o} pathway. However, different agonists can display biased agonism towards one intracellular pathway over another. Biased agonist 1 shows a stronger activation of G protein-associated signaling pathways, while biased agonist 2 rather activates the β -arrestin pathway. Adapted from Ibsen et al., 2017.

The crystal structure of human CB₁R was recently identified, revealing insights into the activation mechanism of agonist and antagonist binding to the receptor (Figure 3A; Hua et al., 2017; Hua et al., 2016; Shao et al., 2016). The suggestion that CB₁Rs possess distinct but overlapping binding sites for the agonists WIN,55,212-2 and CP55,940 (Song and Bonner, 1996b) was supported by analysis of agonist docking in the crystal structure. In addition, a variety of allosteric modulators of CB₁Rs were identified that do not or only partially interact with the orthosteric binding sites where endogenous cannabinoids bind (Saleh et al., 2018). The development and optimization of allosteric modulators for CB₁Rs represent an additional promising approach to target the cannabinoid system for therapeutic purposes.

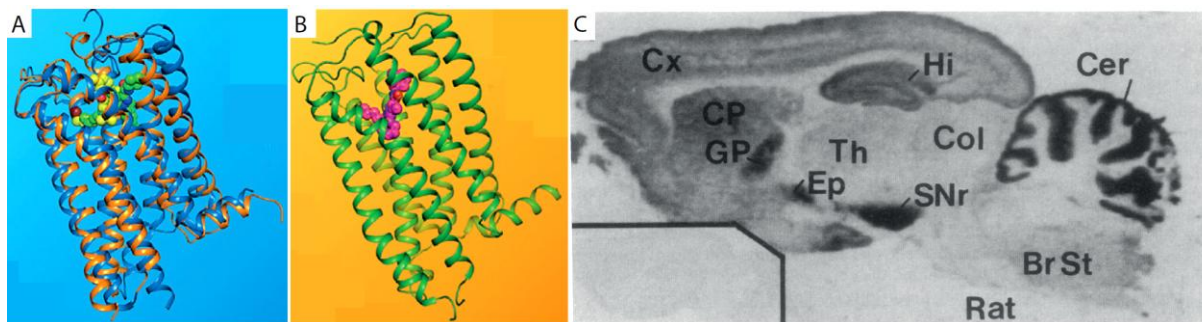


Figure 3: Crystal structure and expression of cannabinoid receptors.

A: Crystal structure of agonist- (orange) and antagonist-bound (blue) human CB₁R (Hua et al., 2017; Li et al., 2019). **B:** Crystal structure of antagonist-bound human CB₂R. Modified from Li et al., 2019. **C:** Autoradiography of [³H]CP55,940 binding in rat brain; Cx: Cortex; Hi: Hippocampus, Th: Thalamus; CP: Caudate putamen, GP: Globus pallidus, Ep: Entopeduncular nucleus, Col: Colliculi, SNr: Substantia nigra, Cer: Cerebellum, BrSt: Brainstem. Modified from Herkenham et al., 1990.

CB₁Rs are encoded by the gene CNR1 located on mouse chromosome 4 and human chromosome 6 and consists of 473 amino acids in rodents and 472 amino acids in human, showing 97-99% sequence identity among these species (Chakrabarti et al., 1995; Gerard et al., 1990; Matsuda et al., 1990). In addition, two alternative splice variants of the CB₁R were discovered: CB₁Ra and CB₁Rb (Ryberg et al., 2005; Shire et al., 1995). These variants possess a shortened N-terminal, show altered ligand binding and are expressed at low levels in a variety of tissues (Ryberg et al., 2005).

Since the discovery and first distribution analysis of CB₁R expression using radiolabeled ligands (Devane et al., 1988; Herkenham et al., 1990; Figure 3C) much progress was achieved in characterizing expression patterns of CB₁R in neuronal tissues. Soon after the first description, CB₁R cDNA was cloned, leading to investigation of regional and cellular distribution of CB₁R mRNA by *in*

situ hybridization (Mailleux and Vanderhaeghen, 1992; Matsuda et al., 1993). The development of specific antibodies shed further light on the subcellular and cell type-specific distribution of CB₁R via immunohistochemical and electron microscopy-based methods (Katona et al., 1999; Tsou et al., 1998). A meta-analysis study on 119 autoradiographic, immunohistochemical and *in situ* hybridization studies summarized the distribution of CB₁R expression in human and rat brain (McPartland et al., 2007). CB₁Rs are highly expressed in the basal ganglia nuclei, hippocampus, cortex and cerebellum. In fact, its distribution correlates with the role of the cannabinoid system in the control of motor function, memory and analgesia. In addition, species-dependent differences in the expression levels were observed: CB₁R density was higher in cognitive regions (cerebral cortex) in human, while rat brains showed a higher expression in movement-associated areas (cerebellum, caudate-putamen; McPartland et al., 2007). Interestingly, two different patterns of CB₁R mRNA distribution were found: In some regions, like the cerebellum or the thalamus, almost all cells express CB₁R. In contrast, in the hippocampus or the cerebral cortex only few neurons express very high levels of CB₁R (Mailleux and Vanderhaeghen, 1992; Matsuda et al., 1993). These findings were supported by immunohistochemical studies detecting strong CB₁R expression in cholecystokinin-positive interneurons, low expression in excitatory cells and no CB₁R in parvalbumin-positive interneurons (Katona et al., 1999; Tsou et al., 1999). However, some discrepancies were described between mRNA expression detected by *in situ* hybridization and protein expression detected by autoradiography or immunohistochemistry. This discrepancy can be explained by the predominant presynaptic location of CB₁Rs (Katona et al., 1999) detected by autoradiography and immunohistochemistry, while *in situ* hybridization stained the perikarya. Further, astroglial cells were shown to express functional CB₁Rs (Han et al., 2012; Navarrete and Araque, 2008).

In addition to the presynaptic location of CB₁Rs, several studies indicate the presence of functional CB₁Rs on different intracellular locations including endosomes, lysosomes (Grimsey et al., 2010) and mitochondria (Benard et al., 2012). Further, CB₁Rs were found in the postsynaptic density and the extrasynaptic membrane of striatal neurons (Kofalvi et al., 2005). Postsynaptic expression was also found in superficial Cornu Ammonis 1 (CA1) pyramidal neurons (Maroso et al., 2016).

1.2.1.2 CB₂R

The CB₂R is encoded by the gene CNR2 and shares only 44% sequence homology with CB₁R at protein level. CB₂R has a greater species differences between rodents and humans compared to CB₁Rs (82% similarity; 360 amino acids in human, 347 amino acids in mice; Kano et al., 2009). In rats four different specific mRNA isoforms were identified (Zhang et al., 2015). In addition, higher level of CB₂R

mRNA was detected in mice in different brain regions and cell types, compared to rats (Zhang et al., 2015).

In contrast to the extensively studied CB₁R, much less is known about the role of CB₂Rs in the CNS. Since the discovery and cloning of the CB₂R cDNA (Munro et al., 1993) it was considered to represent the “non-neuronal” counterpart of the “neuronal” CB₁R (Buckley, 2008). CB₂Rs were mainly detected in immune cells, including macrophages, B-cells, T-cells as well as microglia, while initially no signal could be detected in the brain (Munro et al., 1993). Further, autoradiography studies using a high affinity CB₁/CB₂R agonist showed no signal in the brain of CB₁R knockout (KO) mice, whereas a strong labeling was present in the spleen indicating CB₂R expression (Buckley et al., 2000; Zimmer et al., 1999). A transgenic reporter mouse expressing GFP under the CB₂R promoter supported the finding that CB₂Rs are only present in peripheral tissue and that the major source for GFP-signal in the brain arises from microglia (Schmole et al., 2015). However, the dogma of CB₁R-complementary, strictly non-neuronal CB₂R expression was challenged by several studies that showed expression of CB₂Rs and its mRNA in various brain regions using different methods (immunohistochemistry: Gong et al., 2006; Zhang et al., 2014; *in situ* hybridization: Li and Kim, 2015; Stempel et al., 2016; Zhang et al., 2014; Western blots: Zhang et al., 2019; quantitative real-time polymerase chain reaction: Onaivi, 2006; Onaivi et al., 2008). However, the interpretation of the detected CB₂R signals was often questioned, mainly for two reasons: First, adequate CB₂R KO controls were not performed or generated an unspecific signal. The two available CB₂R KO mouse lines (Buckley et al., 2000; Li and Kim, 2016) represent partial KOs expressing remaining residues of a non-functional truncated CB₂Rs. Second, due to the remaining CB₂R parts in KO mice, and due to the use of anti-rat CB₂R antibodies in mice, many commercially available antibodies generate false-positive signals in KO strains (Zhang et al., 2019). These methodological obstacles may explain the discrepancies of the former studies.

However, in addition to the expression analysis of CB₂Rs, various behavioral and electrophysiological studies support the expression of functional CB₂Rs in neuronal cells (see chapter 1.2.3).

Like the CB₁R, CB₂R is a classical GPCR. Although both receptors share similar intracellular transduction pathways, being most often coupled to G $\alpha_{i/o}$, several signal transduction pathways that have been characterized for CB₁R have not been identified for CB₂Rs: In rare cases CB₁Rs were shown to couple to G α_s whereas CB₂Rs did not (Kano et al., 2009). Controversial findings were published for G $\beta\gamma$ mediated modulation of ion channels: While earlier publications showed a lack of GIRK and P/Q-type channel modulation by CB₂Rs (Felder et al., 1995), more recent findings demonstrated that mouse and human CB₂Rs can modulate these ion channels. However, their activation strongly depends on the used ligand, representing an example of biased agonism (Atwood et al., 2012b;

Soethoudt et al., 2017). Similar to other GPCRs, various CB₂R agonists were identified that, upon binding to the receptor, favor one transduction pathway over another. A recent study profiled the most widely used CB₂R ligands and characterized the ability of certain agonist to activate distinct signaling pathways and to cause off-target effects (Soethoudt et al., 2017). The authors recommend the compounds HU-308, HU-910 and JWH133 as selective CB₂R agonists to study the role of CB₂R in biological processes.

Very recently, the crystal structure of antagonist bound CB₂R (Figure 3B) was published and revealed a distinct, smaller antagonist-binding pocket compared to CB₁R (Figure 3A). In fact, this antagonist-binding pocket is similar with regard to size and ligand-interacting residues to the CB₁R agonist-binding pocket, resulting in a conformational similarity of antagonist-bound CB₂R with agonist bound CB₁R (Li et al., 2019). This study suggests opposing effects of CB₁R and CB₂R and provides the explanation for the experimental finding that CB₂R antagonists can act as agonists on CB₁R (Li et al., 2019).

1.2.1.3 Other targets of endocannabinoids

Next to the two main cannabinoid receptors CB₁R and CB₂R, several orphan receptors (receptor whose endogenous ligand has not yet been identified) have been postulated to be putative cannabinoid receptors. The most promising candidate to represent an additional cannabinoid receptor is GPR55: Despite a low sequence homology to CB₁R and CB₂R (13.5% and 14.4%, respectively) a variety of synthetic, phyto- and endocannabinoids were shown to activate GPR55, including 2-AG and AEA. Although many controversial findings were reported, most studies showed that GPR55 cannot be activated by WIN55,212,2, a synthetic CB₁R/CB₂R agonist. The endogenous lipids lysophosphatidylinositol (LPI) and 2-arachidonoyl lysophosphatidyl inositol (2-ALPI) have been proposed as endogenous agonists of GPR55. In fact, GPR55 has been also been named LPI1 receptor (Kihara et al., 2014; Oka et al., 2007).

GPR18 is also considered to be associated with the endocannabinoid system, even though it displays an even smaller sequence homology to CB₁R and CB₂R (13% and 8%, respectively) compared to GPR55. Next to metastatic melanomas, as well as gastrointestinal and testicular tissues, GPR18 expression was found in neurons in various brain regions and in microglia (McHugh, 2012). The endocannabinoid N-arachidonylglycerine has been suggested to be the endogenous GPR18 ligand and several reports have indicated this receptor as a therapeutic target in the treatment of different pathologies including cancer and intraocular pressure (Morales and Reggio, 2017).

Further, it is well established that the endocannabinoids AEA, N-arachidonoyl dopamine (NADA; Huang et al., 2002) and noladin ether (Duncan et al., 2004) but not 2-AG, bind to transient receptor potential vanilloid 1 (TRPV1) channels at the same binding site as capsaicin, where they act as agonists (Pertwee et al., 2010).

Most GPCRs form homo- or heterodimers to represent their functional structure and both CB₁R and CB₂Rs have been shown to dimerize. When coexpressed with other GPCRs, formation of heterodimers can lead to crosstalk between cannabinoid and non-cannabinoid receptors connecting both endogenous systems. For example μ -opioid receptor/CB₁R heterodimers (Hojo et al., 2008) and CB₂R/chemokine receptor 4 heterodimers (Coke et al., 2016) were identified in which activation of the individual monomers influenced the function of the other component. Moreover, GPR55 were also shown to form functional dimers with CB₁Rs or CB₂Rs, which are present in neurons and in astrocytes (Kargl et al., 2012; Garcia-Gutierrez et al., 2018). CB₁R/CB₂R heterodimers were detected in rat brain pineal gland, nucleus accumbens and globus pallidus. Although the physiological function of such dimers is not known yet, it was shown that antagonization of one monomer blocks agonist activation of the other (Callen et al., 2012). Thus, the pharmacological properties of the heterodimers can be distinct from those of either one of the homodimeric receptors.

In addition, endogenous cannabinoid receptor ligands directly interact with several signaling proteins in a cannabinoid receptor-independent manner. These targets include GPCRs (muscarinic M1 and M3 receptors, adenosine receptor A3, serotonergic 5-HT₁ and 5-HT₂ receptors), ligand gated ion channels (serotonergic 5-HT₃ receptors, nicotinic acetylcholine receptors, glycine receptors, N-methyl-D-aspartate sensitive glutamate (NMDA) receptors), voltage gated Ca²⁺ channels (T-type Ca_v3 channels) and K⁺ channels (ATP-sensitive inward rectifier channels, voltage gated K⁺ channels and Ca²⁺ activated K⁺ channels; reviewed by Pertwee, 2015).

1.2.2 Endocannabinoids

Endocannabinoids are bioactive lipid messenger molecules that bind to cannabinoid receptors. Their lipophilic properties lead to a poor solvability in the hydrophilic extracellular space suggesting local and location-dependent activity. Mainly *in vitro* studies provided evidence that there are at least 15 endogenous compounds that target cannabinoid receptors either orthosterically (12 compounds) or allosterically (3 compounds). Here I describe the five most prominent and so far best studied endocannabinoids in the mammalian CNS.

1.2.2.1 AEA

The first endocannabinoid AEA was isolated from pig brain in 1992 and was named 'anandamide' based on the Sanskrit word *ananda* that means 'bliss' (Devane et al., 1992). Shortly after its discovery, activity dependent production of AEA was shown in cultured neurons (Di Marzo et al., 1994). High frequency stimulation in acute hypothalamic slices induced an increase in AEA levels that was abolished by blocking glutamate signaling (Di et al., 2005).

AEA behaves as a partial agonist to both CB₁Rs and CB₂Rs whereas it acts as a full agonist and represents the endogenous ligand for TRPV1 channels (Pertwee et al., 2010). Synthesis of AEA is considered to occur by multiple complementary and compensatory pathways, varying among brain regions. Different pathways may be favored for distinct physiological and pathophysiological processes. The classical AEA production underlies the metabolism of N-arachidonoyl phosphatidylethanolamines (NAPE), which is synthesized from phosphatidyl-ethanolamines (PE) by N-acyltransferase (NAT) that is activated by PKA. In addition, NAT activity was shown to be strongly stimulated by Ca²⁺ and it is thought to be the rate-limiting step in AEA production. Hydrolysis of NAPE by a NAPE-specific phospholipase D (NAPE-PLD, Figure 4A) represents the major pathway for AEA production. However, different effects on AEA levels were reported in NAPE-PLD KO mice and NAPE-PLD distribution only partially overlaps with CB₁R distribution, indicating the presence of additional metabolic pathways involved in AEA synthesis (Lu and Mackie, 2016). The best-studied alternative pathway describes the cleavage of the NAPE phosphodiester bond by NAPE-selective phospholipase C (NAPE-PLC) followed by dephosphorylation to liberate AEA (Figure 4A). As an additional pathway it was shown that O-deacylation of NAPE by α/β domain hydrolase 4 (ABHD4) leads to the formation of lyso-NAPE that in turn can either be further deacetylated (by ABHD4) to form glycerophospho (GP)-AEA followed by phosphodiesterase reaction to release AEA, or direct hydrolysis of lyso-NAPE by lysophospholipase D (lyso-PLD) to form AEA (Figure 4A). Interestingly, despite the fact that AEA levels were not changed in NAPE-PLD mice (Leung et al., 2006) both lyso-NAPE and GP-AEA levels were increased (Tsuboi et al., 2013). Additionally, by analyzing this KO mouse line, it was suggested that AEA can also be formed not only from NAPE, but also from N-acylated plasmenylethanolamine via both, NAPE-PLD-dependent and -independent pathways (Tsuboi et al., 2013).

Next to the complexity of possible synthesis pathways, degradation of AEA can occur via three different pathways: 1) Hydrolysis by fatty acid amino hydrolase (FAAH), 2) hydrolysis by N-acylethanolamine-hydrolysing acid amidase (NAAA) to arachidic acid (AA) and ethanolamine or 3) oxidation by cyclooxygenase-2 (COX-2) to create prostamides (Figure 4B). Metabolism via FAAH is considered to represent the major pathway for AEA degradation.

However, inhibition of FAAH may be compensated by the alternative pathways, altering cell functions independently of the endocannabinoid system due to the engagement of for example the COX-2 pathways (Tsuboi et al., 2013).

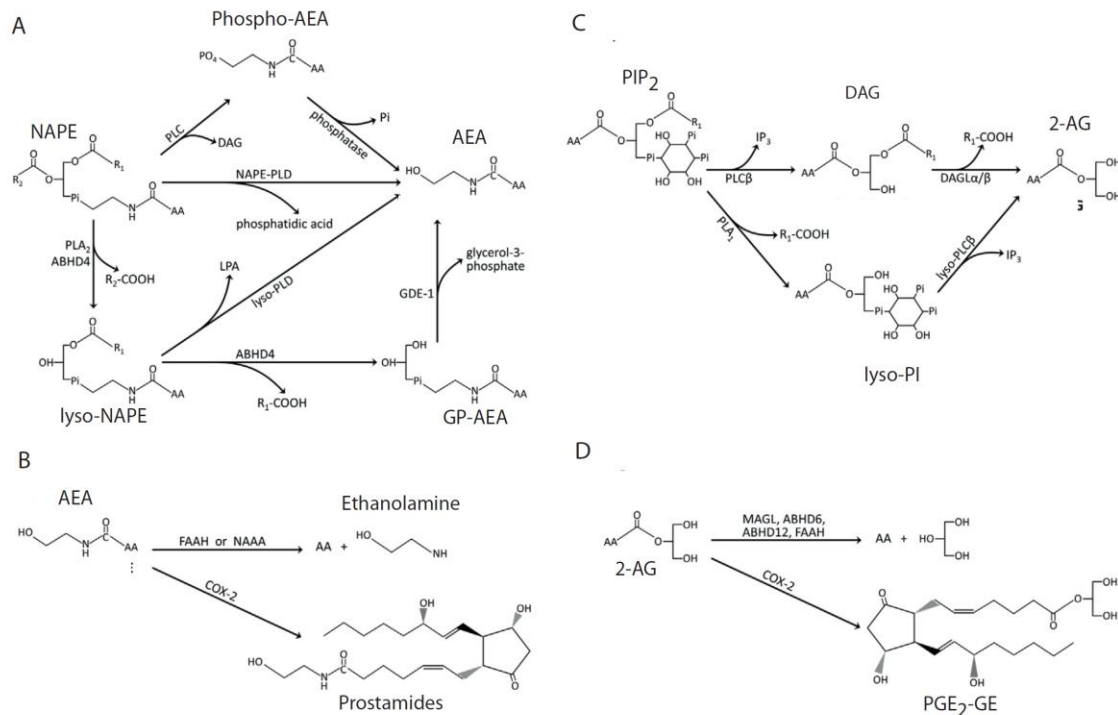


Figure 4: Metabolism pathways for AEA and 2-AG.

A: Synthesis and degradation (**B**) of AEA. **C:** Synthesis and degradation (**D**) of 2-AG. Modified from Lu and Mackie, 2016.

1.2.2.2 2-AG

2-AG is the most prevalent endocannabinoid in the CNS expressing much higher concentrations than AEA and acts as a full agonist to CB₁R and CB₂R, suggesting that 2-AG is a true natural ligand for the cannabinoid receptors (Kano et al., 2009). Same as AEA, 2-AG is synthesized on demand in response to neuronal activity (Di et al., 2005).

The major part of 2-AG is produced by hydrolysis of arachnidonyl-containing phosphatidylinositol 4,5-bisphosphate (PIP₂) by PLCβ followed by hydrolysis of the resulting DAG by DAG lipase (DAGL) to release 2-AG (Figure 4C). The first step of 2-AG synthesis can be engaged by stimulation of GPCRs that activate PLC via Gα_{q/11}, including group I metabotropic glutamate receptors (mGluR; Maejima et al., 2001; Varma et al., 2001) and muscarinic acetylcholine receptors (mACh; Kim et al., 2002; Ohno-

Shosaku et al., 2003). This activation leads to the production of DAG, the precursor of 2-AG. Intracellular Ca^{2+} elevation following depolarization or neuronal activity was shown to trigger 2-AG release (Kreitzer and Regehr, 2001a; Kreitzer and Regehr, 2001b; Ohno-Shosaku et al., 2001; Wilson and Nicoll, 2001) due to a Ca^{2+} -dependent enzymatic activity of PLC β . In fact, synergetic effects of both stimuli (mild GPCR activation combined with weak depolarization) have been reported to prominently enhance 2-AG release (Kim et al., 2002; Ohno-Shosaku et al., 2003; Ohno-Shosaku et al., 2002a; Varma et al., 2001). Although 2-AG can be produced in a Ca^{2+} or PLC β -independent manner, Ca^{2+} -assisted PLC β activation has been suggested to underlie physiological cannabinoid release during synaptic transmission (Kano et al., 2009) in which PLC β acts as a coincidence-detector inducing cannabinoid production (Figure 5). In line with these findings, PLC β 1 was reported to form clusters that were found in somatodendritic locations and in close proximity to mGluR, mACh and DAGL α (Fukaya et al., 2008).

DAGL is a Ca^{2+} -activated enzyme expressed in two isoforms: DAGL α and DAGL β . Generation and analysis of transgenic mice lacking either of the two enzymes showed that DAGL α is exclusively responsible for the production and release of 2-AG at synapses in the CNS (Tanimura et al., 2010). Electronmicroscopical analysis of DAGL α expression reported its postsynaptic location. The opposing excitatory presynaptic sites of the DAGL α -expressing postsynaptic regions were found to be equipped with CB $_1$ Rs supporting the importance of DAGL α in endocannabinoid production. Surprisingly, DAGL α expression was rarely found opposed to CB $_1$ R-expressing inhibitory terminals contacting perisomatic sites of the cells, although these connections show strong expression of endocannabinoid-mediated plasticity mechanisms (see chapter 1.2.4; Katona et al., 2006; Yoshida et al., 2006).

In an additional complementary pathway for 2-AG production phosphatidylinositol (PI) is cleaved by phospholipase A1 (PLA1) to lyso-PI followed subsequent conversion to 2-AG by lyso-PLC (Figure 4C).

Degradation of 2-AG primarily occurs via three hydrolytic enzymes to form arachidonic acid and glycerol (Figure 4D): 85% of 2-AG hydrolysis is performed by monoacylglycerol lipase (MAGL) while the remaining part is mostly catalyzed by α/β -Hydrolase domain containing enzyme (ABHD) 6 and ABDH12 (Blankman et al., 2007). These three enzymes have different cellular and subcellular expression patterns: In contrast to presynaptic localization of MAGL (opposing postsynaptic DAGL α), ABDH6 and 12 are mainly expressed in dendrites and dendritic spines suggesting diverging functions of these enzymes (Figure 5). Additionally, 2-AG can be oxidized by COX-2 or hydrolyzed by FAAH (Lu and Mackie, 2016), representing an overlap with degradation of AEA. Interestingly, metabolism of 2-AG by COX-2 leads to the formation of prostaglandin 2 glycerol ester (PGE2-GE) that was shown to

potentiate synaptic transmission and plasticity (Sang et al., 2006). Thus, different physiological or pathological conditions that modulate the endocannabinoid system might not only alter 2-AG levels, but can also lead to altering degradation pathways that result in modifications of endocannabinoid-independent systems.

1.2.2.3 Noladin Ether

A third putative endocannabinoid is 2-arachinodyl glycerol ether (noladin ether), which was isolated in 2001 from porcine brain. Noladin ether shows a selective binding to CB₁Rs in the nanomolar range but only a weak binding to CB₂Rs (Hanus et al., 2001; Table 2). In addition, noladin ether was shown to act independently of cannabinoid receptors as an agonist for TRPV1 channels (Duncan et al., 2004). Noladin ether production is increased by the cholinomimetic drug carbachol causing sedation, hypothermia, intestinal immobility and mild antinociception in mice (Hanus et al., 2001).

1.2.2.4 NADA

NADA is an endogenous lipid found especially in the hippocampus, cerebellum and striatum. NADA acts as full agonists of CB₁Rs (Bisogno et al., 2000) and TRPV1 channels (Huang et al., 2002). Interestingly, NADA was shown to act on both, CB₁Rs and TRPV1 channels in dopaminergic neurons: While higher NADA concentrations preferentially activate CB₁Rs leading to decreased inhibitory transmission, facilitation of glutamate release via TRPV1 channels only occurs after reuptake of NADA via endocannabinoid membrane transporters (Marinelli et al., 2007). The synthesis pathways for NADA production are not completely understood yet, however it was observed that NADA synthesis occurs almost exclusively in dopaminergic terminals. For degradation, NADA is hydrolyzed by FAAH to dopamine and AA (Huang et al., 2002). Thus, NADA acts as a competitive inhibitor for AEA degradation, suggesting a NADA-dependent potentiation of AEA effects (Grabiec and Dehghani, 2017).

1.2.2.5 Virodhamine

Virodhamine (O-arachidonoyl ethanolamine) is an endocannabinoid that is found in similar concentrations as AEA in human hippocampus and in rat brain. In contrast to the amide linkage of AA and ethanolamine in AEA, virodhamine contains the opposite chemical linkage: An ester. Thus, its name derives from the Sanskrit word *virodha*, which means opposition. Virodhamine acts as antagonist of CB₁Rs and agonist of the CB₂Rs (Porter et al., 2002). A recent study described the

connection between the endocannabinoid and the monoaminergic neurotransmission systems in which virodamine and related analogues inhibited activity of monoamine oxidase (MAO; Pandey et al., 2018).

In summary, unlike most other GPCRs, cannabinoid receptors appear to have more than one endogenous agonist. Different endocannabinoids alter in their affinities to the classical cannabinoid receptors as well as their activation potency for other receptor targets (see chapter 1.2.1.3). Thus, the endocannabinoid system represents a versatile tool for the regulation of various physiological and pathological processes (Di Marzo and De Petrocellis, 2012).

1.2.2.6 Mobilization of endocannabinoids

Although some evidences suggested that pre-formed 2-AG stores exist, it is now considered that endocannabinoids are produced and released on demand in an activity-dependent manner. As lipophilic compounds, endocannabinoid cannot be stored in vesicles and exocytotic endocannabinoid release can be excluded since 2-AG release was not affected by Butolinum toxin (Ohno-Shosaku et al., 2001; Wilson and Nicoll, 2001). The diffusion and spread of the endocannabinoids after their production is further discussed in chapter 1.2.4.2.

It appears intuitively plausible, that cannabinoids interact with the plasma membrane and diffuse laterally within the cell membrane to reach the effector receptors. Despite the fact that multiple orthosteric binding sites on CB₁Rs are associated with the extracellular domain (Saleh et al., 2018), several agonists (including AEA) were shown to interact with intermembrane regions of CB₁Rs (Song and Bonner, 1996a). AEA inserts readily and stably into cholesterol-containing membrane bilayers to form AEA/cholesterol complexes that laterally diffuse in the membrane or facilitate the transport across the cell membrane (Di Pasquale et al., 2009). In addition, the crystal structure of CB₁Rs revealed the association of cholesterol with the receptor for stabilization. A model suggests that cholesterol molecules surrounding CB₁Rs attract the AEA/cholesterol complex and thereby guide AEA to the agonist-binding site of the CB₁R, where the high affinity of AEA to CB₁Rs leads to AEA dissociation from cholesterol followed by binding and activation of CB₁R (Di Scala et al., 2018). Cholesterol enrichment of cell membranes was shown to reduce the binding efficiency and the induced response of AEA to CB₁Rs (Bari et al., 2005).

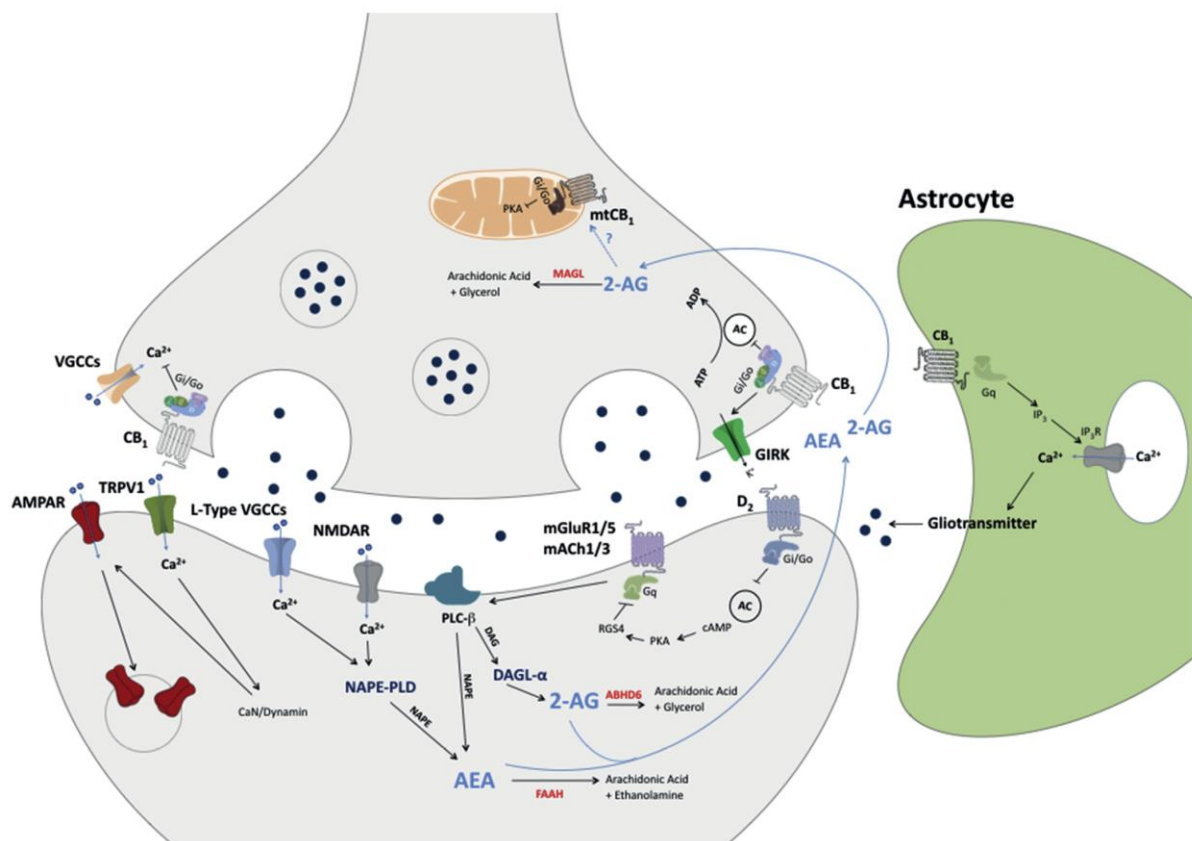


Figure 5: Synaptic function of the endocannabinoid system.

Presynaptic transmitter release (black points) leads to activation of metabotropic receptors (mGluR1/5, mACh1/3) and depolarization at the postsynaptic site. Together both stimuli can induce synthesis of endocannabinoids (2-AG DAGL α and AEA by NAPE-PLD). Endocannabinoids are released after production and can activate CB₁Rs on astrocytes, the presynaptic plasma membrane or presynaptic mitochondria. On the presynaptic site, CB₁R activation leads to inhibition of VGCC, GIRK channels, AC and mitochondrial PKA activity, resulting in suppression of transmitter release. Astrocytic CB₁R activation increases intracellular Ca²⁺ and induces gliotransmitter release. Adapted from Araque et al., 2017.

1.2.3 Role of cannabinoid system in behavior and diseases

Plant extracts of *Cannabis Sativa* have been used for a long time since their medical benefits were known for different applications related to inflammation, pain, anxiety and food-intake. Administration of cannabis or pure THC to animals led to the identification of a classical behavioral patterns tetrad including hypoactivity, hypothermia, antinociception and catalepsy (Martin et al., 1991). Most of these effects were not observed when CB₁Rs were pharmacologically blocked or genetically disrupted (Ledent et al., 1999; Zimmer et al., 1999). However, deletion of CB₁Rs did not alter THC-induced analgesic and immunosuppressive effects as well as several physiological behaviors (Zimmer et al., 1999). In contrast, deletion of CB₂Rs abolished THC effects on immune cells

while the observed cannabinoid effects on the central nervous system were unaltered (Buckley et al., 2000). Although it is still under debate, a broad line of research, including behavioral and electrophysiological experiments, showed evidence for the existence of functional CB₂Rs in neuronal, glial and endothelial cells (reviewed in Jordan and Xi, 2019).

1.2.3.1 Anxiety and depression

Even if there are no direct experimental data on the role of endocannabinoids on anxiety in humans, numerous publications demonstrated this link in animal models. Analysis of CB₁R or DAGL α deficient mice revealed enhanced anxiety, stress and fear responses and depression-like behavior (Jenniches et al., 2016; Martin et al., 2002). Pharmacological inhibition of the endocannabinoid degrading enzymes FAAH and MAGL enhanced brain cannabinoid levels and produced anxiolytic effects in rats, whereas the CB₁R inverse agonist rimonabant induced anxiogenic behavior (Mechoulam and Parker, 2013). Rimonabant was developed by Sanofi (Paris, France) and was marketed under the trade name Acomplia in 2006 as a treatment against obesity. However, patients treated with rimonabant had enhanced depression- and anxiety-related symptoms (Christensen et al., 2007), leading to its worldwide withdrawal in 2008. Interestingly, effects of anxiolytic drugs like bromazepam and buspirone, which are thought to act in a cannabinoid receptor-independent manner, were abolished in CB₁R KO mice (Uriguen et al., 2004). In line with this finding, it was shown that cannabinoids and CB₁Rs activation can modulate the noradrenergic and serotonergic system. This interaction may represent the mechanism by which cannabinoid-related substances induce their anxiolytic and antidepressant effects (Mendiguren et al., 2018).

Unlike for the CB₁R, the role of CB₂Rs in anxiety is controversial: On the one hand, genetic manipulation or pharmacological intervention of the CB₂R showed that CB₂R activation reduces anxiety- and depression-like behavior (Busquets-Garcia et al., 2011; Garcia-Gutierrez and Manzanares, 2010; Ortega-Alvaro et al., 2011). In contrast, chronic activation of CB₂Rs was shown to increase anxiety, while blockade of CB₂Rs had anxiolytic effects (Garcia-Gutierrez et al., 2012). Further, injection of CB₂R antisense oligonucleotide into mouse brain induced anxiolytic behavior in mice. Analysis of the incidence of a polymorphism of the CB₂ gene in humans demonstrated an increased prevalence of one isoform in Japanese patients suffering from depression or alcoholism (Ishiguro et al., 2007; Onaivi, 2006; Onaivi et al., 2008). Analysis of CB₂R protein and gene expression in suicide victims revealed that relative gene expression of CB₂R-A isoform was significantly lower while overall CB₂R protein expression was higher compared to the corresponding control group (Garcia-Gutierrez et al., 2018). In line with this, CB₂R expression was down regulated in mice that

experienced emotional or immunological stress, increasing the risk of depression-like behaviors that may be linked with neuro-immune crosstalk (Ishiguro et al., 2007; Ishiguro et al., 2018). Specific deletion of CB₂Rs on dopaminergic neurons modulates animal behavior in anxiety- and depression-like paradigms (Liu et al., 2017). In addition, the behavioral tetrad induced by cannabinoids, which was classically associated with CB₁R activation, was altered in these animals. It was also shown that hippocampal CB₂R expression can be rapidly upregulated during anxiogenic social interaction and fear conditioning (Robertson et al., 2017).

Despite some contradictions, these studies convincingly showed that CB₂Rs are involved in anxiety-like behaviours. While CB₁Rs activation has clearly anxiolytic effects, CB₂Rs seem to modulate anxiety-related behavior in a more complex pattern.

1.2.3.2 Learning and memory

Research on the effects of marijuana has shown that cannabis intake can lead to memory loss in humans and animals. A systematic review analyzed 105 publications on the acute and chronic effects of cannabinoids in humans and summarized that verbal learning and memory as well as attention is consistently impaired by acute and chronic exposure to cannabis (Broyd et al., 2016). Multiple animal models and a wide range of behavioral paradigms have been used to assess the effects of cannabinoids on various stages of memory formation (acquisition, consolidation, retrieval and extinction). The major effects of cannabinoid application include impairment of working memory and long-term memory formation (Kruk-Slomka et al., 2017). Although the exact cellular mechanisms by which cannabinoids modulate memory-related processes are unknown, several studies showed that these effects are mediated by CB₁Rs expressed on hippocampal GABAergic interneurons (Puighermanal et al., 2009), astrocytes (Han et al., 2012) or by mitochondrial CB₁Rs (Hebert-Chatelain et al., 2016). A recent study demonstrated that endocannabinoids control synaptic plasticity and memory in a cell-autonomous manner by which postsynaptic CB₁Rs modulate the activity of hyperpolarization-activated cyclic nucleotide-gated channels regulating dendritic excitability (Maroso et al., 2016).

Deletion of CB₂Rs in mice impairs long-term fear memory (Garcia-Gutierrez et al., 2013), and manipulation of CB₂R expression in CA1 PC or microglia was shown to induce distinct behavioral phenotypes in mice: While microglial CB₂Rs were involved in contextual fear memory, overexpression or disruption of CB₂Rs in PC lowered anxiety levels or enhanced spatial working memory, respectively (Li and Kim, 2017). In conclusion, although the effects of cannabis administration on learning and memory are well studied in animal models, it is still unclear how the

physiological effects of the endocannabinoid system affect learning and memory. In fact, it was suggested that local repetitive activation of the endocannabinoid system is beneficial for working memory (Carter and Wang, 2007) and low dose of THC reversed an age-related decline in cognitive performance (Bilkei-Gorzo et al., 2017). Activation of CB₂Rs was also shown to restore cognitive function in a mouse model of Alzheimer's disease (Wu et al., 2017).

1.2.3.3 Neuroprotective effects of endocannabinoids

In various pathological states including neuroinflammation and neurodegenerative disorders different components of the endocannabinoid systems (endocannabinoids, CB₁R and CB₂R) were shown to be upregulated (Pertwee, 2015). Combined with the demonstrated neuroprotective effects of the endocannabinoid system (Fernandez-Ruiz et al., 2010) this may reflect the system's response to the pathological brain states. The endocannabinoid system is involved in different beneficial mechanisms during pathological brain states: It plays a key role in the death/survival cell decision, attenuates generation of reactive oxygen species and induces vasodilation to improve blood supply to injured brain areas (Fernandez-Ruiz et al., 2010). It was hypothesized that enhanced glutamatergic signaling and chronic excitotoxicity, which occurs in numerous neurodegenerative diseases (Lewerenz and Maher, 2015) leads to an increased production of endocannabinoids and elevated presynaptic CB₁R activation. In addition, activation of the endocannabinoid system was shown to decrease epileptic activity: 2-AG can suppress seizures and epileptogenesis by reducing excitatory synaptic inputs in the dentate gyrus through CB₁R and CB₂Rs (Sugaya et al., 2016).

Especially, but not exclusively, activation of microglial CB₂Rs was demonstrated to induce potent anti-inflammatory effects. In contrast to low CB₂R expression under physiological conditions, microglial CB₂R expression dramatically increased in a variety of pathological conditions including neuroinflammation (Caslisle et al., 2002; Zoppi et al., 2014), stroke (Yu et al., 2015; Zarruk et al., 2012), Parkinson's disease (Concannon et al., 2015, 2016), Alzheimer's disease (Benito et al., 2003) and Huntington's disease (Palazuelos et al., 2009). Also, neuronal CB₂R expression is increased in neuropathic pain (Svizenska et al., 2013), drug addiction (Zhang et al., 2014, 2017) and CB₂R protein expression was increased in suicide victims (Garcia-Gutierrez et al., 2018). According to these data Pacher and Mechoulam suggested that CB₂R signaling might represent a protective system that prevents tissue and cell damage (Pacher and Mechoulam, 2011).

1.2.3.4 Therapeutic use of cannabinoids

Considering the involvement of the endocannabinoid system in a variety of pathological conditions, a plethora of clinical trials have been performed to determine the therapeutic potential of cannabinoids (search for cannabinoids: 375 registered trials on ClinicalTrials.gov; 696 clinical studies and case reports on database by International Association for Cannabinoid Medicines; accessed on March 22 2019).

Some cannabinoid-based medications have already been approved for the treatment of various pathological conditions: A synthetic analog of THC (Nabilone) and an isoform of THC (Dronabinol) are used for treatment of nausea and vomiting induced by chemotherapy (Fraguas-Sánchez and Torres-Suárez, 2018). Plant extracts from *Cannabis Sativa* (Nabiximols; trade name: Sativex), mainly containing THC and cannabidiol (at a ratio 1:1) are used for the treatment of spasticity and pain associated with multiple sclerosis and for palliative treatments in patients with advanced cancer. Pure plant-derived cannabidiol (trade name: Epidiolex) has recently been approved for treatment of two severe and refractory forms of pediatric-onset epilepsies: Lennox-Gaustat syndrome and Dravet-syndrome (Billakota et al., 2019; Sekar and Pack, 2019). Several studies have shown that cannabidiol interacts with various cannabinoid-related and non-related targets: It acts as an antagonist for CB₁Rs and GPR55 as well as inverse agonist of CB₂R (Ryberg et al., 2007; Thomas et al., 2007) and inhibits AEA uptake and degradation resulting in increased endocannabinoid levels (Billakota et al., 2019; Campos et al., 2012). Further, cannabidiol is an agonist of TRPV1, TRPV2, 5-HT_{1A} and 5-HT_{2A} receptors and an antagonist for 5-HT₃ and TRPM8 receptors. It acts as an allosteric modulator of opioid receptors and blocks reuptake of adenosins (Campos et al., 2012). However, the exact mechanisms by which cannabidiol-induced therapeutic effects are mediated have not been determined.

1.2.3.5 Endocannabinoid system as target for drug-discovery research

Despite the involvement of the endocannabinoid system in a variety of pathological states, only a few compounds targeting the endocannabinoid system have reached the therapeutic market (chapter 1.2.3.4). Due to the ubiquitous expression of CB₁Rs in the CNS and its involvement in multiple physiological processes, pharmacological manipulation of CB₁Rs leads to several side effects including psychotropic actions (Fraguas-Sánchez and Torres-Suárez, 2018).

Hence, CB₂Rs are considered to represent a more promising target for treatment of CNS-related diseases due to their low expression levels in physiological conditions that is upregulated in a variety of pathological states (Dhopeswarkar and Mackie, 2014). This pathology-induced expression of CB₂Rs implicates a disease-associated target for pharmacotherapeutic treatment without strong side

effects in healthy states. Further, CB₂R activation showed to mediate potent anti-inflammatory effects that can be beneficial in most neurological diseases (Basavarajappa et al., 2017). Since specific CB₂R activation does not have psychoactive side effects associated with CB₁R activation (Pertwee, 2012), CB₂Rs represent an excellent potential target for drug-discovery research.

1.2.4 Physiological effects of cannabinoids on synaptic transmission

After the discovery of the endocannabinoid system in the early 1990s, a plethora of the well-known effects of marijuana could be investigated in more detail and were mainly mimicked by CB₁R activation. Numerous studies were performed to identify and locate the key elements of the endocannabinoid system. In addition, the development of transgenic animals lacking the cannabinoid receptors (Buckley et al., 2000; Ledent et al., 1999; Zimmer et al., 1999) shed further light into the role and function of one of the major physiologically important systems. The initial studies of CB₁R KO mice described that transgenic animals did not respond to cannabinoid drugs as opposed to their wild type (WT) littermates indicating the role of CB₁R in analgesia, reinforcement, hypothermia, hypolocomotion, and hypotension (Ledent et al., 1999; Zimmer et al., 1999). In addition several phenotypes of the CB₁R deficient mice were described, including increased mortality, hypoalgesia, hypoactivity (Zimmer et al., 1999) and CB₁Rs were considered to be responsible for all cannabinoid related effects in the CNS. Further, several studies have elucidated the effects of cannabinoids on developing organisms, especially in regard to the CNS as well as characterized the presence of components of the endocannabinoid system during development (Fernandez-Ruiz et al., 2000).

During the 1990s, the discovery of the endocannabinoid system and the systematic study of transgenic KO animals of its key component established a detail understanding of the functional anatomy and the molecular mechanisms for cannabinoid signaling. However, the physiological role of the endocannabinoid system remained elusive, since the physiological stimuli for endocannabinoid production and release were not understood yet.

In the meantime a phenomenon was identified in which an unknown retrograde messenger was released upon depolarization of a postsynaptic neuron to suppress inhibitory input (DSI: Depolarization-induced suppression of inhibition, Figure 6; Pitler and Alger, 1992). Four publications from different laboratories were published in three different journals on the 29th March 2001 and unequivocally demonstrated that cannabinoids represent the long-sought retrograde messengers. One publication proposed a model suggesting that endocannabinoids represent retrograde messengers (Elphick and Egertova, 2001), and experimental data from hippocampal (Wilson and Nicoll, 2001) and cerebellar brain slices (Kreitzer and Regehr, 2001a), as well as from cultured

hippocampal neurons (Ohno-Shosaku et al., 2001) supported the hypothesis that endocannabinoids are produced and release postsynaptically to inhibit neurotransmitter release from presynaptic terminals.

1.2.4.1 Short-term plasticity

Endocannabinoids were shown to act as retrograde messengers: Activation of the postsynaptic cell, by Ca^{2+} increase or due to activation of $\text{G}\alpha_{q/11}$ GPCRs lead to activation of endocannabinoid synthesizing enzymes and the release of endocannabinoids. The endocannabinoids bind to presynaptic CB_1Rs (Figure 5) and transiently inhibit transmitter release for tens of seconds. In acute hippocampal brain slices and in cultured hippocampal neurons DSI in PC was mimicked and occluded by activation of CB_1Rs and DSI was abolished with CB_1R antagonists (Ohno-Shosaku et al., 2001; Wilson and Nicoll, 2001). At cerebellar excitatory synapses a similar phenomenon was identified in which endocannabinoids inhibit glutamate release upon binding to presynaptic CB_1Rs and it was called depolarization-induced suppression of excitation (DSE; Kreitzer and Regehr, 2001a, b). This inhibition of glutamate release was accompanied with presynaptic Ca^{2+} decrease and was blocked by application of Ca^{2+} chelators into the postsynaptic cell.

2-AG is considered to represent the major endocannabinoid responsible for modulation of synaptic transmission since both DSI and DSE were absent in $\text{DAGL}\alpha$ deficient animals (Tanimura et al., 2010). Strong activation (one brief depolarization step or several APs) of the postsynaptic cell leads to an increase in intracellular Ca^{2+} via voltage-gated Ca^{2+} channels (VGCC; Pitler and Alger, 1992) or NMDA receptors (Ohno-Shosaku et al., 2007), which induces $\text{PLC}\beta$ and $\text{DAGL}\alpha$ to produce 2-AG. In addition, a Ca^{2+} -independent mechanism was described in which activation of GPCRs (including mGluR, mACh and cholecystinin-receptors) activate $\text{PLC}\beta$ via the $\text{G}\alpha_{q/11}$ subunit to produce DAG that is subsequently metabolized to 2-AG (metabotropic suppression of inhibition/excitation; MSI/MSE; Lu and Mackie, 2016). Despite the Ca^{2+} -independency of MSI/MSE, the Ca^{2+} sensitivity of $\text{PLC}\beta$ results in synergetic action of metabotropic and depolarization-induced 2-AG production and suppression of transmitter release. Thus, these two forms of endocannabinoid production can serve as coincidence-detector of $\text{G}\alpha_{q/11}$ signaling, postsynaptic depolarization and Ca^{2+} influx. Importantly, it was reported that stimulation of presynaptic neurons can induce postsynaptic 2-AG production via mGluR1 and NMDA receptors to inhibit presynaptic transmitter release (Beierlein and Regehr, 2006).

After production and release, 2-AG binds to presynaptic CB₁Rs on inhibitory (for DSI and MSI) or excitatory (for DSE and MSE) axon terminals resulting in reduction in transmitter release via inhibition of VGCC (mainly N-type, under some conditions also L-type Ca²⁺ channels; Foldy et al., 2006; Lenz et al., 1998). In addition, mitochondrial CB₁Rs were shown to contribute to DSI in hippocampal PCs by regulating neuronal respiration and energy production (Benard et al., 2012).

Short term modulation of synaptic transmission by endocannabinoids was described for numerous synapses in multiple brain regions including hippocampal CA1 and CA3 PC, dentate granule cells, hilar mossy cells and hippocampal cholecystokinin-positive interneurons, cerebellar Purkinje cells, basket cells and stellate cells, striatal medium spiny neurons, neurons in the globus pallidus and in substantia nigra pars reticulata and pars compacta, in layers 2/3 and 5 PC of the somatosensory cortex, in the amygdala, the hypothalamus as well as in the brainstem (reviewed by Kano et al., 2009).

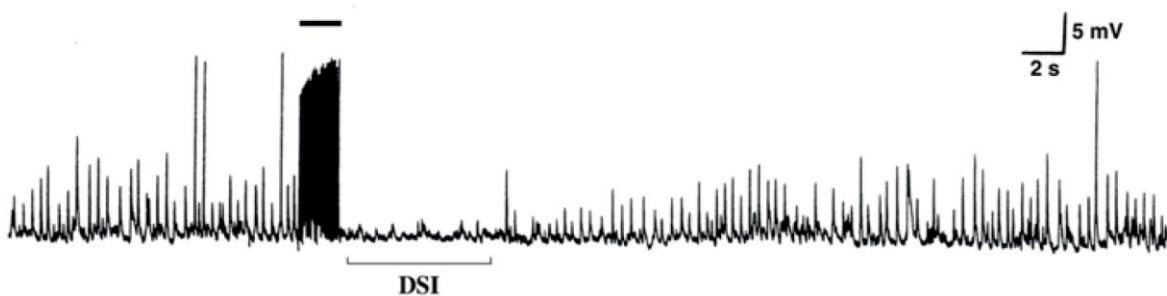


Figure 6: High-frequency trains of APs transiently reduce inhibitory potentials in hippocampal PCs.

Spontaneous inhibitory potentials were recorded in CA1 PCs with KCl-filled electrodes (positive voltage deflection; Pitler and Alger, 1992). Voltage-clamp recordings were performed in the presence of ionotropic glutamate receptor antagonist and carbachol to isolate and increase inhibitory transmission, respectively. Example trace shows that a brief AP train (black bar) induced a transient suppression of inhibitory events (depolarization-induced suppression of inhibition: DSI). Modified from Pitler and Alger, 1992.

1.2.4.2 Spread of endocannabinoids

The hydrophobic nature of endocannabinoids allows the lateral diffusion in the cell membrane to activate adjacent cannabinoid receptors but it raised the question of how these lipid molecules can diffuse through the synaptic cleft to act on the presynaptic site. It was also unknown whether these diffusible messengers can spread to modulate nearby synapses. It was reported for neighboring hippocampal PCs that depolarization of one neuron caused a suppression of inhibition in the adjacent neurons when they were separated by 20 μ m or less (Ohno-Shosaku et al., 2000; Wilson

and Nicoll, 2001). In the cerebellum it was demonstrated that MSE does not spread to neighboring cells (Maejima et al., 2001), while DSI can spread from one Purkinje cell to another at a distance of 70 μm (Vincent and Marty, 1993). Further studies reported that depolarization of a Purkinje cell can inhibit neighboring excitatory and inhibitory cells at room temperature but only inhibitory cells at physiological temperature (Kreitzer et al., 2002). However this inhibition is not mediated by the direct long-range spread of the endocannabinoids but rather occurs due to activation of somatic K^+ channels at the interneurons, which can project over several hundred micrometers (Kreitzer et al., 2002). Thus, the biophysical mechanism by which the hydrophobic endocannabinoids can spread even short distances remains unclear.

1.2.4.3 Termination of endocannabinoid signaling

The short time course of DSI/DSE and MSI/MSE is caused by the rapid termination of the endocannabinoid signal due to enzymatic degradation. It is thought that both neurons and glial cells express transporters and degradation enzymes for endocannabinoids, and that they collaborate in endocannabinoid clearance of the extracellular space (Pertwee, 2015). While a lot of research was performed on AEA reuptake, relatively little is known about 2-AG. However, uptake parameters of both endocannabinoids share similar properties including temperature dependency, saturability and sensitivity to endocannabinoid reuptake blockers (including AM404 and OMDM-2). Additionally, AEA uptake is also inhibited by 2-AG, AA and noladin ether suggesting the presence of a general endocannabinoid plasma membrane transporter. Although putative endocannabinoid transporters have not been identified yet, specific endocannabinoid reuptake blockers are widely used in research to enhance extracellular endocannabinoid levels. Interestingly, these uptake blockers were reported to inhibit endocannabinoid release suggesting a bidirectional endocannabinoid transport across the plasma membrane (Seillier and Giuffrida, 2018).

It is still under debate if membrane bound transporters exist or if alternative models could explain the experimental observation. One alternative model for endocannabinoid transport utilizes the lipid structure of AEA and 2-AG and hypothesizes their association with the cell membrane and passive diffusion into the cell without the need for a specific membrane transporter. Passive diffusion would only be possible until extra- and intracellular level would reach equilibrium. However, activity of intracellular degrading enzymes (FAAH, MAGL) creates an endocannabinoid gradient that enables further translocation of endocannabinoids into the cell. For AEA it is adequately described that it diffuses across the cell membrane and is subsequently transported by intracellular carriers to the effector molecules (such as intracellular CB_1Rs or TRPV1 channels) or catabolic enzymes (Di Scala et

al., 2018; Fowler, 2013). These carriers are inhibited by endocannabinoid membrane transporter inhibitors. In addition, endocytosis was proposed to represent an important route for AEA uptake (McFarland et al., 2008). Different entry routes might even co-exist, meaning that the uptake of AEA might depend on the cell type as well as the physiological state of the cells, and a lot more research is needed to shed further light on this process and especially on the uptake of 2-AG.

1.2.4.4 Long-term plasticity

Next to the short-term modulation of synapses endocannabinoids are also involved in the induction of long-term changes of synaptic strength. High frequency stimulation of excitatory cortico-striatal synapses paired with postsynaptic depolarization induced long-lasting depression of presynaptic transmitter release due to postsynaptic AEA production (Gerdeman et al., 2002). In nucleus accumbens, presynaptic stimulation induced postsynaptic activation of mGluR5 receptors triggering endocannabinoid release that induced long-lasting presynaptic decrease in transmitter release (Robbe et al., 2002). Pairing of presynaptic stimulation with postsynaptic depolarization also induces long term depression (LTD) in cortical layer 5 PCs in which coincident activation of presynaptic NMDA receptors and CB₁R causes long-lasting synaptic depression (Sjöström et al., 2003). In addition, a heterosynaptic form of LTD was described in CA1 PC in which presynaptic stimulation of excitatory synapses leads to mGluR-mediated endocannabinoid release that induces LTD on nearby GABAergic terminals (Chaveleyre and Castillo, 2003).

In contrast to the inhibition of N-type VGCC by Gβγ for endocannabinoid induced short-term plasticity, the predominant mechanism for endocannabinoid induced long-term LTD requires reduction of the cAMP/PKA pathways by Gα_{i/o} following CB₁R activation (Cheveleyre et al., 2007). Moreover, CB₁R activation alone (pharmacologically or via repeated DSI induction) is not sufficient to induce LTD. Simultaneous presynaptic neuronal activity is crucial for LTD induction and CB₁R activation is only important during the induction phase but not in the expression phase (Castillo et al., 2012).

Besides the presynaptic forms of LTD, an endocannabinoid-dependent form of postsynaptic LTD was also described (Grueter et al., 2010). Presynaptic glutamate release triggers postsynaptic AEA production via mGluR5. In addition to acting on presynaptic CB₁R to induce LTD, AEA activates TRPV1 channels resulting in AMPA receptor endocytosis (Grueter et al., 2010).

In contrast to the general inhibitory action of endocannabinoids, several recent studies indicated that endocannabinoids can also participate in the induction of unconventional forms of long-term

potentiation (LTP). High frequency stimulation of the lateral perforated path triggers a presynaptic form of LTP, which is induced by CB₁R activation. Presynaptic neuronal activity results in transmitter release that leads to postsynaptic activation of mGluR5 and NMDA receptors. This induces endocannabinoid production and release to stimulate presynaptic CB₁Rs (Wang et al., 2016). In addition, layer 5 PC were shown to express a brain-derived neurotrophic factor-dependent form of LTP, where AP firing triggers endocannabinoid production and results in decreased inhibition onto the cell enabling increased Ca²⁺ influx and brain-derived neurotrophic factor production to induce LTP on excitatory synapses (Maglio et al., 2018). Paired pre- and postsynaptic stimulation of cortical or striatal principal cells resulted in an endocannabinoid dependent form of LTP that is NMDA receptor-independent but requires the simultaneous activation of CB₁Rs and TRPV1 receptors (Cui et al., 2016, 2018).

1.2.4.5 Involvement of glial cells in cannabinoid mediated synaptic modulation

Cannabinoid receptors as well as their synthesizing and degrading enzymes are also present in glial cells including astrocytes, oligodendrocytes and microglia. CB₁R and CB₂R expression in microglia changes depending on their phenotype and activation profile: While only low expression levels can be detected in healthy brains, especially CB₂R expression is highly increased under pathological conditions (see chapter 1.2.3).

Several studies confirmed the expression of CB₁R in astrocytes (Araque et al., 1999, 2017; Navarrete and Araque, 2010; Gomez-Gonzalo et al., 2015). These cells extend their processes to the synaptic cleft and can influence synaptic transmission, creating a functional entity with the pre- and postsynaptic site that has been named tripartite synapse (Araque et al., 1999). Activation of CB₁Rs on hippocampal astrocytes leads to increased intracellular Ca²⁺ that is mediated via activation of G $\alpha_{q/11}$ proteins and leads to PLC stimulation and release of Ca²⁺ from intracellular stores (Araque et al., 2017). Increase of the intracellular Ca²⁺ can trigger release of gliotransmitter that were shown to activate pre- or postsynaptic sites of the neighboring synapses (Figure 5). Stimulation of presynaptic excitatory cells with paired depolarization of postsynaptic layer 2/3 PC in somatosensory cortex leads to endocannabinoid release from the postsynaptic cell. These endocannabinoids can activate astrocytic CB₁Rs resulting in astrocytic glutamate release and presynaptic NMDA receptor activation to induce LTD (Min and Nevian, 2012). Additionally, while endocannabinoids acting on homosynaptic neuronal CB₁Rs induce DSE, they can also induce heterosynaptic short-term facilitation through activation of astrocytic CB₁Rs (Navarrete and Araque, 2010). Thus, astrocytes might also be involved in heterosynaptic regulation of synaptic strength since they span over several hundred micrometers

and form contacts to numerous dendrites and synapses. Interestingly, an *in vivo* study using cell type-specific CB₁R KO mice showed that impairment of working memory by marijuana and other cannabinoids exclusively relies on activation of astrocytic CB₁Rs and is associated with astroglial-dependent hippocampal LTP (Han et al., 2012). Gómez-Gonzalo et al. described another form of astrocytes-mediated long-term plasticity in 2015: Endocannabinoids were shown to induce LTP at a single hippocampal synapse through astrocyte activation when coincided with postsynaptic activity. Endocannabinoid-mediated activation of astrocytic CB₁Rs resulting in glutamate release that binds to presynaptic mGluR5 receptors. Simultaneous postsynaptic nitric oxide production and presynaptic activation of PKC results in potentiation of the excitatory synapse (Gomez-Gonzalo et al., 2015). In addition to glutamate, multiple different gliotransmitters contributing in synaptic plasticity were described to be released from astrocytes upon ligand binding to CB₁Rs. For example, activation of astrocytic CB₁Rs enabled induction of LTP via exocytosis of ATP from astrocytes (Rasooli-Nejad et al., 2014).

It is still unclear to which extent glial cells contribute to the production of endocannabinoids for its synaptic action. Astrocytes as well as oligodendrocytes were shown to be able to synthesize endocannabinoids through Ca²⁺- and ATP-dependent pathways (Oliveira da Cruz et al., 2016). Further, a recent study showed that neurons and astrocytes coordinately regulate 2-AG content via MAGL-mediated 2-AG metabolism and transcellular shuttling of AA (Viader et al., 2015).

In conclusion, glial cells, especially astrocytes, might represent an important cellular component of the endocannabinoid system, since they bridge pre- and postsynaptic sites and contribute to heterosynaptic regulation of synaptic strength. In addition, glia cells are involved in the production and degradation of endocannabinoids regulating its temporal and local activity. Together, the involvement of astrocytes in cannabinoid signaling adds an additional level of complexity to the endocannabinoid system.

1.2.5 Cell-autonomous action of endocannabinoids

Beside the modulation of synaptic transmission, endocannabinoids were reported to influence cell excitability in an autocrine or cell-autonomous manner. Postsynaptic CB₁Rs were shown to regulate dendritic excitability by modulating the key dendritic current I_h due to activation of hyperpolarization-activated cyclic nucleotide-gated channels. CB₁R activation leads to enhancement of I_h via a c-Jun-N-terminal kinases, nitric oxide synthase, and intracellular cyclic Guanosine monophosphate (cGMP) dependent pathway resulting in an impairment of dendritic integration of excitatory inputs, LTP and spatial memory formation (Maroso et al., 2016). Intracellular CB₂Rs in PCs

of the medial prefrontal cortex were reported to open Ca^{2+} -activated Cl^- channels in an IP_3R -dependent manner (den Boon et al., 2012). AP-firing triggers 2-AG synthesis that activates intracellular CB_2Rs resulting in reduction of neuronal excitability as a putative mechanism to prevent excessive neuronal firing (den Boon et al., 2014). Moreover, 2-AG was reported to increase spontaneous firing of isolated dopaminergic neurons by reducing A-type K^+ currents in a cannabinoid receptor-independent manner (Gantz and Bean, 2017).

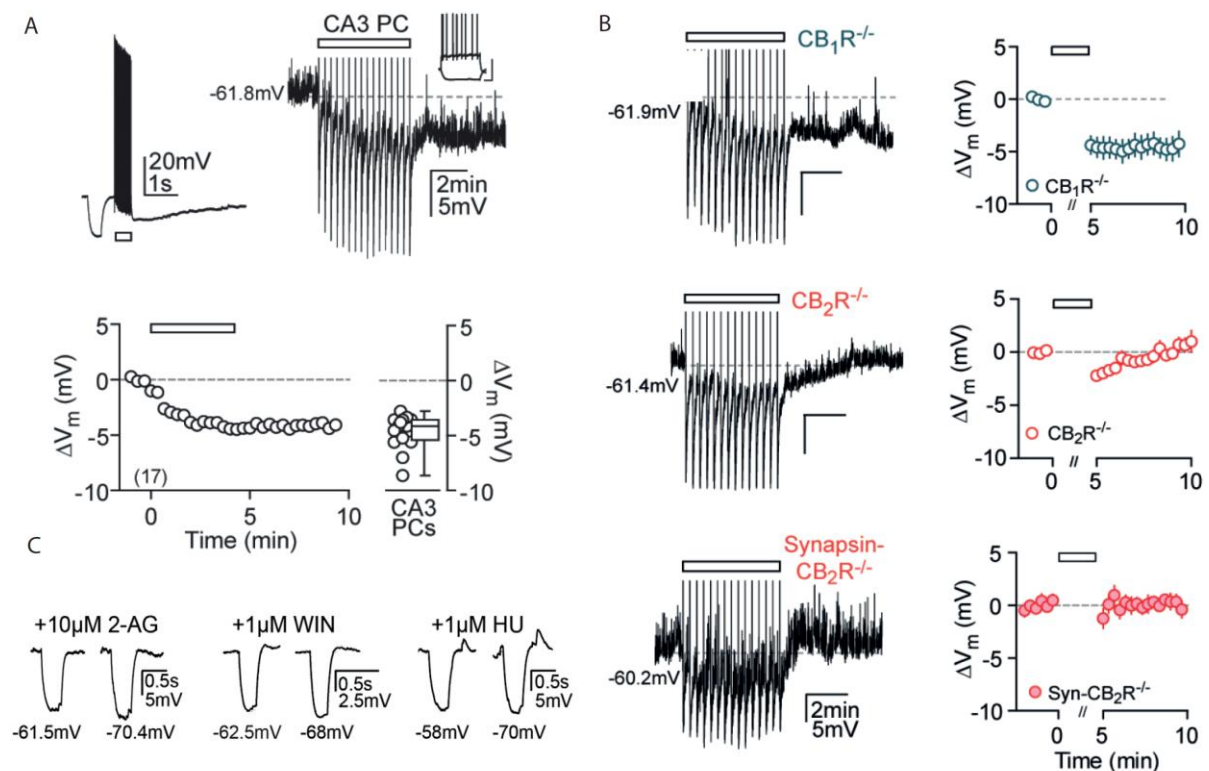


Figure 7: Hippocampal SSI is mediated by neuronal CB_2Rs and does not change the input resistance.

A: Trains of APs induce SSI in CA3 PCs recorded in perforated patch configuration (Stempel et al., 2016). Raw traces (upper part) show that trains of APs (white bars) elicit a long-lasting hyperpolarization. Lower part shows the time course of the average hyperpolarization induced by AP trains, as well as individual values of hyperpolarization. **B**: SSI is still present in $\text{CB}_1\text{R}^{-/-}$ mice (top), but abolished in constitutive (middle) and synapsin promoter-driven (bottom) $\text{CB}_2\text{R}^{-/-}$ mice. Left: Example of membrane potential in response to AP trains (white bars). Right: Average hyperpolarization induced by AP trains. **C**: Hyperpolarizing test-pulses (40 pA; in current-clamp configuration) were used to monitor input resistance of recorded cells. Agonist applications result in long-lasting hyperpolarization (membrane potential written under test pulses) but do not affect input resistance of the cells. Modified from Stempel et al., 2016.

Low-threshold spiking interneurons (LTS) in layer 5 of the somatosensory cortex express a form of self-inhibition that is mediated by CB₁Rs and was named slow self-inhibition (SSI; Bacci et al., 2004). Trains of action potential induce the synthesis of 2-AG and lead to activation of GIRK channels (Bacci et al., 2004; Marinelli et al., 2008). This effect was blocked by preincubation with the CB₁R antagonist AM-251 as well as by disrupting the intracellular Ca²⁺ increase via the Ca²⁺ chelator BAPTA or by blocking VGCC with Cd²⁺ (Bacci et al., 2004). Next to LTS interneurons, a subset of PC (approx. 30%) in layer 2/3 of the somatosensory cortex was shown to express SSI (Marinelli et al., 2009). A similar phenomenon was described in hippocampal principal cells, where trains of APs induced a long-lasting hyperpolarization in CA3 PCs (Figure 7A; Stempel et al., 2016). Surprisingly, pharmacological and genetic approaches demonstrated that hippocampal SSI is mediated by neuronal CB₂Rs (Figure 7B, C; Stempel et al., 2016). A further difference in hippocampal and cortical SSI represents the mechanism for the hyperpolarization: While in cortical neurons SSI is mediated via activation of GIRK channel resulting in reduced input resistance (Bacci et al., 2004; Marinelli et al., 2009), hippocampal SSI is not accompanied with a change in input resistance (Figure 7C; Stempel et al., 2016).

1.3 Aim of this study

In my thesis I investigated the presence, function and cellular mechanisms of SSI in different hippocampal and cortical cell types. SSI is an endocannabinoid-mediated cell-autonomous effect that modulates neuronal excitability. When we started this project, it was not known exactly which cell types are capable of inducing SSI and by which mechanism it is implemented. Based on the literature it was unclear whether cortical SSI depends exclusively on CB₁Rs or whether CB₂Rs may contribute to its induction. The overall aim of the study was to address the question whether cortical and hippocampal SSI differ in their induction and establishment mechanisms, or if their occurrence and underlying mechanisms rely on generalized biological principles.

First, we analyzed the cellular mechanism underlying SSI in hippocampal pyramidal neurons. Based on the finding that the input resistance did not change during SSI, we demonstrated that activity modulation of ion pumps represents the underlying mechanism (chapter 3.1). Second, we investigated whether SSI is only present in hippocampal principle cells or if interneurons also are able to induce SSI (chapter 3.1.1). Third, we studied SSI in different types of cortical neurons and intended to characterize the involvement of different cannabinoid receptors in SSI induction as well as the underlying mechanism (chapter 3.2).

2. Materials and methods

2.1 Materials

2.1.1 Technical Equipment

Vibratome	VT 1200S (Leica, Germany)
Interface storage chamber	Haas-type (Haas et al., 1979), custom-made (Charité Berlin, Germany)
Water baths	WBT series (Carl Roth, Germany)
Peristaltic pump	Puls 3 (Gilson, USA)
Recording chamber	submerged (Luigs and Neumann, Germany)
Heatable perfusion cannula	with temperature sensor PH01 and temperature controller TC02 (Multichannel Systems, Germany)
Oscilloscope	HM1507-3 (Hameg Instruments, Germany)
Amplifier	Axoclamp 700B (Molecular Devices, Canada)
Digitizer	BNC 2090 (National Instruments, USA)
A/D Board	PCI 6035E (National Instruments, USA)
Micromanipulators	Mini 25, 3 axes (Luigs and Neuman, Germany)
Stimulus generator	Master 8 (A.M.P.I, Israel)
Extracellular stimulation unit	Iso Flex (A.M.P.I, Israel)
Glass electrode puller	DMZ Universal Puller (Zeitz Instrumente, Germany)
Borosilicate glass capillaries	GC150TF-10 (Harvard Apparatus, UK)
Recording and bath electrodes	AG-8W silver wire, chlorided (Science products, Germany)
Upright microscope	BX-51 WI with differential interference contrast (DIC) optics and video microscopy (Olympus, Japan)

Water immersion objective	LumPlan FL/IR 60x 0.9NA (Olympus, Japan)
Phase objective	UPlanFL N 4X×0.13 PhP (Olympus, Japan)
Confocal microscope	DMI 6000; SP5 (Leica, Germany)
Plastic syringes	(B. Braun, Germany)
Perfusion tubing	(Carl Roth, Germany)

2.1.2 Software

IGOR Pro 6.12 (WaveMetrics Inc., USA) with custom-written plug-ins

NeuroMatic (<http://www.neuromatic.thinkrandom.com>)

Prism 5 (GraphPad Software, USA)

Illustrator (Adobe Systems Inc., USA)

Office 2007 (Microsoft, USA)

Image J (Research Services Branch, National Institute of Health, USA)

FIJI (Schindelin et al., 2012)

neuTube (Feng et al., 2015)

2.2 Experimental preparations

2.2.1 Ethical Statement and Animal Handling

Animal husbandry and experimental procedures were performed in accordance with the guidelines of local authorities (Berlin, Germany), the German Animal Welfare Act, and the European Council Directive 86/609/EEC. Animals were housed on a 12:12h reversed day-night cycle with food and water *ad libitum*.

2.2.2 Transgenic animals

All knockout animals used in this study were kindly provided by Prof. Andreas Zimmer (Department of Molecular Psychiatry, University of Bonn, Bonn, Germany). CB₁R- and CB₂R-deficient mice (Buckley et al., 2000; Zimmer et al., 1999) were maintained on a C57BL/6n genetic background, and homozygous KO mice and their WT littermates were obtained from heterozygous breedings.

In addition, a somatostatin reporter mouse line was used in which a somatostatin/Cre-expressing mouse line (Taniguchi et al., 2011) was crossed with a floxed-Ai9 mouse line (Madisen et al., 2010) resulting in tdTomato expression in somatostatin-expressing interneurons.

Animal breeding and genotyping was performed by technical assistances of the laboratory.

2.2.3 Preparation of brain slices

Coronal or horizontal slices were prepared from the somatosensory cortex and the hippocampus, respectively, mice aged postnatal day 21-35. Animals were anesthetized with isoflurane and decapitated. Brains were removed and transferred to ice-cold sucrose-based artificial cerebrospinal fluid (sACSF; containing in mM: 87 NaCl, 26 NaHCO₃, 50 sucrose, 10 glucose, 2.5 KCl, 1.25 NaH₂PO₄, 3 MgCl₂, and 0.5 CaCl₂). Tissue blocks were mounted on a vibratome (Leica VT 1200S, Leica Microsystems), cut at 300 μm thickness, and stored in an interface chamber (Haas et al., 1979; Figure 8) at 33 °C.

Interface storage of acute slices was chosen for this study, as previous work from our laboratory demonstrated advantages over submerged storage in terms of excitability and network preservation (Maier et al., 2009). In addition, structural analysis by electron microscopy revealed an improved maintenance of perisynaptic astroglial processes in interface storage, which are lost or retracted when slices are maintained under submersion conditions (Bourne and Harris, 2012).

The interface chamber was perfused with ACSF (containing in mM: 119 NaCl, 26 NaHCO₃, 10 glucose, 2.5 KCl, 1 NaH₂PO₄, 2.5 CaCl₂ and 1.3 MgCl₂). Temperature of the ACSF was maintained at 32°C and slices were incubated for at least 60 min before recordings started. All ACSF solutions were equilibrated with carbogen (95% O₂ and 5% CO₂).

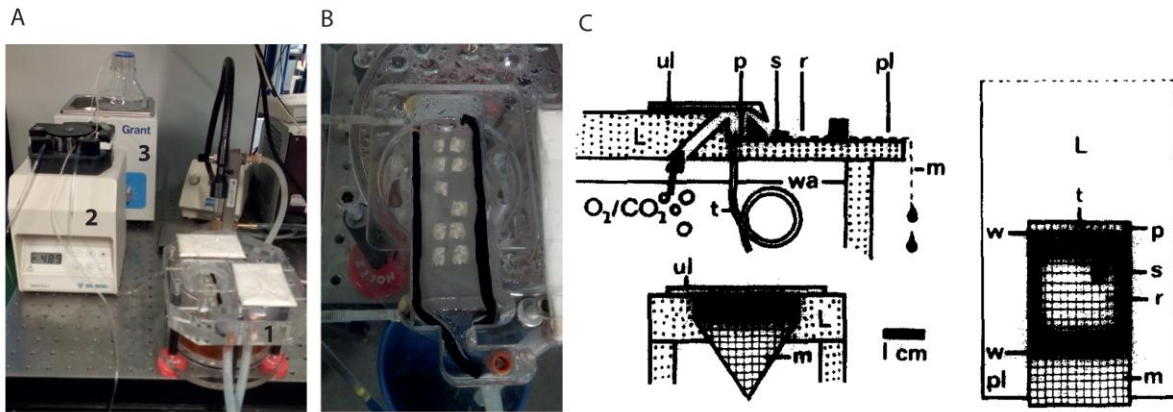


Figure 8: Interface chamber for slice storage.

Brain slices were placed on lens cleaning tissues in the interface chamber. ACSF is transported through polyethylene tubing and reaches the lower part of the brain slices. Top parts of brain slices are not covered by ACSF. ACSF and water in the interface chamber are oxygenated by carbogen. **A:** 1) Interface chamber containing horizontal hippocampal brain slices; heated to 33°C. 2) Perfusion pump for ACSF circulation. 3) Water bath with ACSF (in bottle). **B:** Higher magnification of interface chamber in which ACSF is transported from top to bottom to supply horizontal brain slices. **C:** Schematic drawing of the interface chamber; modified from Haas et al., 1979. Top: Side view. Right: View from above. Bottom left: Front view. L: Lid; m: Nylon mesh; p: Prechamber; pl: Projecting part of lid; r: Recording chamber; s: Slice; t: Polyethylene tube; ul: Upper lid; w: Ground wires; wa: Water line; Plexiglas forming the water bath and the lid is shaded, the frame forming the storage chamber is black.

2.2.4 Electrophysiology

2.2.4.1 General setup

For recordings, individual brain slices were transferred to a submerged chamber, perfused with ACSF (~5 ml/min, pre-heated to 33°C in a water bath, in addition heated via a PH01 heatable perfusion cannula mounted on the solution inlet into the recording chamber). Cells were visualized with infrared differential interference contrast optics on an Olympus BX-51 WI microscope. Patch clamp recordings were performed with a MultiClamp 700B amplifier and monitored using an HM1507-3 oscilloscope. Data were low-pass filtered at 3 kHz, digitized and sampled at 10 - 20 kHz with 16-bit resolution using a BNC-2090 interface board (connected to a PCI 6035E A/D board), and recorded in IGOR Pro 6.12 with custom-made plug-ins.

2.2.4.2 Whole-cell patch clamp recordings

Patch pipettes were pulled from filamented borosilicate glass capillaries (outer diameter 1.5 mm, inner diameter 1.17 mm) with a DMZ Universal Puller and fire-polished to a final resistance of 2-3 M Ω for patch clamp recordings. Unless stated otherwise, pipettes were backfilled with filtered KMeSO₃-based intracellular solution (containing in mM: 130 KMeSO₃, 10 KCl, 10 HEPES, 4 NaCl, 4 Mg-ATP, 0.5 Na-GTP, 5 phosphocreatine; 285 - 290 mOsm, pH was adjusted to 7.3 with KOH).

Putative hippocampal principal cells (in CA3 and CA1) were identified based on their location in *stratum pyramidale*, their pyramidal shaped soma and a prominent apical dendrite reaching towards *stratum radiatum*. Oriens lacunosum-moleculare (OLM) cells were located in *stratum oriens* and were identified by their spindle-shaped soma. Cortical interneurons were visually differentiated from PCs based on two criteria: A lack of apical dendrite projecting towards the pial surface and horizontally orientated and spherical shaped somata compared to the pyramidal shaped somata of pyramidal cells (PCs).

All recordings were performed in current-clamp mode. Resting membrane potential and input resistance (R_{in}) were determined directly after establishing the whole-cell configuration. Experiments were only performed if cells had a resting membrane potential more hyperpolarized than -55 mV (without correction for liquid junction potential) and a series resistance below 25 M Ω . Cells were characterized by recording their membrane response and firing pattern by applying hyperpolarizing and depolarizing current steps (-200 to + 600 pA, increment: 40 pA, 1 s).

Hippocampal PC showed a moderate spiking frequency and no pronounced sag-potential. OLM cells were identified by their faster spike frequency, their saw-tooth like firing pattern upon mild depolarization and a pronounced voltage sag following hyperpolarization. Cortical fast-spiking (FS) interneurons showed high frequency AP firing (>200 Hz) with no frequency adaptation. Both cortical regular spiking non-pyramidal cells (RSNPCs) and PCs showed moderate spiking frequency (20 - 60 Hz) and increasing inter-spike intervals during the depolarization step. The AP slope ratio was calculated by dividing maximal positive slope with the maximal negative slope of the AP. Series resistance was monitored and bridge balance was performed throughout the recording.

2.2.4.3 Substitution experiments

Different intracellular and extracellular solutions were used in order to determine the ions that contribute to SSI in hippocampal principal cells. Whole-cell recordings were performed in CA1 and CA3 PCs and long-lasting hyperpolarization was induced by direct CB₂R activation using HU-308. Recordings with K⁺-free intracellular solution (containing in mM: 130 CsMeSO₃, 10 HEPES, 10 NaCl, 4 Mg-ATP, 0.5 Na-GTP, 5 Na-Phosphocreatine) were performed in order to analyze the lack of intracellular K⁺ ions on SSI. The involvement of Cl⁻ on SSI was determined by using either high-Cl⁻ intracellular solution (containing in mM: 135 KCl, 10 HEPES, 4 NaCl, 4 Mg-ATP, 0.5 Na-GTP, 5 Na-Phosphocreatine) or low-Cl⁻-ACSF (containing in mM: 99 Na-gluconate, 20 NaCl, 25 NaHCO₃, 10 glucose, 2.5 KCl, 1 NaHPO₄, 2.5 CaCl₂, 1.3 MgCl₂). NMDG-based ACSF (containing in mM: 112 NMDG, 7 Na-ascorbate, 26 NaHCO₃, 10 glucose, 2.5 KCl, 1 NaHPO₄, 2.5 CaCl₂, 1.3 MgCl₂) was used to determine a reduced Na⁺-driving force on SSI.

Table 1: Pharmacological compounds used to determine mechanism of hippocampal SSI.

Name	Function	Final concentration	Supplier
SCH23390	GIRK channel blocker	10 μM	Tocris
S0859	NBC blocker	10-30 μM	Sigma-Aldrich
Oubaine	Na ⁺ /K ⁺ ATPase inhibitor	5 μM	Tocris
BAPTA	Ca ²⁺ - chelator (in patch pipette)	30 mM	Tocris
Bumetanide	NKCC inhibitor	10 μM	Tocris
VU0240551	KCC2 inhibitor	10 μM	Tocris
DNDS	Cl ⁻ channel blocker (in patch pipette)	500 μM	Sigma-Aldrich
Cariporide	NHE1 inhibitor	10 mM	Tocris
Rotenone	Inhibits complex I of the mitochondrial electron transport chain	2.5 μM	Tocris
Cyclopiazonic acid	SERCA-ATP inhibitor	30 μM	Tocris
NBQX	AMPA antagonist	100 nM	Tocris

2.2.4.4 Pharmacological agents

All drugs were purchased from Sigma-Aldrich or Tocris (both Germany). In hippocampal cells, experiments were performed in the continuous presence of GABA_A and GABA_B receptor blockers (1 μ M Gabazine and 1 μ M CGP55845) to isolate excitatory transmission, and 100 nM NBQX to prevent epileptiform activity. Other drugs were either added to the intracellular solution or bath-applied (see Table 1). In the case of bath-application of the drugs, slices were preincubated for at least 10min before SSI induction. Pharmacology targeting the cannabinoid receptors was used to determine the involvement of CB₁Rs and CB₂Rs in SSI in cells of the somatosensory cortex. Agonists and inverse agonists were used in concentrations according to literature for preferential activation or deactivation of either CB₁Rs or CB₂Rs (Table 2).

Table 2: Pharmacological tools to study involvement of cannabinoid receptors in cortical SSI.

Name	Function	Final concentration	K _i CB ₁ R	K _i CB ₂ R	References
2-Arachidonyl glyceryl ether (Noladin ether)	Endogenous CB ₁ R agonist	300 nM	21.2 nM	> 3 μ M	(Hanus et al., 2001)
HU-308	CB ₂ R agonist	1 μ M	> 10 μ M	22.7 nM	(Hanus et al., 1999)
SR144258	CB ₂ R inverse agonist	1 μ M	400 nM	0.6 nM	(Rinaldi-Carmona et al., 1998)
Ly 320135	CB ₁ R inverse agonist	1 μ M	220 nM	>10 μ M	(Felder et al., 1998)

2.2.4.5 Action potential protocols

The standard action potential (AP) protocol used to elicit SSI consisted of 15 AP trains in hippocampal cells and 10 trains in cortical neurons with 50 AP each (750 or 500 APs, respectively, 10 ms inter-stimulus interval, 20 s inter-train interval). Individual APs were elicited by 2 ms, somatic current injections (4 nA).

2.2.4.6 Data analysis

Data were analyzed in IGOR Pro 6.12 using the IGOR analysis software package Neuromatic. Statistical comparisons between groups were performed in Prism 5. Sample sizes are given as the number of experiments (n). The input resistance was calculated from a 50 ms average of the steady-state membrane potential response to a hyperpolarizing test pulse (400 ms, -40 pA). Individual membrane potential values (denoted as V_m in figures) were determined from a 10 ms average around the detected minimum within a 100 ms time window every 20 s. Baseline membrane potential values were calculated as the average of a 2 min baseline (6 values) before the action potential induction protocol or drug application. Given V_m values are not corrected for liquid junction potential (10 mV; calculated with JPCalcWin; Barry, 1994).

Changes in membrane potential (ΔV_m) were calculated as relative difference from the baseline V_m by subtracting the average V_m over 2 min (starting 60 s after the last AP train, or when V_m reached a stable state for agonist-induced hyperpolarization). Changes in input resistance after SSI were calculated by normalizing the average input resistance after SSI induction to the average baseline input resistance. Cells were classified as responding when ΔV_m was higher than three times the standard deviation of the baseline V_m . For average ΔV_m values, responding and non-responding cells were analyzed together and given as mean \pm SEM, unless otherwise stated.

For summary time plots of the global membrane potential average, the individual values of all experiments were averaged per point in time. Exemplary membrane potential recordings are unfiltered raw traces if not indicated otherwise.

Data distribution was assessed with the D'Agostino and Pearson omnibus normality test. Normally distributed datasets were compared using a two-tailed unpaired Student's t-test. Stated p -values refer to comparison of hyperpolarization amplitude (ΔV_m) between different datasets by using unpaired Student's t-test, unless otherwise stated. If datasets were not normally distributed the Mann-Whitney test was performed to compare the groups. If more than two groups were compared, 1-way-ANOVA (Kruskal-Wallis Test) followed by post-hoc Dunnett's Multiple Comparison Test was performed. Error bars correspond to the mean \pm SEM in normally distributed datasets or to median (25th percentile to 75th percentile) in not-normally distributed datasets. Box plots are shown as median with 25th and 75th percentile.

2.2.5 Immunohistochemistry and morphological reconstruction

Biocytin-containing intracellular solution (0.1% Biocytin, Sigma-Aldrich, USA) was used for post-hoc identification of the recorded neuron. After the recording, brain slices were fixed overnight in 4% paraformaldehyde in PBS (pH 7.4) at 4°C. Subsequently the sections were washed three times (10 min each) in PBS and incubated in a blocking solution composed of 5% normal goat serum (NGS, Biozol, Germany), 0.1% Triton-X (Sigma-Aldrich, USA) and PBS for three hours at room temperature with gentle agitation. Primary antibodies (mouse anti-GAD67, 1:500; mouse anti-Reelin, 1:1000, Millipore, USA) and conjugated streptavidin-Alexa488 (Invitrogen, USA) were diluted in a 2.5% NGS blocking solution and sections were incubated for 48 hours at 4°C. Following this, sections were washed three times (10 min each) with PBS and secondary antibodies (goat anti-mouse Alexa647, Life Technologies, USA) were applied, diluted to 1:500 in PBS for 3 hours at room temperature. Finally, slices were washed 4 times (10 min each) before being mounted on glass slides in mounding medium (Mowiol, Sigma-Aldrich, USA).

Stained slices were imaged with a laser confocal microscope (Leica DMI 6000) using a 20x or 63x objective and a z-step size of 1 μm . Morphological reconstruction was performed using Neutube (Feng et al., 2015) and Fiji software (Schindelin et al., 2012).

3. Results

3.1 Hippocampal SSI

3.1.1 Mechanism underlying SSI in hippocampal PCs

Brief trains of APs induce CB₂R-mediated SSI in hippocampal PCs (Figure 7A), which can be mimicked by application of the selective CB₂R agonist HU-308 (Stempel et al., 2016). Unlike in cortical SSI (Bacci et al., 2004; Marinelli et al., 2009), this hyperpolarization is not accompanied by a decrease in input resistance (Figure 7C; Stempel et al., 2016). The input resistance of a cell describes the reciprocal value of its conductance. A change in conductance of the cell membrane is usually linked to opening or closing of ion channels, in case of cortical SSI opening of GIRK channels (Bacci et al., 2004).

Since the input resistance remains unchanged during CB₂R mediated hyperpolarization in CA3, it is unlikely that modulation of ion channels represent the underlying mechanism, suggesting the involvement of a different mechanism underlying hippocampal SSI. One putative explanation is the activation of an electrogenic ion transporter for CB₂R-driven hyperpolarization of the cell. In contrast to ion channels, ion transporters can perform an active transport of ions across a cell membrane by moving ions against their electrochemical gradient. To overcome this gradient, ion transporters need to consume energy, such as ATP (primary transporters) or a concentration gradient of a different ion (secondary transporters).

Due to the high number of potential targets we performed a screening approach using pharmacological inhibitors of key molecules of different transduction pathways to abolish SSI. In this approach we used either AP trains or direct CB₂R activation to elicit the long-lasting hyperpolarization in the presence of different inhibitors. If we were able to elicit the long-lasting hyperpolarization in at least one recording (> 30% responding cells), we considered the given manipulation as not relevant for SSI. A cell was considered to be responding, if the AP- or agonist induced hyperpolarization was higher than three times the standard deviation of the baseline (dashed line in Figure 9A, B, E).

In a first attempt to demonstrate that an active ion transport is the underlying expression mechanism of hippocampal SSI, we used several approaches to alter the energy metabolism of the recorded neurons. After hydrolysis of ATP to ADP, ATP has to be regenerated to serve as an energy source for a variety of ion pumps. Phosphocreatine acts as a temporal energy buffer in cells to promote rapid regeneration of ATP (Guimarães-Ferreira, 2014). However, when we used an intracellular solution without ATP and phosphocreatine added, we could still elicit SSI (Figure 9A). Next, we preincubated the slices with cyclopiazonic acid (CPA 30 μM, inhibitor for Sarcoplasmic/endoplasmic reticulum Ca²⁺-

ATPase: SERCA) or rotenone (2.5 μM , a mitochondrial electron transport chain inhibitor) to inhibit ATP production. However, it was still possible to elicit long-lasting hyperpolarization in presence of these drugs (Figure 9A; Table 3), suggesting an ATP-independent mechanism. Hence, it seemed unlikely that an active form of ion transport is the underlying mechanism for SSI.

Since our data indicated that SSI is independent of ATP as an energy source, we hypothesized that a secondary ion transporter might be activated during the induction of SSI. To delimit the ion pumps that could be the target of CB_2R activation we performed substitution experiments (Figure 9B, C): We removed individual ions from the extracellular or the intracellular solutions in order to abolish the ion gradient across the cell membrane and prevent the induction of the long-lasting hyperpolarization. Substitution of extracellular Cl^- (with Na^+ -gluconate) or increase of intracellular Cl^- (by a KCl -based intracellular solution) as well as removing intracellular K^+ ions (with a CsMeSO_3 -based intracellular solution) did not block long-lasting hyperpolarization (Figure 9B, C). In fact, by reducing the K^+ gradient, the amplitude of the long-lasting hyperpolarization seemed to increase. However, replacing Na^+ with NMDG completely abolished the agonist-induced hyperpolarization (Figure 9B, D; Table 3), indicating that the Na^+ gradient across the cell membrane is necessary to establish the long-lasting hyperpolarization.

To determine the identity of the specific transporter that mediates hippocampal SSI, we performed a set of experiments in which we pharmacologically deactivated several ion pumps. Thus, we blocked the $\text{Na}^+/\text{K}^+/\text{Cl}^-$ transporter NKCC (with 10 μM bumetanide), the Na^+/H^+ exchanger (with 10 μM cariporide), the Na^+/K^+ ATPase (with 10 μM Ouabain), the K^+/Cl^- transporter KCC2 (with 10 μM VU0240551) and anion transporters (with 500 μM DNDS, in the patch pipette). However, we could not antagonize the long-lasting hyperpolarization (Figure 9E, F; Table 3). In contrast, a specific blocker of the electrogenic $\text{Na}^+/\text{bicarbonate}$ transporter (NBC; antagonized with S0859 10-30 μM) prevented both, agonist and AP-induced long-lasting hyperpolarization (Figure 10; Table 3).

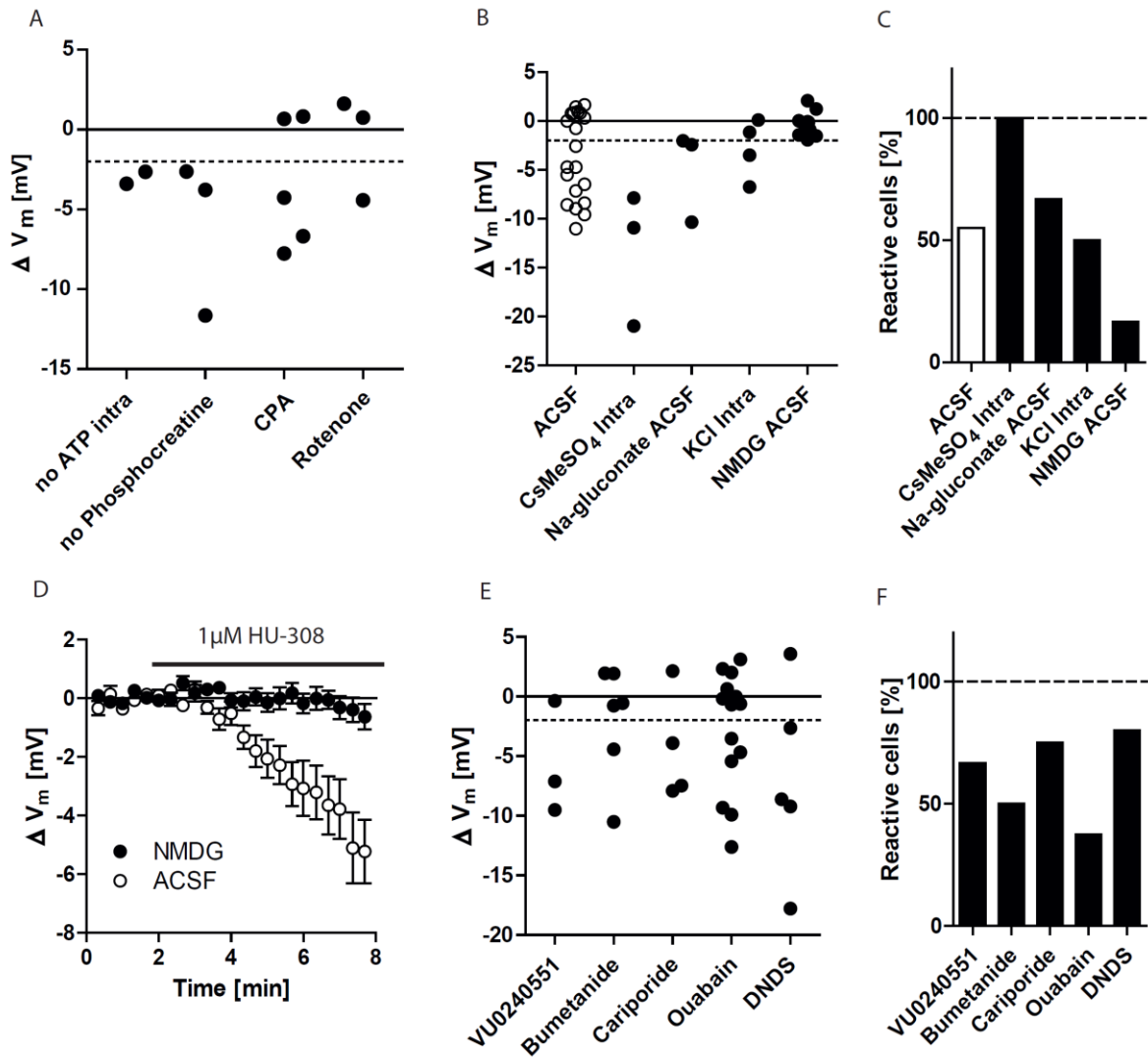


Figure 9: Mechanism underlying hippocampal SSI.

A: Different attempts to manipulate the cellular energy metabolism failed to block SSI induction. Dashed line: Approximate threshold for successful SSI induction (three times the standard deviation of the baseline). **B - D:** Removal of individual ions showed that substitution of extracellular Na⁺ ions by NMDG blocked the long-lasting hyperpolarization whereas it was still present in the absence of a K⁺ or Cl⁻ gradient. **B:** Amplitude of long-lasting hyperpolarization; **C:** Occurrence of long-lasting hyperpolarization. **D:** Time course of agonist induced long-lasting hyperpolarization in NMDG-containing and control ACSF solutions. **E - F:** Pharmacological inactivation of several ion transporters showed no effect on HU-308-induced long-lasting hyperpolarization. Amplitude (**E**) and occurrence (**F**) of HU-308-induced long-lasting hyperpolarization in presence of different ion transporter inhibitors.

In order to get more insight on the intracellular mechanism linking the AP trains with the activation of the NBC, we performed a series of experiments in which we added the Ca²⁺ chelator BAPTA into the intracellular solution. It is well-known that an intracellular Ca²⁺ increase can lead to the

production of endocannabinoids, thus interfering with the intracellular Ca^{2+} signal should prevent this process (Ohno-Shosaku et al., 2001). In line, SSI was abolished when recordings were performed with BAPTA-containing (30 mM) intracellular solution, indicating a Ca^{2+} -dependent mechanism for establishment of the long-lasting hyperpolarization (Figure 11A, C). However, a transient hyperpolarization was still present during the induction trains, but the membrane potential returned to baseline as soon as the AP trains stopped (Figure 11A). Interestingly, disruption of intracellular Ca^{2+} signaling also prevented CB_2R agonist-induced long-lasting hyperpolarization, indicating a Ca^{2+} -dependent mechanism downstream of CB_2R activation for SSI (Figure 11B, C).

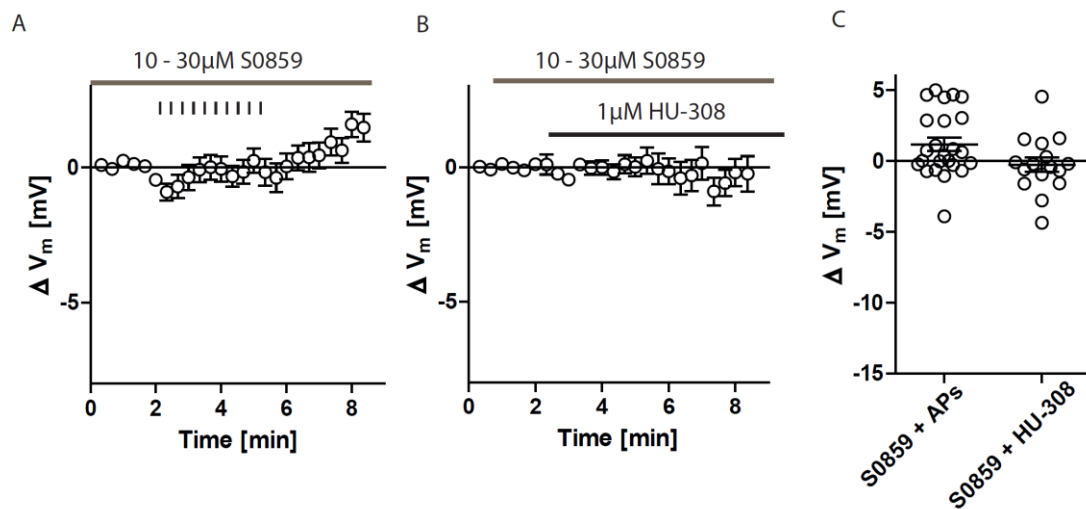


Figure 10: Deactivation of the NBC prevented both AP trains and agonist-induced long-lasting hyperpolarization.

A - B: Average time course of cells that were preincubated with the NBC antagonist S0859 (10-30 μM). AP trains (**A**) and application of HU-308 (**B**) did not induce a long-lasting hyperpolarization. **C:** Individual display of ΔV_m for the two conditions of SSI-induction in presence of the NBC blocker S0859.

Together, these results demonstrate that (1) hippocampal SSI is dependent on the Na^+ gradient across the cell membrane, and (2) that the hyperpolarization is mediated via NBC that are activated after ligand binding to CB_2Rs . These results have been published as part of the manuscript entitled “Cannabis Type 2 Receptors Mediate a Cell Type-Specific Plasticity in the Hippocampus” (Stempel et al., 2016).

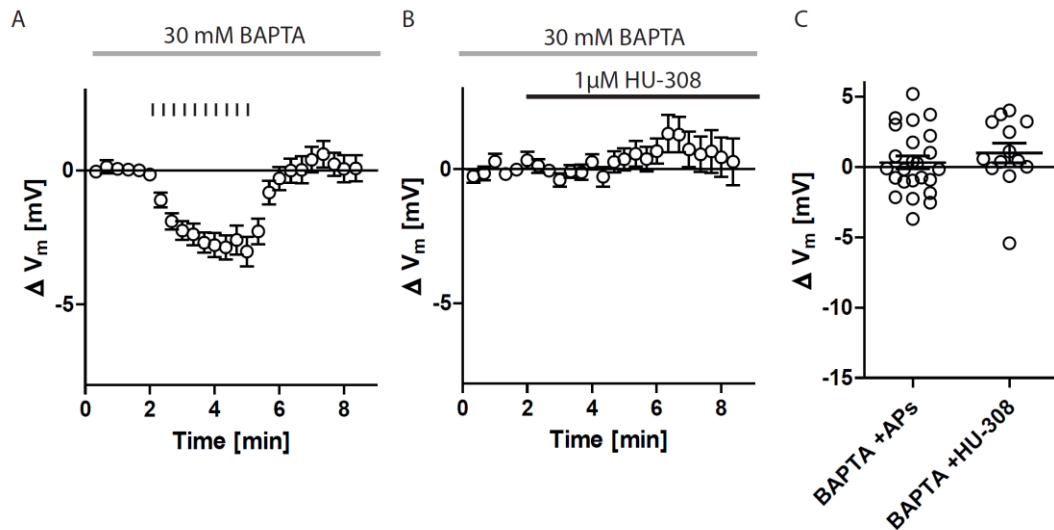


Figure 11: Intracellular Ca^{2+} signaling is necessary for induction of both AP train and agonist-induced hyperpolarization.

A - B: Average time course of changes in membrane potential for cells recorded with BAPTA (30 mM) containing intracellular solution. Intracellular BAPTA abolished the induction of the long-lasting hyperpolarization by AP trains (**A**) and HU-308 (**B**). AP trains induced a transient hyperpolarization during the induction. **C:** Individual display of ΔV_m for the two conditions of SSI-induction in presence of intracellular BAPTA. BAPTA + APs: $n = 24$; BAPTA + HU-308: $n = 13$.

To conclude, SSI in hippocampal CA3 PCs is mediated by CB_2Rs that activate the NCB transporter (via a still unknown intracellular signal cascade). Thus, hippocampal SSI is established by a mechanism that does not affect the input resistance, which is in contrast to cortical neurons, where SSI depends on the activation of GIRK channels downstream of cannabinoid receptors (Bacci et al., 2004; Marinelli et al., 2009).

Table 3: Amplitude and occurrence of SSI in hippocampal PC under different recording conditions

	Nr. of experiments	Average ΔV_m (mV)	Responding cells
“No ATP” intra	2	-3.02 ± 0.37	2/2
“NoPhosphocreatine” intra	3	-6.02 ± 2.83	3/3
CPA	5	-3.44 ± 1.80	3/5
Rotenone	3	-0.69 ± 1.89	1/3
ACSF	20	-3.60 ± 0.98	10/20
CsMeSO4 Intra	3	-13.28 ± 3.95	3/3
Na-Gluconate ACSF	3	-4.95 ± 2.71	2/3
KCl Intra	4	-2.84 ± 1.51	2/4
NMDG ACSF	12	-0.51 ± 0.34	2/12
VU0240551	3	-5.663 ± 2.74	2/3
Bumetanide	6	-2.10 ± 1.94	3/6
Cariporide	4	-4.29 ± 2.32	3/4
Ouabain	14	-2.78 ± 1.33	5/14
DNDS	5	-6.94 ± 3.57	4/5
S0859 + APs	24	1.17 ± 0.47	1/24
S0859 + HU-308	16	-0.27 ± 0.50	2/16
BAPTA + APs	24	0.32 ± 0.46	5/24
BAPTA + HU-308	13	0.99 ± 0.70	1/13

Average ΔV_m values are given as mean \pm SEM including responding and non-responding cells.

3.1.2 SSI in OLM cells

We have demonstrated that hippocampal CA3 pyramidal cells show a long-lasting hyperpolarization after brief AP firing (Figure 7A; Stempel et al., 2016) that is mediated by CB₂R activation. In contrast, CA1 PCs did not show SSI after AP trains, but still hyperpolarized after direct CB₂R activation with the specific agonist HU-308 (Stempel, 2015; Stempel et al., 2016), indicating CB₂R expression. Additionally, granule cells of the dentate gyrus did not hyperpolarize with both induction protocols (Stempel, 2015; Stempel et al., 2016). Thus, in the hippocampus SSI was so far only identified in a subset of excitatory neurons. In light of these findings, two questions arose: 1) Is SSI also present in inhibitory cells in the hippocampus? 2) Are SSI expression mechanisms different in different cell types?

To analyze the occurrence of SSI in inhibitory cells, we investigated hippocampal oriens lacunosum-moleculare (OLM) interneurons that have a distinctive location, firing pattern and morphology. OLM interneurons are somatostatin-expressing cells (Forro et al., 2015) that are located in *stratum oriens* of the hippocampus. The axons of OLM cells project towards stratum lacunosum-moleculare (verified in post-hoc biocytin staining, Figure 12A). In addition, OLM cells can be identified by their saw-tooth like firing pattern upon mild depolarization (Pangalos et al., 2013; Figure 12A). In line with previous studies (Pangalos et al., 2012), the input resistance of the recorded OLM cells was on average $377.2 \pm 37.4 \text{ M}\Omega$ (data not shown), supporting the identity of the recorded cells as OLM interneurons.

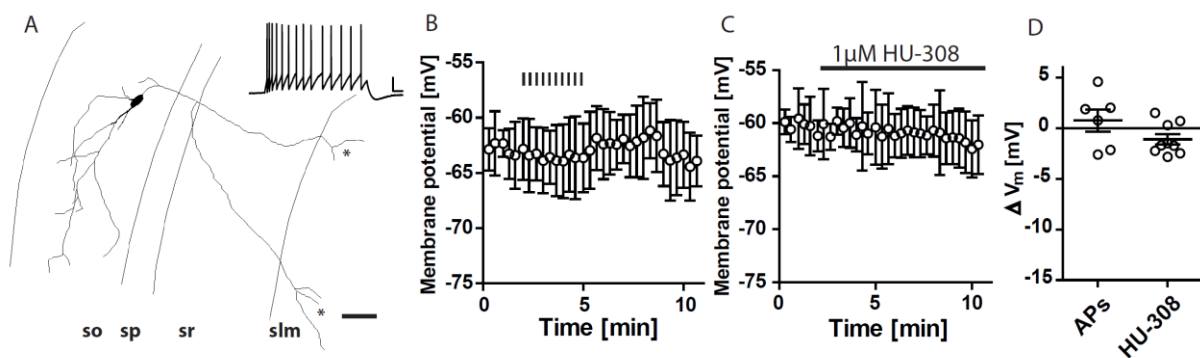


Figure 12: SSI is not present in hippocampal OLM cells.

A: Morphological reconstruction and firing pattern (inset: Scale bar: 0.1 s/20 mV) of biocytin-filled OLM cell. Scale bar: 50 μm . Spindle-shaped somata of OLM cells are located in *stratum oriens* (so) and axons project through *stratum pyramidale* (sp) and *stratum radiatum* (sr) towards *stratum lacunosum-moleculare* (slm) and ramify in slm (asterisk). **B - C:** Average membrane potential of OLM cells during AP trains (black lines, **B**) and agonist HU-308 application (black bar, **C**). **D:** individual amplitudes of hyperpolarization. AP trains and HU-308 application did not lead to a long-lasting hyperpolarization in OLM cells. APs: $n = 6$; HU-308: $n = 9$.

Trains of APs did not elicit SSI in OLM cells (Figure 12B, D). Additionally, application of the CB₂R agonist HU-308 did not change the membrane potential of OLM cells (Figure 12C, D) suggesting a lack of CB₂Rs or the downstream transduction pathway for SSI in this cell type. To summarize, OLM cells that were analyzed as an example of an inhibitory cell type hippocampus showed no hyperpolarization after activation with AP trains or pharmacological CB₂R activation.

In the hippocampus, expression of SSI was only found in a subset of excitatory cells (CA3 and CA2 PCs but not in CA1 PCs and dentate gyrus granule cells; Stempel et al., 2016). In these cells, SSI was exclusively induced by CB₂R activation. Remarkably, up to this point, it remained unclear whether in cortical neurons only CB₁Rs mediate SSI, or whether CB₂Rs also contribute to its induction.

Furthermore, it was not clear if all or just a subset of cortical neurons, can express SSI, and by which mechanism it is implemented. Therefore, in the final part of my PhD project, I investigated the expression and underlying mechanism of SSI in different neurons of the somatosensory cortex (chapter 3.2).

3.2 Cortical SSI

Our findings show that hippocampal SSI differs from the previous description of cortical SSI (Bacci et al., 2004; Marinelli et al., 2009) in terms of utilization of the cannabinoid receptor type and its downstream mechanism implementing the long-lasting hyperpolarization. Hence, we were wondering whether the establishment of SSI is, in fact, so variable in different celltypes and brain regions, or if we could identify similarities.

3.2.1 Cell type-specific expression of SSI in cortical neurons

In order to further investigate SSI induction and expression in different cell types, we performed whole-cell patch clamp recordings in three types of cortical neurons in the somatosensory cortex layer 2/3: Pyramidal cells (PCs), regular spiking non-pyramidal cells (RSNPCs) and fast-spiking interneurons (FSs). Cells were distinguished based on their morphology and their firing pattern (Figure 13).

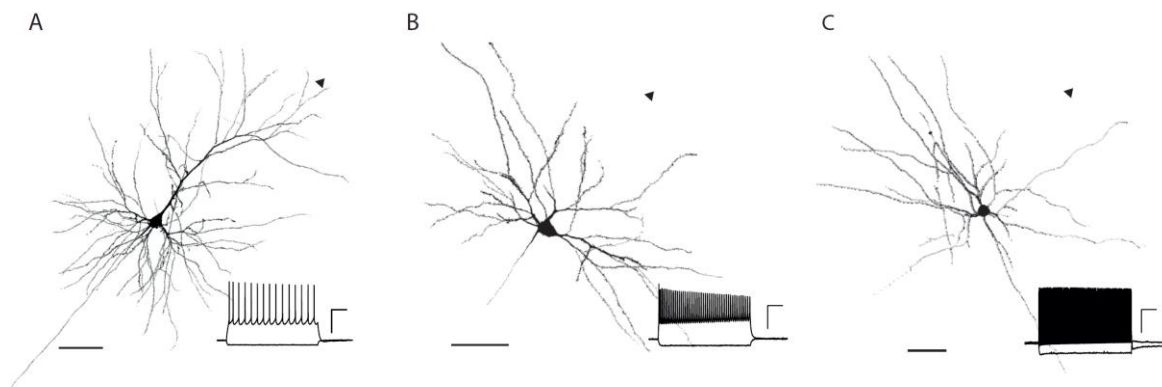


Figure 13: Morphological and electrophysiological properties of the three recorded cell types in the somatosensory cortex.

Characteristic cell morphology and firing pattern of a PC (A), a RSNPC (B) and a FS (C), visualized by post-hoc biocytin staining and morphological reconstruction. Scale bar: 50 μ m; arrow head depicts the direction of the pial surface. Insets show neuron type-specific firing pattern evoked by depolarizing current injection. Scale bars: 0.2 s/20 mV.

PCs showed a typical, eponymous pyramid-shaped cell soma, a prominent apical dendrite exceeding the pyramidal layer towards the pial surface (Figure 13A) and a regular firing pattern (Table 4). The firing pattern of RSNPCs was undistinguishable from PCs (Table 4); however, their horizontally orientated and spherical soma shape (Figure 13B) allowed clear discrimination between the two cell types. Finally, FSs also displayed a characteristic firing pattern (Table 4) and a non-pyramidal soma shape without an apical dendrite projecting towards the pial surface (Figure 13C). FSs also showed a depolarized resting membrane potential and a smaller input resistance compared to regular firing cells (Table 4). Additionally, AP half-widths and AP slope ratio were smaller and AP threshold was detected at more depolarized membrane potentials in FSs. Lastly, FSs were able to fire at much higher frequencies compared to regular spiking cells (Table 4).

Table 4: Cell properties of cortical neurons in somatosensory cortex layer 2/3

	PCs (11)	RSNPCs (21)	FSs (6)
Resting membrane potential [mV]	-81.9 ± 2.0	-80.6 ± 1.2	-65.2 ± 1.9
Input resistance [M Ω]	153.1 ± 11.6	189.3 ± 13.9	80.6 ± 9.7
AP half-width [ms]	1.0 ± 0.1	1.6 ± 0.1	0.3 ± 0.2
AP threshold [mV]	-33.9 ± 1.3	-36.0 ± 1.0	-46.8 ± 2.6
AP slope ratio	4.5 ± 0.2	4.5 ± 0.2	0.9 ± 0.1
AHP [mV]	-16.7 ± 0.7	-15.0 ± 0.5	-18.1 ± 0.6
Maximal firing frequency [Hz]	36.8 ± 2.3	41.17 ± 2.3	360 ± 39.9

Values are given as mean \pm SEM, PCs: Pyramidal cells; RSNPCs: Regular spiking non-pyramidal cells; FSs: Fast spiking interneurons; AHP: Afterhyperpolarization; numbers of recorded cells are displayed in parentheses.

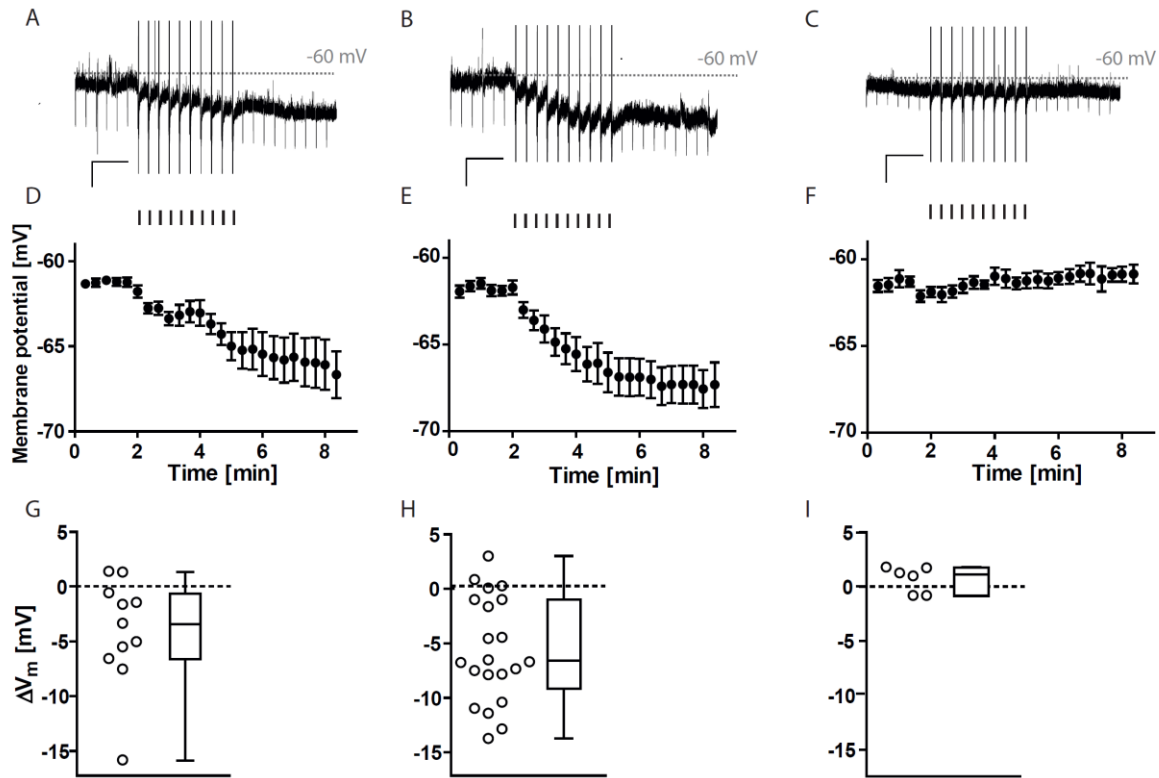


Figure 14: Trains of APs elicit a cell type-specific hyperpolarization.

AP trains induce SSI in PCs (A, D, G, $n = 11$) and RSNPCs (B, F, H, $n = 21$) but not in FSs (C, E, I, $n = 6$). A - C: Example trace of SSI induction in different cell types. Scale bar: 0.1 s/5 mV. D - F: Average membrane potential before during and after SSI induction. G - I: Hyperpolarization amplitudes in different cell types. AP trains are depicted as black lines.

In these three cell types, we intended to induce SSI by eliciting AP trains with 2 ms long somatic current injection (10 AP trains, 20 s inter-train interval; 50 APs/train at 100 Hz). Trains of APs elicited long-lasting SSI in PCs (Figure 14A, D, G; ΔV_m : -4.1 ± 1.5 mV) and in RSNPCs (Figure 14B, E, H; ΔV_m : -5.6 ± 1.1 mV), but not in FSs (Figure 14C, F, I; ΔV_m : -0.7 ± 0.5 mV). It was shown before that in whole-cell recordings only subsets of cell respond to the SSI-inducing stimulus: In hippocampal CA3 PC 50-60% showed a long-lasting hyperpolarization (Table 3; Stempel et al., 2016); 78% of layer 5 LTS-Interneurons (Marinelli et al., 2008) and 26-30% of layer 2/3 PC (Marinelli et al., 2009). We considered a cell as responding if ΔV_m after SSI induction was larger than three times the standard deviations of the baseline membrane potential. Accordingly, 73 % (8/11) of PCs and 71% (15/21) of RSNPCs exhibited a significant hyperpolarization after AP trains, whereas none of the FS were responding. Here, both responding and non-responding cells were included in averaged values and statistics (Figure 14). Taking into account only responding cells, PCs hyperpolarize by -6.0 ± 1.6 mV (data not shown) and RSNPCs by -7.6 ± 1.0 mV (Figure 15).

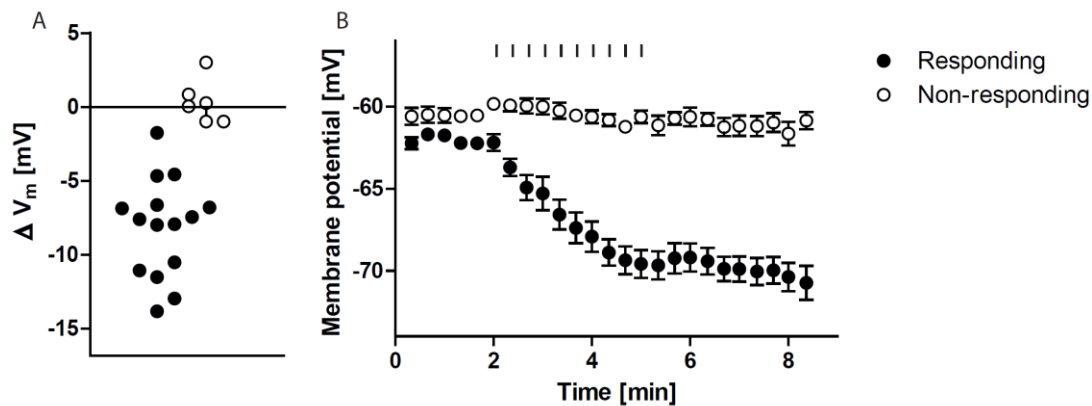


Figure 15: Responding and non-responding RSNPCs to SSI inducing AP trains.

Trains of AP induced a long-lasting hyperpolarization in the majority of RSNPCs while a subset of cells maintained a constant membrane potential. **A:** Amplitude of hyperpolarization after AP trains. **B:** time course of hyperpolarization in response to AP trains (black lines) in responding (black circles, $n = 15$) and non-responding (open circles, $n = 6$) RSNPCs.

In an additional set of experiments, we analyzed multiple parameters of the APs during the cell type characterization and found that they were both stable and of comparable magnitude in responding and non-responding cells (Figure 16). A notable difference was only observed in the AP half-width in RSNPCs (measured at 50% of maximum amplitude), which was shorter in cells that did not respond with SSI to the induction-trains (Figure 16H; responding: 1.8 ± 0.1 ms vs. non-responding: 1.3 ± 0.1 ms; $p = 0.0012$). In PCs the AP half-width also showed a tendency to shorter values in non-responding cells, but the difference to cells with SSI was not significant (Figure 16 D; responding: 1.2 ± 0.1 ms, vs. non-responding: 1.1 ± 0.1 ms; $p = 0.26$ n.s.).

Additionally, we analyzed the properties of the induction trains in the different cell types as well as in responding and non-responding cells. In each case there were no failures of APs nor substantial declines in AP amplitude or alterations in AP time course during the train (Figure 17).

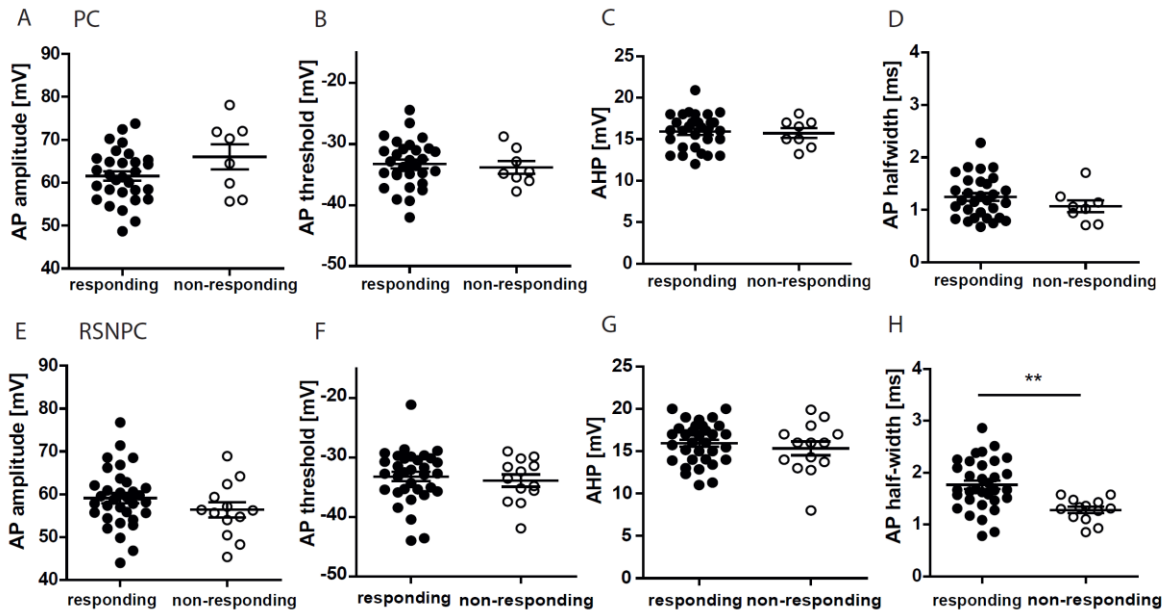


Figure 16: AP properties of responding and non-responding PCs and RSNPCs.

Several active properties were analyzed in PCs (responding: $n = 30$; non-responding: $n = 8$) and RSNPCs (responding: $n = 33$; non-responding: $n = 13$) during cell characterization (1 s depolarization step). **H:** Responding RSNPCs showed higher AP half-width compared to non-responding cells ($p = 0.0012$, Student's t-test). All other parameters analyzed did not show any significant differences between responding and non-responding cells.

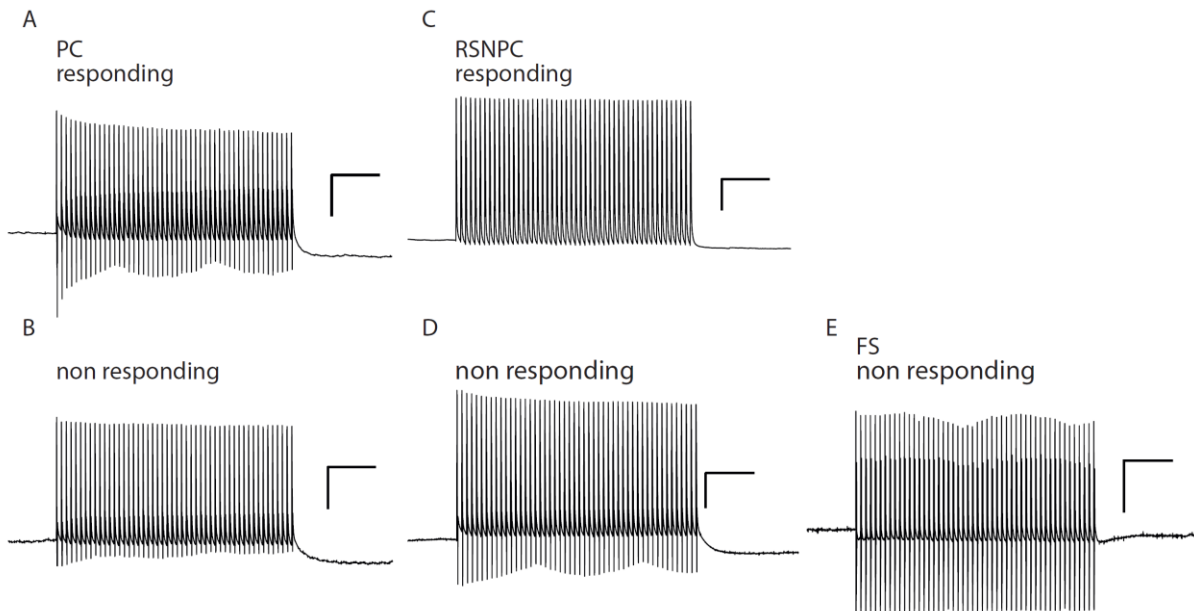


Figure 17: AP trains for SSI induction in responding and non-responding cells of different cell types.

Induction trains (50 APs, 100 Hz) show stable responses with no failures or substantial declines in AP amplitude throughout the trains. Scale bars: 0.1 / 20 mVs.

An additional group of cells showed different firing patterns during characterization (Figure 18A), distinct from RSNPCs, PCs and FSs. These firing patterns were similar to those reported for somatostatin-expressing interneurons (Jiang et al., 2015). Characterization of somatostatin interneurons in a somatostatin-Cre/Ai9 reporter mouse line (Madisen et al., 2010; Taniguchi et al., 2011) supported the assumption that these cells represent somatostatin-expressing interneurons (Figure 18B). In WT animals, trains of APs did not elicit SSI in these putative somatostatin interneurons (Figure 18C, D).

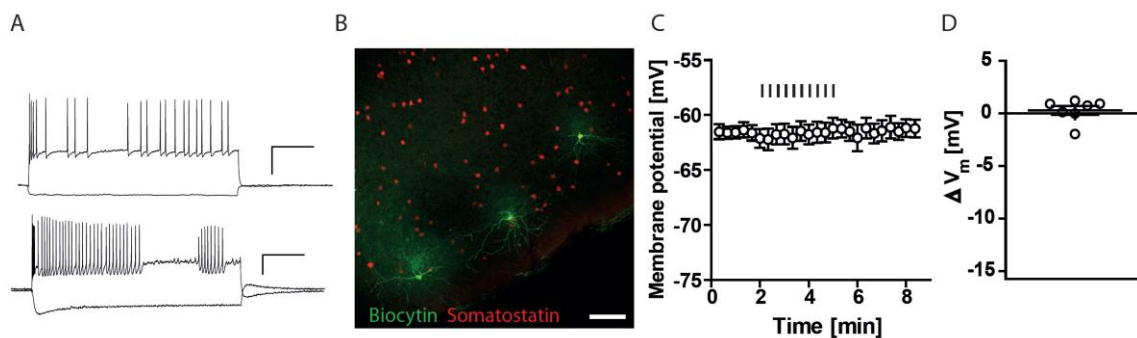


Figure 18: Putative somatostatin-expressing cells do not express SSI.

A: Characteristic AP firing pattern of putative somatostatin-expressing interneurons in BL6/N mice. **B:** Immunohistochemical image of Ai9 x somatostatin reporter mouse: tdTomato is expressed under the somatostatin-promoter (red). Patched cells were filled with biocytin and visualized with streptavidin conjugated with Alexa 488 (green). Scale bar: 100 μ m. **C:** Average membrane potential of putative somatostatin cells in WT animals before, during and after SSI induction. **D:** Hyperpolarization amplitudes elicited by AP trains. $n = 7$.

Further, we characterized the properties of the established hyperpolarization after SSI induction in RSNPCs. After SSI-inducing AP trains, the cells remained stably hyperpolarized during the entire time of the recording (up to 40 minutes) and we did not observe a rundown of the SSI effect (Figure 19A). This persistency of the long-lasting hyperpolarization was also observed in CA3 PCs (Stempel et al., 2016), in LTS interneurons (Bacci et al., 2004) and in PCs (Marinelli et al., 2009) in the somatosensory cortex after SSI induction. In another set of experiments, we elicited two additional trains of APs after successful induction of SSI, with an interval of several minutes between those applications (Figure 19B, C). The initial first train was sufficient to maximally evoke SSI and subsequent trains did not lead to any further significant additional hyperpolarization of the cells.

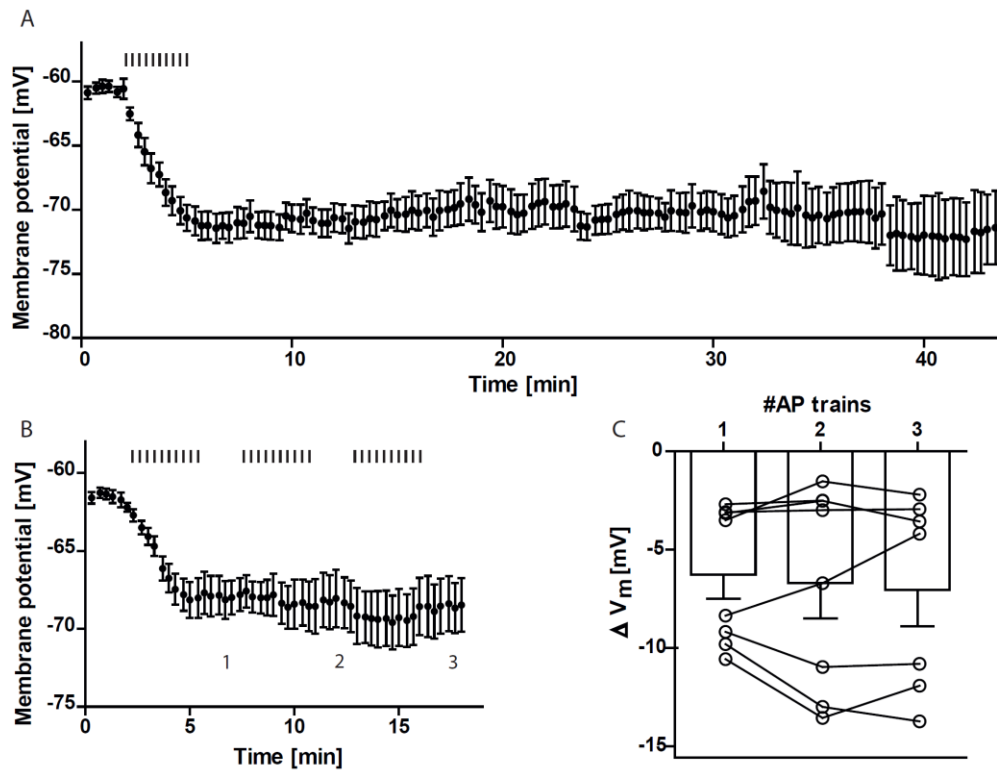


Figure 19: Characterization of SSI in RSNPCs.

A - B: Average time-course of membrane potential in RSNPCs before during and after SSI induction. Black lines depict trains of AP. **A:** One SSI-inducing AP train hyperpolarizes the cell long-lastingly for up to 40 min. 0 - 23 min: $n = 7$; 23 - 28 min: $n = 6$; 28 - 33 min: $n = 5$; 33 - 38 min: $n = 4$; 38 - 44 min: $n = 3$. **B - C:** Additional AP trains do not lead to any further hyperpolarization. **C:** Hyperpolarization amplitudes compared to baseline before first AP train. 1) $n = 8$; 2) $n = 8$; 3) $n = 7$.

3.2.2 Mechanism underlying cortical SSI in RSNPCs

We have previously shown that trains of APs induce a cell-autonomous CB_2R -dependent SSI in hippocampal PCs by activation of a Na^+ /bicarbonate cotransporter (NBC; chapter 3.1; Stempel et al., 2016). In contrast, both layer 2/3 PCs and layer 5 interneurons of the somatosensory cortex were suggested to utilize an alternative mechanism in which activation of CB_1Rs induces a GIRK channel-driven hyperpolarization (Bacci et al., 2004; Marinelli et al., 2009).

The cellular mechanisms of SSI have not been characterized before in layer 2/3 RSNPCs, despite the fact that of all cells in layer 2/3, RSNPCs show the most pronounced SSI (Figure 14). Thus, we focused on RSNPCs to further investigate the SSI mechanism: In RSNPCs, the magnitude of hyperpolarization correlated with the decrease in input resistance (Figure 20A), indicating an increase in ion channel conductance. Preincubation with an inhibitor of NBC (10 μM S0859) did not alter SSI in RSNPCs (Figure 20B, C, D; ΔV_m : -4.4 ± 0.9 mV; 11/13 responding cells).

In contrast, preincubation with a GIRK channel blocker (10 μ M SCH23390) prevented the long-lasting hyperpolarization (Figure 20B, D; control ΔV_m : -5.6 ± 1.1 mV; 15/21 responding cells; SCH23390 ΔV_m : -0.2 ± 0.3 mV; 1/11 responding cells).

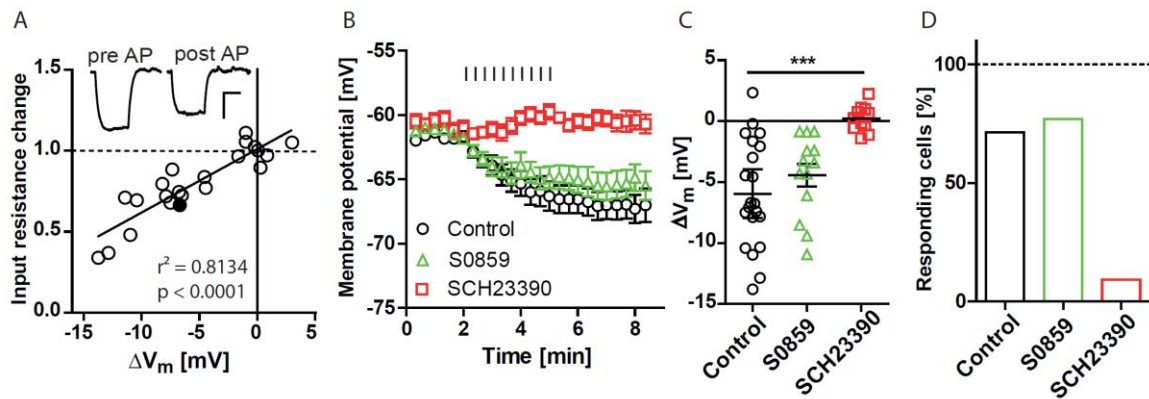


Figure 20: SSI is mediated via GIRK channels.

A: The amplitude of the hyperpolarization (ΔV_m) correlates with the reduction in input resistance (normalized to pre-AP average; $r^2 = 0.81$, $p < 0.0001$). Inset: example traces of -40 pA test pulses before and after AP trains. Scale bar: $0.2s/5$ mV; filled circle in the plot depicts recording for example traces. **B:** Preincubation with the GIRK blocker SCH23390 (10 μ M) abolished SSI whereas SSI was still intact in the presence of the NBC antagonist S0859 (10 μ M). **C:** SCH23390 reduced the average SSI magnitude (1-way-ANOVA: $p = 0.0001$; Dunnett's Multiple comparison Test: *** control vs SCH23390) and percentage of hyperpolarizing cells (**D**), while S0859 had no effect on cortical SSI. Control: $n = 21$; S0859: $n = 13$; SCH23390: $n = 11$.

Application of SCH23390 after SSI induction strongly depolarized the cells and increased input resistance (test pulse amplitude returns to baseline amplitude after SCH23390 application, Figure 21A), reversing the AP-induced effects (Figure 21A, B). In contrast, only a weak baseline depolarization occurred when SCH23390 was applied to non-stimulated RSNPCs (Figure 21C). Thus, the AP-induced hyperpolarization in RSNPCs is mediated via activation of GIRK channels and not by the NBC as in hippocampal SSI.

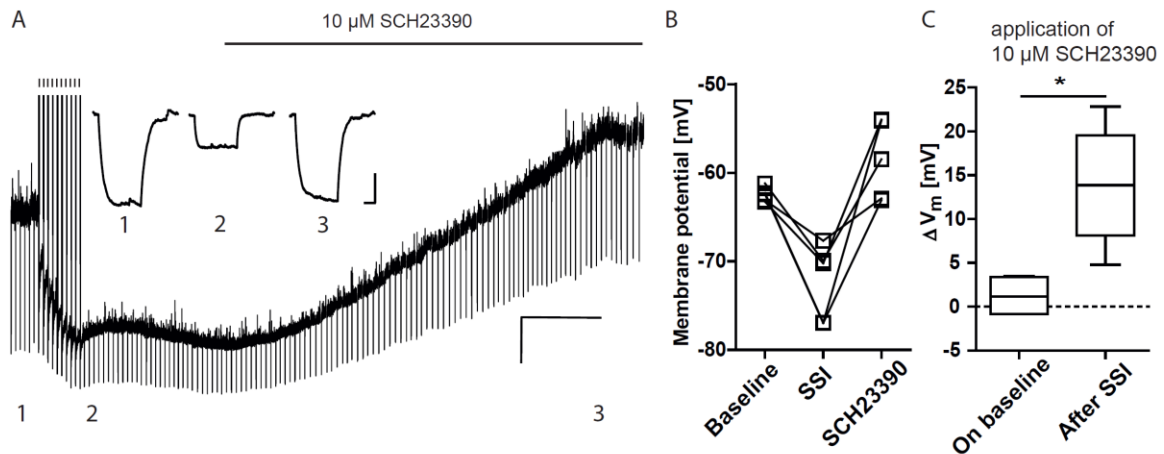


Figure 21: Application of GIRK-channel blocker reverses SSI.

A: Single cell example of the depolarization induced by SCH23390 (10 μM) after SSI induction. Black lines depict AP train, black bar represents SCH23390 application. Scale bar: 5min/ 5 mV. Inset: higher magnification of test pulses (40 pA) to determine input resistance. Membrane potentials: 1) Baseline (-61 mV); 2) SSI (-76 mV); 3) SCH23390 (-54 mV). Scale bar: 0.1 s/ 5mV **B:** Single membrane potential values before SSI induction (baseline), after AP train (SSI) and after application of SCH23390 ($n = 5$). **C:** Application of SCH23390 on non-stimulated cells (on baseline) causes only a minor depolarization compared to the effect after SSI ($p = 0.0159$, Mann-Whitney test; On baseline: $n = 4$; After SSI: $n = 5$).

3.2.3 Pharmacological investigation of the cannabinoid receptor involved in SSI of RSNPCs

SSI was previously characterized as an endocannabinoid-dependent mechanism in which either CB₁Rs (Bacci et al., 2004; Marinelli et al., 2009) or CB₂Rs (Stempel et al., 2016) induce a long-lasting hyperpolarization after periods of AP firing, via different mechanisms. In order to identify the responsible cannabinoid receptor in RSNPCs we applied specific agonists for the two receptor types. In neocortical RSNPCs, the specific CB₂R agonist HU-308 (1 μM) mimicked the AP-induced hyperpolarization, whereas application of the endocannabinoid noladin ether (300 nM), which displays selectivity for CB₁Rs over CB₂Rs (Hanus et al., 2001), did not cause a hyperpolarization (Figure 22; ΔV_m represent median (25th percentile to 75th percentile): HU-308 ΔV_m: -4.8 mV (-9.4 mV to -2.3 mV), 8/11 responding cells; NE: ΔV_m: -0.1 mV (-2.9 mV to 1.3 mV), 3/10 responding cells).

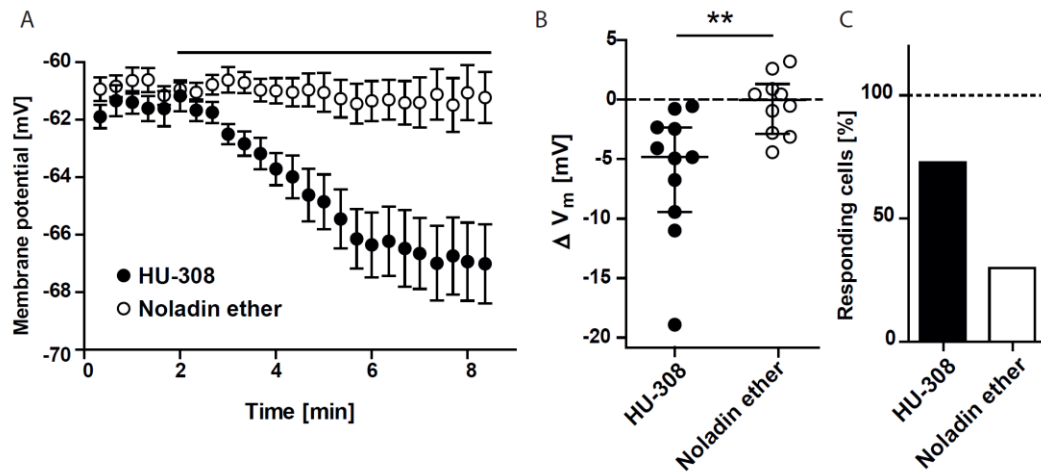


Figure 22: CB₂R specific agonist mimics long-lasting hyperpolarization.

A: Time course of average membrane potential in response to application of the specific CB₂R agonist HU-308 (1 μ M) and the endocannabinoid noladin ether (300 nM) that displays selectivity for CB₁Rs over CB₂Rs. Agonist application is indicated by the black line. **B:** Individual magnitudes of agonist-induced hyperpolarization. Noladin ether does not cause a hyperpolarization, while HU-308 mimics SSI (** $p = 0.005$, Mann-Whitney test; HU-308: $n = 10$; NE: $n = 11$); error bars represent median with interquartile range. **C:** Percentage of cells in which drug application evoked hyperpolarization.

To further substantiate the assumption of a shared CB₂R dependent mechanism in AP train and agonist-induced hyperpolarization, we performed occlusion experiments. When HU-308 was applied after successful SSI induction in RSNPCs, the agonist failed to further hyperpolarize the membrane potential (Figure 23A, D). The same effect occurred when the induction protocols were applied in the reverse order (AP trains after HU-308 application) supporting the finding that both procedures are acting via CB₂Rs to activate the same cellular mechanism (Figure 23B, E). As a control, we performed the occlusion experiment for CB₁R activation: CB₁R activation by noladin ether application (300 nM) failed to induce a long-lasting hyperpolarization and subsequent AP trains lead to SSI induction (Figure 23C, F). To conclude, activation of CB₂Rs (via AP trains or agonist application) leads to a long-lasting hyperpolarization that does not lead to an additional hyperpolarization after further stimulation with CB₂R-activating stimuli. However, if CB₁Rs are activated by noladin ether, it is still possible to elicit SSI in RSNPCs, supporting the hypothesis of an effect exclusively mediated by CB₂R.

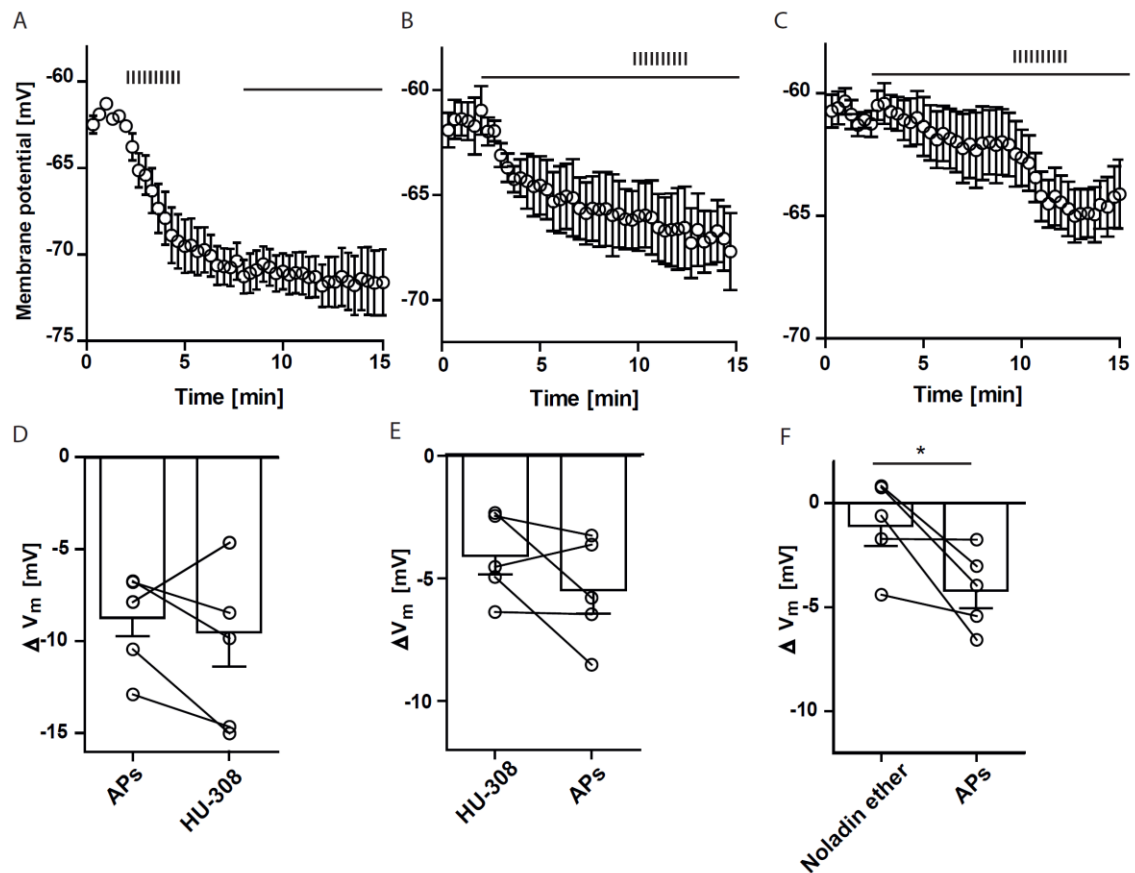


Figure 23: Occlusion of SSI induction by AP trains and cannabinoid receptor agonists.

A - C: Time course of average membrane potential. **D - F:** Individual magnitudes of hyperpolarization after agonist application or AP train. **A, D:** SSI induction by AP trains (black lines) occludes further hyperpolarization via CB₂R activation by HU-308 (1 μ M, black bar) and vice versa (**B, E**). **C, F:** CB₁R activation by noladin ether (300 nM, black bar) did not lead to a significant hyperpolarization. Subsequently, SSI could be still elicited by AP trains (black lines). **F:** Mann-Whitney-test $p = 0.0496$. APs/HU-308: $n = 5$; HU-308/APs: $n = 5$; Noladin ether/APs: $n = 5$.

After demonstrating that CB₂R activation is sufficient to induce SSI, we focused the next series of experiments on investigating whether CB₂R are also necessary for SSI induction. Preincubation with cannabinoid receptor inverse agonists SR144528 (1 μ M, CB₂R inverse agonist) or LY320135 (1 μ M, CB₁R inverse agonist) reduced the magnitude of SSI (Figure 24A, B; ΔV_m represent median (25th percentile to 75th percentile): control $\Delta V_m = -6.7$ mV (-9.2 mV to -1.0 mV); LY320135 $\Delta V_m = -2.0$ mV (-5.0 mV to 1.2 mV); SR144528: $\Delta V_m = 0.2$ mV (-1.7 mV to 1.3 mV)).

However, only the antagonization of CB₂Rs lead to a reduction in SSI occurrence, since the percentage of responding cells was comparable between LY320135 preincubated cells and control conditions (Figure 24C; control: 15/21 responding cells; SR144258: 3/15 responding cells; Ly320135: 14/19 responding cells). Although we cannot completely exclude a role of CB₁Rs in SSI induction, the pharmacological experiments suggest that CB₂Rs are mainly responsible for SSI in RSNPCs.

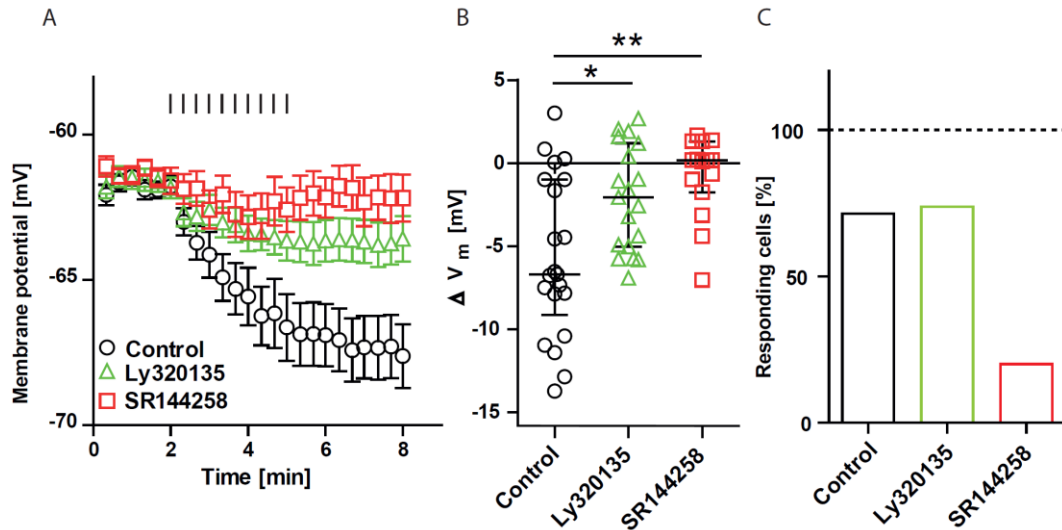


Figure 24: Inverse agonists for CB₁R and CB₂Rs reduce SSI.

A: Time course of average membrane potential before, during (Black lines) and after AP trains in presence or absence of cannabinoid receptor inverse agonists (Ly320135: CB₁R inverse agonist, 1 μ M; SR144259: CB₂R inverse agonist, 1 μ M). **B:** Individual magnitudes of AP-induced hyperpolarization in the presence of cannabinoid receptor inverse agonists. Error bars correspond to median with interquartile range. Both inverse agonists reduced the magnitude of SSI (1-way-ANOVA: ** $p = 0.005$; Dunn's Multiple Comparison Test: control vs. Ly320135 *; control vs. SR144258 **; control: $n = 21$; Ly320135 $n = 19$; SR144258: $n = 15$) but only SR144258 reduced its occurrence. **C:** Percentage of cells in which AP trains evoked hyperpolarization. Error bars represent median with interquartile range.

3.2.4 Characterization of the cannabinoid receptor responsible in cortical SSI by use of specific knockout mice

In order to verify the major role of CB₂Rs in cortical SSI, we used transgenic KO mice lacking CB₁R or CB₂R and their corresponding littermates (Buckley et al., 2000; Zimmer et al., 1999) to further corroborate the involvement of the major cannabinoid receptors in AP-induced SSI. In both CB₁R KO mice and WT littermates, trains of APs elicited a long-lasting hyperpolarization of similar magnitude in RSNPCs (Figure 25A - C; CB₁R KO: ΔV_m : -3.7 ± 0.9 mV, 12/17 responding cells; CB₁R WT: ΔV_m : -5.2 ± 1.5 mV, 7/10 responding cells).

In contrast, CB₂R-deficient mice showed a marked reduction of SSI, both in the SSI amplitude (Figure 25D, E; CB₂R KO: ΔV_m : -0.4 ± 0.6 mV; CB₂R WT: ΔV_m : -3.6 ± 0.8 mV) as well as in the number of responding cells (Figure 5F; CB₂R KO: 2/12; CB₂R WT: 9/12).

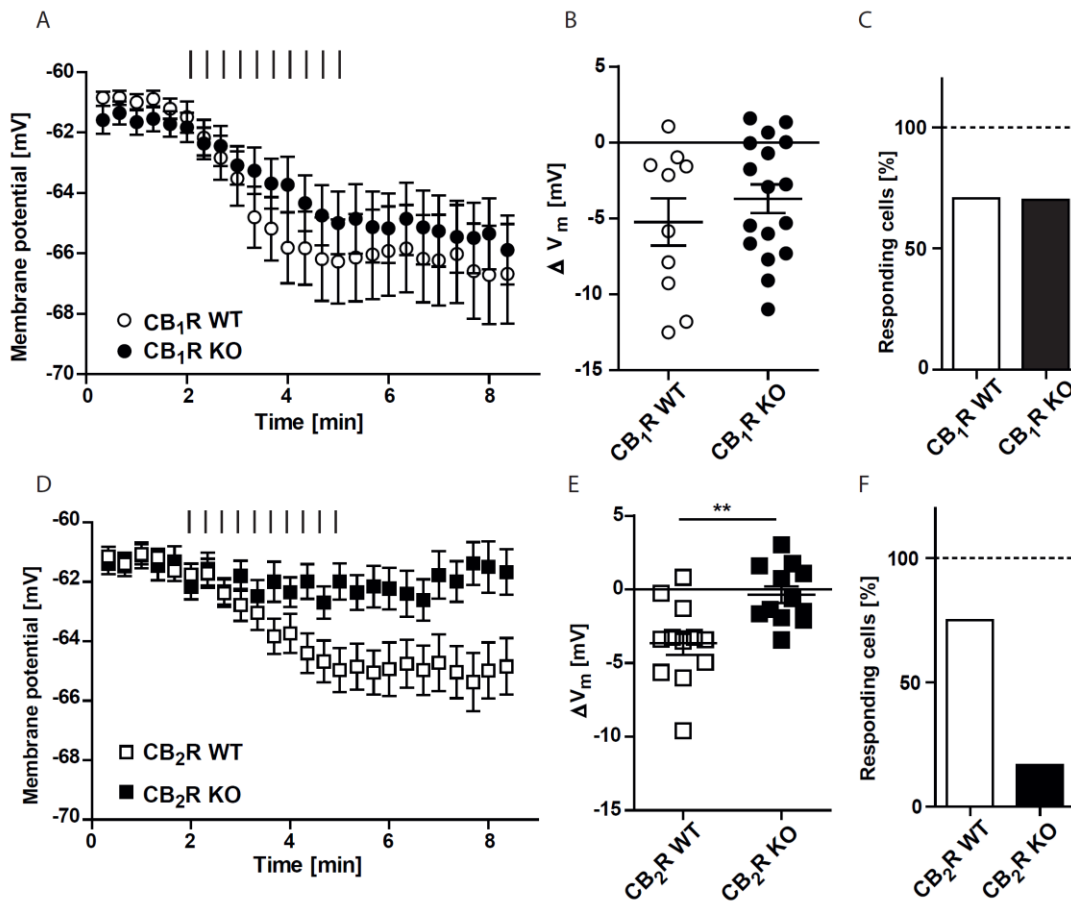


Figure 25: AP-induced hyperpolarization in RSNPCs is absent in CB₂R-deficient mice but present in CB₁R-deficient mice.

A - C: AP train-induced SSI in RSNPCs of CB₁R-deficient mice is indistinguishable from SSI in WT-littermates ($p = 0.4$ Student's t-test; CB₁R KO $n = 17$; CB₁R WT $n = 10$). **A:** Time course of the average membrane potential in WT (open circles) and CB₁R KO mice (black circles). **B:** Overview on individual magnitudes of AP-induced hyperpolarization. **C:** Percentage of cells in which AP trains evoked hyperpolarization. **D - F:** Trains of APs failed to induce SSI in CB₂R-deficient mice compared to WT-littermates (** $p = 0.003$ Student's t-test; CB₂R KO $n = 12$; CB₂R WT $n = 12$). **D:** Time course of the average membrane potential in WT (open circles) and CB₂R KO mice (black circles). **E:** Overview on individual magnitudes of AP-induced hyperpolarization. **F:** Percentage of cells in which AP trains evoked hyperpolarization. AP trains are indicated by black lines.

Corresponding phenotypes were also observed in recordings of PCs in transgenic cannabinoid receptor KO animals: in CB₁R-deficient mice and their WT littermates trains of APs induced SSI of similar magnitude (Figure 26A - C; ΔV_m represent median (25th percentile to 75th percentile): CB₁R WT: ΔV_m : -2.7 mV (-5.6 mV to -1.9 mV); 10/12 responding cells; CB₁R KO: ΔV_m : -4.3 mV (-7.2 mV to -0.1 mV), 7/12 responding cells).

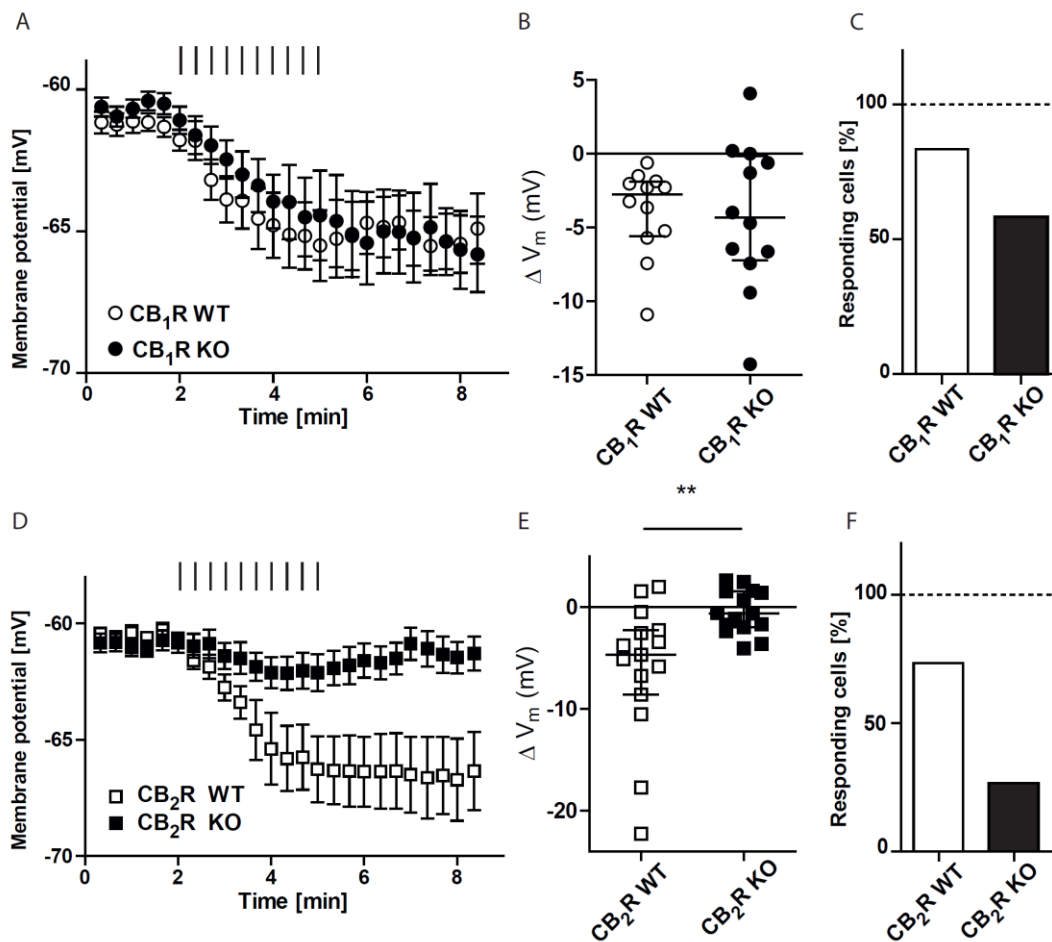


Figure 26: AP-induced hyperpolarization in PCs is absent in CB₂R-deficient mice but present in CB₁R-deficient mice.

A - C: AP train-induced SSI in RSNPCs of CB₁R-deficient mice is indistinguishable from SSI in WT-littermates ($p = 0.93$ Mann-Whitney test; CB₁R KO $n = 12$; CB₁R WT $n = 12$). **A:** Time course of the average membrane potential in WT (open circles) and CB₁R KO mice (black circles). **B:** Overview on individual magnitudes of AP-induced hyperpolarization. **C:** Percentage of cells in which AP trains evoked hyperpolarization. **D - F:** Trains of APs failed to induce SSI in CB₂R-deficient mice compared to WT-littermates (** $p = 0.004$ Mann-Whitney test; CB₂R KO $n = 15$; CB₂R WT $n = 15$). **D:** Time course of the average membrane potential in WT (open circles) and CB₂R KO mice (black circles). **E:** Overview on individual magnitudes of AP-induced hyperpolarization. **F:** Percentage of cells in which AP trains evoked hyperpolarization. AP trains are indicated by black bars. Error bars represent median with interquartile range.

In contrast, the genetic deletion of CB₂R abolishes SSI also in PCs (Figure 26 D - F; ΔV_m represent median (25th percentile to 75th percentile): CB₂R WT: ΔV_m : -4.7 mV (-8.6 mV to -2.2 mV), 11/15 responding cells; CB₂R KO: ΔV_m : -0.6 mV (-1.9 mV to 1.5 mV), 4/15 responding cells). Thus, CB₂R dependence of cortical SSI may represent a general phenomenon that is expressed in different cell types.

Finally, we tested the specificity of the CB₂R agonist HU-308 for inducing a long-lasting hyperpolarization in RSNPCs. In CB₁R-deficient mice as well as in their corresponding littermates, HU-308 application mimicked AP-induced SSI while it failed to hyperpolarize RSNPCs in CB₂R-deficient mice (Figure 27; CB₁R KO: ΔV_m : -4.9 ± 1.9 mV, 7/10 responding cells; CB₁R WT: ΔV_m : -5.5 ± 1.7 mV, 7/10 responding cells; CB₂R KO: ΔV_m : 0.5 ± 0.5 mV, 0/8 responding cells; CB₂R WT: ΔV_m : -4.1 ± 1.8 mV, 7/11 responding cells). These experiments rule out potential off-target effects of HU-308 in the induction of SSI and underline its specificity for CB₂R at a concentration of 1 μ M.

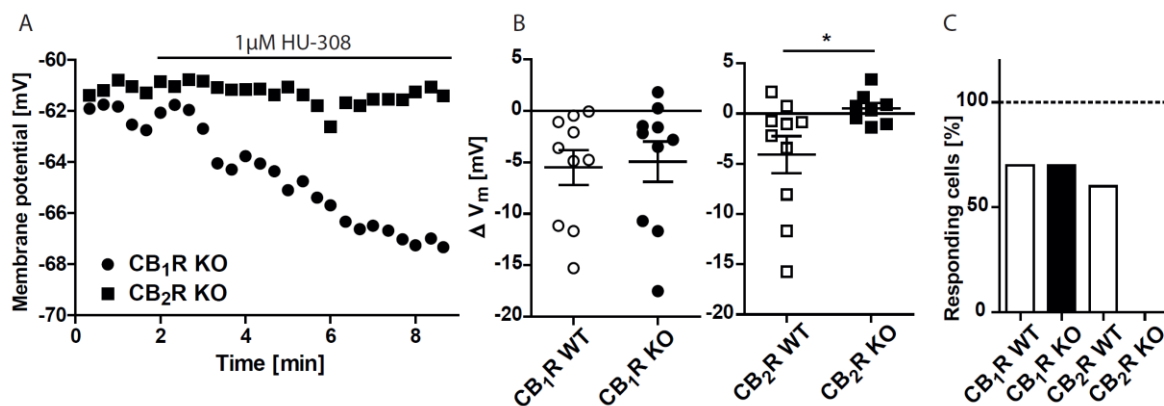


Figure 27: CB₂R agonist mimics SSI in CB₁R deficient mice but not in CB₂R KO animals.

A: Exemplary time course of the membrane potential of RSNPCs in response to HU-308 application (black line). Note the hyperpolarization in the CB₁R KO (black circles), and the lack of hyperpolarization in the CB₂R KO (black squares). **B:** Individual magnitudes of agonist-induced hyperpolarization in different genotypes. HU-308 (1 μ M) hyperpolarized RSNPCs in CB₁R deficient mice and WT-littermates of transgenic animals (CB₁R KO $n = 10$; CB₁R WT $n = 10$), but not in CB₂R-deficient mice ($p = 0.046$ Student's t -test; CB₂R KO $n = 8$; CB₂R WT $n = 10$). **C:** Percentage of cells in which agonist application evoked hyperpolarization.

3.2.5 Identity of RSNPCs

In order to further understand the physiological role of SSI, it is of major importance to know the physiological function of the cell types that express SSI. As the RSNPCs are an ill-defined group of neurons, we performed post-hoc immunohistochemical staining with different cellular markers of the recorded neurons to delimit the cellular identity of RSNPCs. The morphological properties of these cells (lack of apical dendrite) led to the suggestion that these cells are interneurons. To prove this hypothesis we stained the slices for glutamic acid decarboxylase (GAD) 67, an enzyme that catalyzes the decarboxylation of glutamate to GABA and can be used as an interneuron marker (Figure 28A). 63 cells determined as RSNPCs were stained for GAD67, of which 31 cells showed a positive staining (49%). It is not clear whether the GAD67-negative cells did not express this interneuron marker, or if it was washed out from the cytosol during the whole-cell recording. In a subset of RSNPCs that were subsequently stained for GAD67, AP trains (Figure 28C) of HU-308 applications (Table 5) was used to elicit SSI. Amplitude and incidence of SSI were indistinguishable between GAD67-positive and GAD67-negative cells (Figure 28C; Table 5) indicating a physiological homology between these groups, independent of the detectability of GAD67 expression.

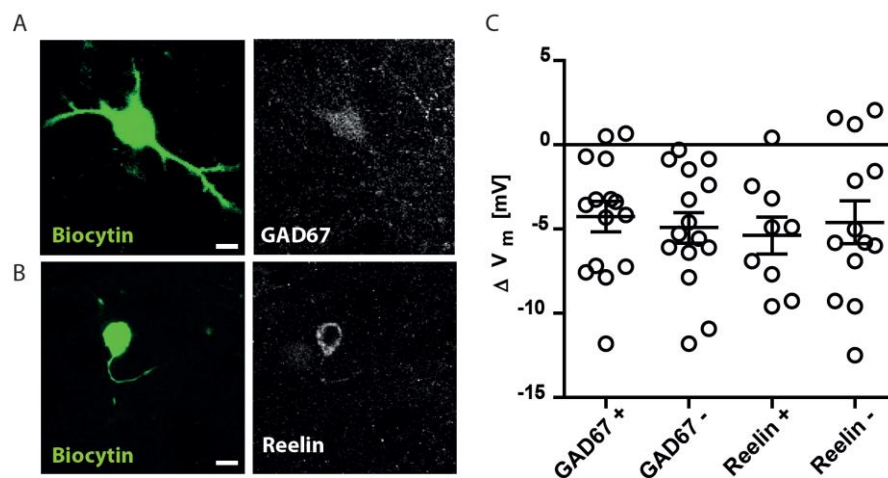


Figure 28: RSNPCs express the cellular markers GAD67 and Reelin.

A - B: Post-hoc immunohistochemical analysis of the recorded cells (green: Biocytin) identified as RSNPCs revealed that a subset of these cells express the cellular markers GAD67 (**A**) and Reelin (**B**). Scale bar: 20 μm . **C:** Trains of APs induced SSI to a similar extend in RSNPCs that were positive (+) or negative (-) for the respective markers. GAD67 +: $n = 15$; GAD67 -: $n = 15$; Reelin +: $n = 9$; Reelin -: $n = 13$.

Cortical interneurons can be divided in three major groups: parvalbumin, somatostatin and serotonin receptor type 3A (5HT_{3A})-expressing interneurons (Rudy et al., 2011). We have found that FSs (putative parvalbumin-expressing) and putative somatostatin-expressing interneurons show a different firing pattern compared to RSNPCs, indicating that the latter cell type is rather part of the 5HT_{3A} subgroup of interneurons. This group can be subdivided in vasoactive intestinal peptide (VIP)-expressing and non-VIP-expressing interneurons, while 80% of the latter group express the cellular marker Reelin (Rudy et al., 2011). 57 cells that were distinguished as RSNPCs were stained for Reelin (Figure 28B) and 18 cells showed a positive staining (31%). In 22 RSNPCs that were subsequently stained for Reelin, AP trains were applied to elicit SSI and both groups showed pronounced SSI expression (Figure 28C; Table 5).

In conclusion, we show that at least a subset of RSNPCs express GAD67 or Reelin indicating that RSNPCs are putatively part of the 5HT_{3A}-expressing subgroup of interneurons.

Table 5: Parameters of SSI in RSNPCs that were post-hoc immunohistochemically stained for cell markers.

	Nr. of experiments	Average ΔV_m (mV)	Responding cells
GAD67-positive (APs)	15	-4.3 ± 0.9	11/15
GAD67-negative (APs)	15	-4.9 ± 0.9	11/15
Reelin-positive (APs)	9	-5.4 ± 1.1	8/9
Reelin-negative (APs)	13	-4.6 ± 1.3	9/13
GAD67-positive (HU-308)	4	-6.1 ± 3.0	3/4
GAD67-negative (HU-308)	5	-4.0 ± 1.7	3/5

SSI induction protocol is indicated in brackets; Average ΔV_m values are given as mean ± SEM including responding and non-responding cells

4. Discussion

4.1 Hippocampal SSI

4.1.1 Mechanism of hippocampal SSI

Upon the discovery of SSI in the hippocampus, it was shown that the long-lasting hyperpolarization was not accompanied with a change in input resistance (Stempel et al., 2016) arguing against the involvement of a conductance-based mechanism like gating of ion channels. Thus, we considered ion pumps or transporters to mediate the hyperpolarization since pump or transporter activation can lead to hyperpolarization without affecting the membrane conductance. To identify the underlying mechanisms, we performed experiments in which we altered different components involved in the energy metabolism of the cell; however, we were still able to elicit the long-lasting hyperpolarization suggesting the involvement of an ATP-independent ion transporter (Figure 9A). By systematically substituting several ions from the intra- and extracellular solution we identified Na^+ as necessary ion for SSI induction (Figure 9B, C). It was previously shown that cannabinoid receptors can modulate the activity of the Na^+/H^+ exchanger (Bouaboula et al., 1999), thus we pharmacologically blocked several transporters to determine their involvement in hippocampal SSI (Figure 9E, F). Finally, we could identify a specific antagonist of the electrogenic Na^+ /bicarbonate cotransporter (NBC) that blocked both AP- and agonist-induced long-lasting hyperpolarization (Figure 10), suggesting the NBC as downstream target of CB_2Rs in hippocampal PCs.

However, the molecular transduction pathway underlying CB_2R -mediated activation of the NBC is not clear. An IP_3 receptor-binding protein (IRBIT) was shown to specifically bind and activate NBC (Shirakabe et al., 2006). At low IP_3 concentrations IRBIT binds to IP_3 receptors at the ER, inhibiting their action and acting as a gatekeeper (Ando et al., 2003). It was demonstrated that NBC activity is stimulated by PIP_2 and IP_3 (Thornell and Bevensee, 2015; Thornell et al., 2012). Thus, increased IP_3 production via PLC activation leads to its binding to IP_3 -receptors releasing IRBIT and inducing Ca^{2+} efflux from the ER. Cannabinoids can elicit intracellular Ca^{2+} transients via activation of CB_1Rs (Sugiura et al., 1997) or CB_2Rs (Zoratti et al., 2003) by increasing PLC activity (Hillard and Auchampach, 1994) in a $\text{G}\alpha_{i/o}$ -dependent manner (Lograno and Romano, 2004). A speculative transduction mechanism could be therefore that upon CB_2R activation, $\text{G}\alpha_{i/o}$ or the $\text{G}\alpha_q$ activate PLC, which metabolizes PIP_2 to DAG and IP_3 . Subsequently, IP_3 binds to ER-bound IP_3 receptors and releases IRBIT, which then binds to and activates NBC (Figure 29).

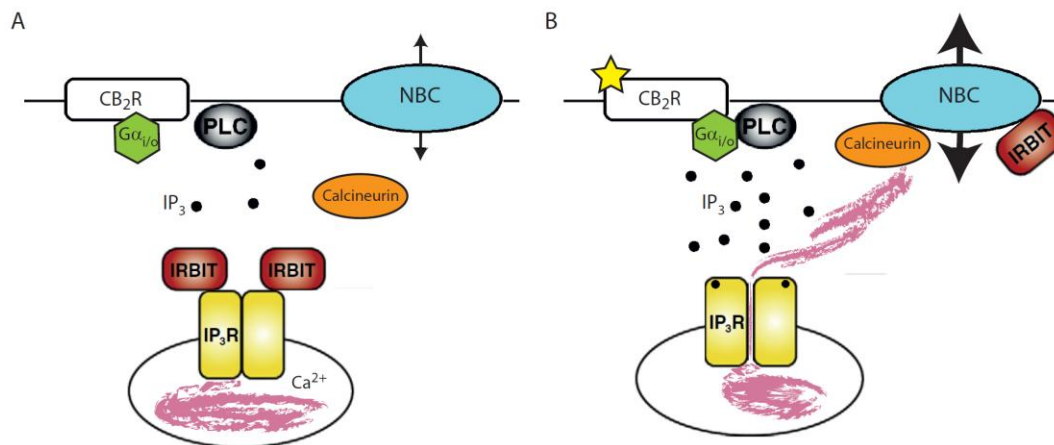


Figure 29: Possible model for NBC activation downstream of agonist binding to CB₂R.

A: Resting state. **B:** Agonist binding to CB₂R increases PLC activity and intracellular IP₃ concentration via Gα_{i/o}. IP₃ binds to IP₃R and releases IRBIT that in turn binds to NBC and enhances its activity. Further, IP₃R opening leads to Ca²⁺ influx from the ER, activating calcineurin that stimulates NBC activity. Modified from Ando and Mikoshiba 2014.

In addition, we performed a series of experiments with intracellular application of the Ca²⁺ chelator BAPTA and saw that not only the AP-induced SSI was abolished, but also agonist-induced long-lasting hyperpolarization was prevented (Figure 11). This hints towards a Ca²⁺-dependent mechanism downstream of CB₂R activation mediating activation of the NBC. Although, it is not clear how CB₂R activation and Ca²⁺ signaling might be connected in this process, it is possible that the Ca²⁺ influx from intracellular stores via IP₃Rs might be crucial for either direct activation of NBCs or for exocytosis of additional NBCs to increase surface expression (Ando et al., 2014). Calcineurin, a Ca²⁺-dependent protein phosphatase, was shown to interact with NBCs to stimulate its activity upon raise in intracellular Ca²⁺ (Danielsen et al. 2013). This stimulation was inhibited by BAPTA supporting our finding of Ca²⁺ dependency for NBC activation (Danielsen et al. 2013). In addition, PLC activity was shown to be regulated by both, intracellular Ca²⁺ concentration as well as GPCR-activation. Thus, the hypothesized coupling mechanism of CB₂Rs with NBC, might be regulated by intracellular Ca²⁺ and PLC could act as a coincidence-detector for CB₂R activation and neuronal activity. Future studies have to address the molecular transduction pathway of SSI downstream of CB₂R activation in more detail. Ca²⁺ imaging experiments could help to understand the role of alteration in intracellular Ca²⁺ concentration after CB₂R activation and could show whether certain cell organelles such as the ER or mitochondria take part in this process.

Activation of NBC changes intra- and extracellular pH values that can alter neuronal activity. Generally, increase in extracellular pH stimulates neuronal activity, while reduced pH decreases it

(Sinning and Hübner, 2013). This arises from the pH-sensitivity of several metabolic enzymes and ion channels. Neuronal activity is thought to cause a transient extracellular alkalosis, thus excessive neuronal firing leads to an initial extracellular alkalization followed by a more prolonged acidification. Electrogenic NBCs are expressed in CA3 PCs, are upregulated during extracellular acidosis (Oehlke et al., 2013) and couple changes in pH with neuronal activity (Majumdar et al., 2008). Vice versa, activation of NBCs may affect neuronal excitability by influencing local pH (Chesler, 2003). Intracellular pH of neurons was shown to be linked to depolarizing stimuli: Ca^{2+} entry leads to a fall in intracellular pH due to $\text{Ca}^{2+}/\text{H}^+$ exchange by Ca^{2+} -ATPases located in the plasmamembrane and ER (SERCA; Chesler, 2003). In response to low cytosolic pH, neurons can either actively extrude H^+ from the cytosol or import bicarbonate into the cells via NBC, a mechanism termed depolarization-induced alkalization (DIA). This effect is present in astrocytes and in hippocampal neurons (Svichar et al., 2011) and is thought to represent a mechanism to preempt a large, prolonged, Ca^{2+} -dependent acidosis. However, it is not clear by which mechanism NBCs get activated in DIA.

In hippocampal PCs, it is unclear whether the Na^+ transport or the pH change is the more important component for the hyperpolarization and establishment of SSI. The Na^+ gradient might act as the energy source for the transport of bicarbonate resulting in deacidification of the intracellular space. Despite having different time-courses, the induction protocols for both SSI and DIA share several characteristics including membrane depolarization and Ca^{2+} -dependency (Figure 11; Svichar et al., 2011), speculatively suggesting similar mechanisms involved. Thus, activation of NBC during SSI not only hyperpolarizes the cell, but may also lead to deacidification of the cell and a decrease in extracellular pH. Since these effects converge to decrease neuronal activity, it is conceivable that hippocampal SSI may represent a cell-protective effect to prevent cell damage due to over-excitability. In addition, it is possible that cell-autonomous CB_2R activation might represent the cellular mechanism for DIA in which excessive Ca^{2+} influx leads to activation of NBCs. Future studies have to analyze if SSI induction alters the extra- and intracellular pH, whether SSI may be occluded by acute manipulation of the pH of the extracellular solution and by which terms SSI and DIA are mechanistically connected.

In summary, excessive activity in hippocampal PCs leads to a strong Ca^{2+} influx into the cell that stimulates 2-AG production. 2-AG activates cell-autonomously CB_2Rs , resulting in SSI. On a speculative note, simultaneous CB_2R activation and prolonged elevated Ca^{2+} may stimulate PLC, which activates NBC in an IP_3 - and IRBIT-dependent manner (Figure 29). For the neuronal physiology, this might represent a protective mechanism that reduces excitability by hyperpolarization and prevents damages by Ca^{2+} -induced acidosis via DIA.

4.1.2 Cell type-specific expression of SSI

We demonstrated that brief trains of APs induce SSI in hippocampal CA3 and CA2 PCs, but not in CA1 PCs, dentate gyrus granule cells (Stempel et al., 2016), nor OLM cells (Figure 12). Surprisingly, direct activation of CB₂Rs by the specific inverse agonist HU-308 induced a long-lasting hyperpolarization in a similar occurrence and amplitude in CA1 PCs as in CA3 PCs. This effect was abolished with NMDG-ACSF as well as in presence of the NBC blocker S0859. Thus, CA1 PCs seem to express functional CB₂Rs that are probably coupled through the same molecular mechanism to NBC. Further evidences for the expression of functional CB₂R in CA1 PCs exists: CB₂R mRNA was detected in CA1 PCs (Stempel et al., 2016) and deletion of CB₂Rs was shown to reduce synaptic transmission and LTP in CA1 (Li and Kim, 2016). Further, cell type-specific deletion or overexpression of CB₂Rs in CA1 PCs enhanced spatial working memory or reduced anxiety levels, respectively (Li and Kim, 2017). Several studies demonstrated that CA1 PCs are capable to produce and release endocannabinoids in different physiological conditions including DSI (Wilson and Nicoll, 2001), DSE (Ohno-Shosaku et al., 2002b) and LTD (Chaveleyre and Castillo, 2003). However, CB₂Rs on CA1 PCs could not be activated by AP trains, even with increased stimulation intensities (Stempel et al., 2016), hinting towards an induction failure of SSI. It is possible that the cellular location of endocannabinoid production and CB₂Rs are different in CA1 and CA3 PCs hindering cell-autonomous CB₂R activation in CA1 PCs under physiological conditions. The presence of SSI in CA3 PCs might highlight its relevance as a cell protective mechanism in CA3, since CA3 PCs form recurrent connections that enhance network excitation, rendering them sensitive to hyperexcitability-induced damage (Guzman et al., 2016). A recent study demonstrated in a model of pilocarpine-induced epilepsy that after *status epilepticus* the number of neurons decreased in CA3 and CA1 due to increased apoptosis, while the number of CB₂R-positive cells as well as the CB₂R expression increased (Wu and Wang, 2018), supporting the hypothesis of a neuroprotective mechanism. It is conceivable that under physiological conditions some unknown factors impede SSI induction in CA1 PCs although these cells express functional CB₂Rs (Stempel et al., 2016). Under pathological conditions, however, these unknown factors might change and SSI induction could be facilitated. Future studies investigating SSI under hyperexcitable conditions will probably elucidate the conditions for successful SSI induction in CA1 to deepen our understanding of the physiological relevance of this effect under different conditions and in different cell types.

Our data show that OLM interneurons do not express SSI and direct activation of CB₂Rs does not hyperpolarize the cells (Figure 12). It is unclear whether this cell type expresses CB₂Rs or the NBC. In general, SSI is not restricted to excitatory cells since another type of interneuron in the somatosensory cortex was shown to express SSI: Trains of APs induce a long-lasting hyperpolarization

in layer 5 LTS interneurons (Bacci et al., 2004; Marinelli et al., 2008). However, it would be interesting to study additional hippocampal interneuron cell types to determine the presence of SSI in inhibitory cells in the hippocampus. It remains unclear why only distinct cell types express SSI.

4.2 Cortical SSI

4.2.1 Responding and non-responding cells

SSI is expressed in a cell type-specific manner, and most studies find that only a fraction of cells from one cell type express SSI (Figure 14; Bacci et al., 2004; Marinelli et al., 2009; Stempel et al., 2016). In light of the existing literature and our data, it is possible to identify potential explanations for this: We showed that trains of AP induce SSI in RSNPCs and PCs in layer 2/3 of the somatosensory cortex but not in FSs (Figure 14). This cell type-specific expression of SSI was also described for layer 5 of the somatosensory cortex, where only LTS interneurons, but not FS neurons exhibited SSI (Bacci et al., 2004). It was suggested, that SSI represents a form of self-inhibition to alter intrinsic excitability of LTS neurons as an alternative mechanism to autaptic synapses that were found on FSs (Bacci et al., 2003, 2004). For excitatory cortical networks SSI might represent a self-regulatory dampening mechanism (Marinelli et al., 2009).

In cortex layer 2/3 PC Marinelli et al. were able to elicit SSI in 26% of PCs with average hyperpolarization amplitude of 4.75 mV (Marinelli et al., 2009), while in our recordings approximately 70% of the PCs were responding to the AP trains with average amplitude of 5.9 mV (Figure 13). This increased prevalence might be explained by the use of different intracellular solutions: While Marinelli et al. were using K-gluconate-based intracellular solution our solution was K-Methylsulfate-based. In our previous study we demonstrated that it was not possible to induce SSI in hippocampal PC with K-gluconate based intracellular solution (Stempel et al., 2016). This induction-failure can be explained by the Ca^{2+} buffering effects of gluconate (Woehler et al., 2014). We showed that a BAPTA-containing intracellular solution blocked both, AP-induced as well as agonist-induced long-lasting hyperpolarization in hippocampal PC (Figure 11). Thus, gluconate in the patch pipette could prevent or reduce either the Ca^{2+} -dependent production of endocannabinoids or the Ca^{2+} -dependent down-stream mechanism after CB_2R activation.

However, we also found a fraction of cells not responding to the induction stimuli (AP trains or agonist application) when recorded in whole-cell configuration, although they belonged to cell types generally capable of SSI expression (Figure 14; Figure 15; Stempel et al., 2016). The AP trains for SSI inductions were similar in amplitude and no substantial decline could be observed in responding and

non-responding cells (Figure 17). Further, we showed that responding and non-responding cells (for both RSNPCs and PCs) had similar electrophysiological properties (Figure 16). However, we noticed that the AP half width was significantly higher in responding RSNPCs compared to the non-responding cells. This trend was also observed in PCs although the difference was not statistically significant (Figure 16). The shorter AP durations could cause less Ca^{2+} to enter the cell, thus it may be insufficient to trigger endocannabinoid production. On the other hand, the percentage of responding to non-responding cells was similar when the long-lasting hyperpolarization was induced by CB_2R agonist application, arguing against an induction failure of SSI due to reduced Ca^{2+} entry. Moreover, in our previous study (Stempel et al., 2016) we showed that SSI was present in all pyramidal cells when recorded in perforated patch configuration, which renders the intracellular milieu intact. This argues in favor of non-biological, experimental factors being responsible for 'successful' SSI induction. To summarize, we think that unsuccessful SSI induction depends on the recording conditions rather than on biological differences regarding firing properties of cells.

It was previously suggested that the responsiveness of PCs to SSI induction depends on the PC subtype (Marinelli et al., 2009): Dendrites of responding cells were found more branched but less extended towards the superficial layers compared to dendrites of non-responding cells. Further, repeated AP trains decreased the amplitude of evoked IPSCs more reliably in responding cells than in non-responding cells. DSI could be evoked less frequently in non-responding cells (Marinelli et al., 2009), arguing for a biological heterogeneity of PCs regarding their cannabinoid signaling. Remarkably, RSNPCs are not able to induce DSI, despite receiving CB_1R sensitive inhibitory input, which led to the suggestion that endocannabinoid production in RSNPCs is impaired (Lemtiri-Chlieh and Levine, 2007). However, we demonstrate that RSNPCs are capable of producing sufficient endocannabinoids for successful SSI induction. In addition, we showed that under our recording conditions, it is sufficient to apply the induction protocol once (10 trains of 50 APs) to induce SSI (Figure 19A), and that SSI cannot be further potentiated (Figure 19B, C; Figure 23).

It is conceivable that the recording conditions used in Marinelli et al. (whole-cell recordings, K-gluconate intracellular solution) lead to the high occurrence of non-responding cells (Marinelli et al., 2009) due to wash-out or Ca^{2+} buffering resulting in impairment of endocannabinoid production. All this could lead to the impression of a biological heterogeneity in PCs, which could have been misinterpreted in regard to cannabinoid signaling. In order to unequivocally identify the true nature of the occurrence of SSI and other cannabinoid mediated effects in cortical PCs, future studies using perforated-patch recordings are required.

4.2.2 CB₂Rs are mediating SSI

We investigated the underlying mechanism of SSI in detail using pharmacological tools (Figure 22; Figure 23) as well as CB₁R- and CB₂R-deficient mice (Figure 25; Figure 26). We found that SSI is selectively mediated by CB₂Rs in both RSNPCs as well as PCs. This is somewhat unexpected as CB₁Rs were previously implicated in SSI of PCs in layer 2/3 of somatosensory cortex (Marinelli et al., 2009). It is conceivable that the finding of CB₁R-dependency in SSI arose due to several factors: Marinelli et al. used the CB₁R inverse agonist AM-251 in a concentration (3 μM) that also inhibits CB₂Rs (Stempel et al., 2016). Thus, the abolishment of SSI in the presence of AM-251 does not prove the involvement of CB₁Rs in this effect. Further, it was shown that SSI incidence was reduced in CB₁R KO mice (Marinelli et al., 2009). However, since only 26% of the PCs in WT mice could induce SSI, and approximately 8% of the tested PCs in the CB₁R deficient mice were still able to express SSI (Marinelli et al., 2009), the involvement of CB₂Rs cannot be excluded.

Our data show that in cortical regular spiking neurons SSI is mediated via activation of CB₂Rs. Application of the selective CB₂Rs agonist triggers a long-lasting hyperpolarization, while pharmacological activation of CB₁Rs does not change the membrane potential (Figure 22). Additional experiments showed that SSI and agonist-induced CB₂R activation occlude each other suggesting a shared intracellular transduction pathway (Figure 23). In line with this finding, preincubation with a CB₂R specific inverse agonist prevented induction of SSI. However, the CB₁R inverse agonist Ly320135 also decreased the amplitude of SSI, while the occurrence of responding cells was comparable to control conditions (Figure 24). The reported K_i values for Ly320135 at CB₂Rs determined in cell culture assays and binding studies is much higher (>10 μM; Felder et al., 1998) as the used concentration (1 μM) arguing against a direct interaction with CB₂Rs. However, it is still possible that application of this compound might affect CB₂R activity: One possible explanation is the presence of CB₁R/CB₂R heterodimers which were found to be expressed and functional in several brain regions (Callen et al., 2012; Sierra et al., 2015). Since these heterodimers show bidirectional cross-antagonism, it is conceivable that the CB₁R-selective inverse agonists might affect CB₂Rs due to direct interaction in CB₁R/CB₂R heterodimers. Despite the uncertainty of the functional relevance of these heterodimers, experimental data indicate a crosstalk between different effects mediated by both cannabinoid receptors. In addition, cells expressing both receptor types were shown to exhibit reduced biased agonism, suggesting that heterodimers reduce functional selectivity of agonists (Navarro et al., 2018).

Several recent studies have described the role of CB₂Rs in neuronal self-inhibition: In hippocampal pyramidal neurons CB₂Rs mediate SSI after trains of APs (Stempel et al., 2016). Intracellular CB₂Rs reduce firing frequency in PCs of the prefrontal cortex (den Boon et al., 2012). Furthermore,

application of CB₂R agonists hyperpolarizes dopaminergic neurons of the ventral tegmental area and inhibits spiking due to activation of M-type K⁺ channels (Ma et al., 2019; Zhang et al., 2014). Together these findings illustrate that CB₂R activation can modify excitability in several different cell types and brain regions. Our work demonstrates an additional CB₂R-mediated mechanism for cell-autonomous self-inhibition. Further determination of the inhibitory properties of CB₂R activation would help us understand whether this effect represents a brain wide phenomenon or if it is restricted to specific brain regions.

4.2.3 Mechanism of cortical SSI

CB₁R-mediated GIRK channel activation was described as the mechanism responsible for SSI in layer 2/3 PCs and layer 5 LTS interneurons (Bacci et al., 2004; Marinelli et al., 2009). In the present study, we demonstrate that hippocampal and cortical SSI show different transduction pathways. Despite sharing the foregoing CB₂R activation, hippocampal SSI is established by the activation of NBC (Figure 10) while cortical SSI is based on GIRK activation (Figure 20; Figure 21). GIRK activation by CB₂Rs most likely occurs via direct activation by the Gβγ subunit (Guo and Ikeda, 2003), while the activation of NBC is not yet worked out, but may occur in the above suggested pathway (chapter 4.1; Figure 29).

Given the variability of intracellular transduction protein expression across different classes of neurons, it is not surprising that multiple mechanisms and downstream signaling cascades are involved in a phenomenon such as SSI (Arey, 2014). Several studies have shown that CB₂Rs activation can lead to selective utilization of different transduction pathways (Atwood et al., 2012a; Dhopeswarkar and Mackie, 2016). Thus, cell type-specific variations of the intracellular signaling machinery may determine which transduction pathway is implemented after agonist binding. The recruitment of different intracellular pathways in hippocampal and cortical neurons by CB₂Rs could be explained by the presence of CB₁R/CB₂R heterodimers expressed in these cell types, leading to altered conformational properties of CB₂Rs resulting in different coupling to intracellular cascades by favoring of one G protein over another (chapter 1.2.1.3). Different expression of intracellular binding proteins was also shown to influence the conformation of GPCRs resulting in biased recruitment of intracellular pathways (DeVree et al., 2016). For example, activation of the GPCR M₃ muscarinic receptor mediates very specialized tissue-specific responses upon activation in different cell types: while it regulates membrane excitability in neurons, it mediates contraction and cell growth in smooth muscle cells (Torrecilla et al., 2007). It was shown that M₃ muscarinic receptors can be differently phosphorylated in different cell types due to expression of different protein kinases resulting in recruitment of different signaling pathways (Torrecilla et al., 2007). Thus intracellular

properties and expression profiles (location and expression levels) of CB₂Rs, their corresponding binding partners and specific protein kinases might lead to cell type-specific coupling to different transduction pathways. It is conceivable that this leads to the recruitment of Gβγ signaling in cortical neurons that directly activates GIRK channels, while hippocampal SSI is mediated via Gα_q proteins to activate NBC. The exact molecular transduction pathways still have to be identified for both cortical and hippocampal SSI in the different cell types.

The possibility of utilizing different transduction pathways upon agonist binding and the presence of biased agonism on CB₂Rs might represent a promising strategy to use CB₂Rs as therapeutic targets for several pathological conditions (chapter 1.2.3). Thus, the development of specific CB₂R agonists, which favor one beneficial intracellular pathway over another, might improve the therapeutic effects while reducing possible side effects. However, for CB₂Rs it is still unclear which intracellular pathways will elicit the most beneficial effects in which cell type and brain region to treat pathological conditions.

4.2.4 Physiological relevance

4.2.4.1 Activation pattern

In terms of the physiological relevance of the phenomenon under study, it has been shown before that SSI can be induced with more naturally spaced activity patterns than the induction patterns used in this study: physiological spike trains from *in vivo* recordings were applied in slices and induced SSI in CA3 pyramidal neurons of similar magnitude as the regular-spaced AP trains (Stempel et al., 2016). Similarly, Marinelli et al. could reliably induce SSI in cortical PCs with spike trains of lower (10-50 Hz) frequencies (Marinelli et al., 2009). In this context it is noteworthy that for somatosensory cortex layer 2/3 regular spiking pyramidal neurons, firing frequencies of up to 60 Hz have been reported (Kinnischtzke et al., 2012). Therefore, SSI can be induced by activity patterns of neurons that occur *in vivo*. In this study, we purposefully used an induction protocol of slightly higher activity levels with aiming at a robust SSI amenable to pharmacological dissection of the mechanism. However, the specific role of SSI under physiological conditions has to be addressed experimentally in more detail.

4.2.4.2 Network effects

Although all layers of the somatosensory cortex receive sensory information from the thalamus, the highest density of thalamocortical axons can be found in cortical layer 4, which is regarded as the major input layer. From layer 4, the incoming thalamocortical excitation spreads most prominently to

layer 2/3 PCs, which connect locally to neighboring L2/3 PCs as well as vertically to layer 5 cells and horizontally to different cortical columns to layers 2/3 and 5 (Feldmeyer, 2012). The main outputs of the somatosensory cortex are projections from PCs in layer 5. Excessive neuronal activity, due to strong sensory stimulation or due to pathological conditions, might induce SSI in PCs of layer 2/3 resulting in an inhibition on a cellular level preventing hyperexcitability of the cell (Figure 30). Next to the hyperpolarization, decrease of the cellular input resistance supports the inhibitory effects during SSI. Thus, on the network level, SSI induction in PCs might affect the inter- and intralaminar spread of excitation to the following cells.

Next to this classic excitatory circuitry, layer 2/3 interneurons receive inputs from excitatory cells of layer 2/3 as well as from layer 4 (Helmstaedter et al., 2008). In line with our observation, RSNPCs were described as the most common type of interneuron in layer 2/3 of the somatosensory cortex (Lemtiri-Chlieh and Levine, 2007). Cortical interneurons can be divided into three: somatostatin-, parvalbumin- and 5-HT_{3A}-expressing interneurons (Rudy et al., 2011). Due to the characteristic firing pattern (Figure 13; Table 4), the FSs recorded in this study represent most likely parvalbumin-expressing interneurons. We also showed that putative somatostatin-expressing neurons show a different firing pattern compared to RSNPCs and do not express SSI (Figure 18). Immunohistochemical analysis showed that a subset of RSNPCs expressed the interneuron marker GAD67 and cellular marker Reelin (Figure 28). Since whole-cell recordings lead to washout of cellular markers that cannot be stained after recordings (Marinelli et al., 2008), it is conceivable that the percentage of the positively stained cells do not represent the physiological distribution of the cell markers in RSNPCs.

It is likely that RSNPCs belong to the subgroup of 5HT_{3A}-expressing interneurons, which preferentially synapse onto other interneurons, preferably somatostatin-expressing interneurons (Tremblay et al., 2016). This interneuron class can be subdivided in VIP-expressing and non-VIP-expressing interneurons, while 80% of non-VIP-expressing neurons express Reelin, and are mainly but not exclusively located in layer I of the somatosensory cortex. Further, 60% of VIP-expressing interneurons are located in layer 2/3 and represent the most prominent interneurons class in this layer (Rudy et al., 2011). Since our experiments were conducted in layer 2/3, most of the recorded RSNPCs are probably 5HT_{3A}-expressing interneurons (both, VIP expressing and non-VIP-expressing).

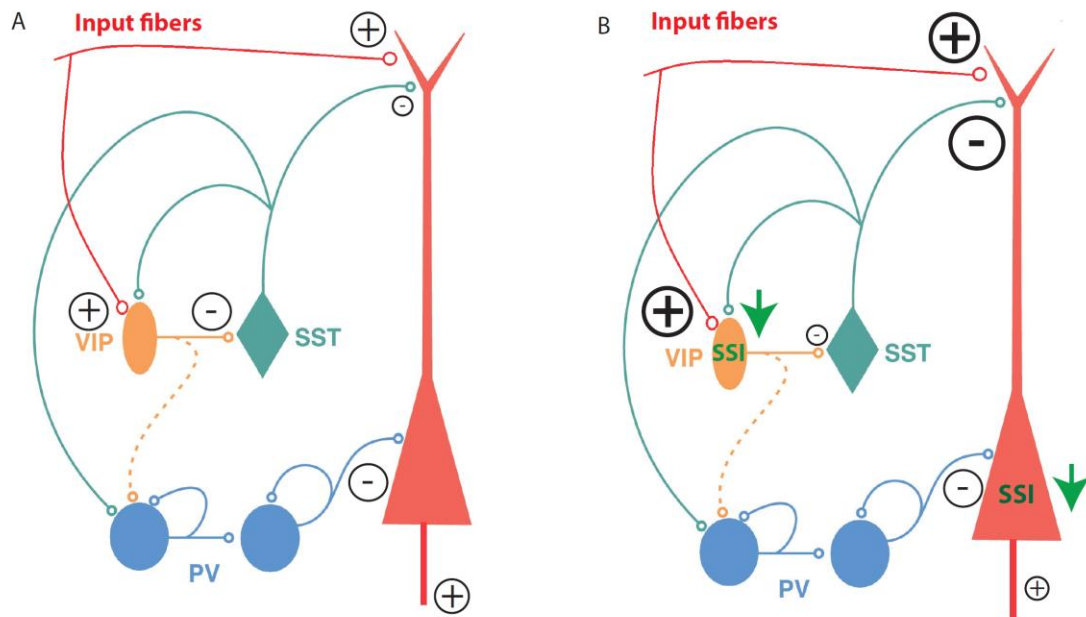


Figure 30: Simplified scheme of cortical circuit demonstrating putative role of SSI on information processing.

A: Somatostatin (SST)-expressing cells connect to dendritic regions of PCs and parvalbumin (PV)-expressing interneurons (putative FSs). PV interneurons connect to each other and to somatic regions of PCs, while VIP interneurons (putative RSNPCs) connect most prominently to SST interneurons. (+): excitatory connection; (-): inhibitory connection **B:** Excessive excitatory input (red fibers; depicted by increased (+) sign) induces SSI in VIP and in PCs leading to their inhibition (decreased excitability depicted by green arrow). Inhibition of VIP neurons renders disinhibition of SST-interneurons supporting the inhibition of PCs. Together SSI in both cell types might reduce or even shunt information transmission from the PC to following structures. Modified from Deleuze et al., 2014.

In vitro analysis of the interaction scheme of the three main interneuron populations and principal cells in the visual cortex revealed that VIP-expressing interneurons establish fewer synaptic contacts to PCs with low synaptic strength compared to the other interneuron types. However, VIP-expressing cells primarily target other interneurons: most prominently somatostatin-expressing cells (Pfeffer et al., 2013). The inhibition of somatostatin-expressing neurons by VIP was shown to be fundamental for motor integration in the somatosensory cortex (Lee et al., 2013) as well as for information processing in the medial prefrontal cortex and the auditory cortex (Pi et al., 2013). The net effect of VIP-positive neuron recruitment is a disinhibition of PCs, resulting in increased firing of principal neurons (Pi et al., 2013). Conversely, it is likely that inhibition of VIP-positive neurons by SSI leads to decrease in PC firing. Excessive excitatory signaling may converge onto layer 2/3 RSNPCs, eliciting SSI resulting in a disinhibition of other interneurons, effectively adding to the excitation protection of

PCs (Figure 30B). Additionally, if the input fibers target also somatostatin- and parvalbumin-expressing interneurons (Isaacson and Scanziani, 2011), elevated excitatory input would increase feedforward inhibition and support the inhibition of PCs induced by SSI in RSNPCs and PCs. Since parvalbumin-expressing interneurons and putative somatostatin-expressing interneurons do not express SSI (Figure 13; Figure 18) this feedforward inhibition would not be attenuated by this cell-intrinsic mechanism.

The long-term stability of SSI after induction (Figure 19A) is a further indication that it might occur in specific events when excessive activity must be prevented for a longer period of time. The finding that SSI cannot be repetitively induced (Figure 19B, D) supports its association as an intrinsic safety-switch to prevent cellular damage arising from excitotoxicity.

In summary, the presence of SSI in both, RSNPCs as well as PC of layer 2/3 in the somatosensory cortex might present an activity-dependent safety mechanism preventing the spread of over-excitability to adjacent brain regions by reducing both cellular and network excitability. By inducing SSI, PCs hyperpolarize which renders the cell less excitable and prevents the propagation of excitation. SSI in RSNPCs might support the inhibition of PCs by disinhibition of interneurons that target PCs (Figure 30). Further experiments should be performed in which whole-cell patch clamp recordings of PCs in layer 2/3 determine the effect of CB₂R agonist application on the incoming inhibitory currents: Does global CB₂R activation types lead to increased inhibition on PCs? In addition, extracellular stimulation of excitatory inputs on PCs should be performed to determine if CB₂R activation reduces spike probability in cortical PCs, giving insight in the role of SSI in information transmission for the network.

It was hypothesized that LTS-interneurons of layer 5 might express SSI to control the flow of sensory information to the PC in layer 5, since LTS neurons target the dendrites of the latter. Thus, induction of SSI in LTS interneurons would result in disinhibition of layer 5 PCs to increase excitation (Bacci et al., 2004), in contrast to decreased excitation in layer 2/3 PCs showed in this study.

Neuronal CB₂Rs modulate oscillatory activity – more specific theta-gamma-coupling in the hippocampal formation (Stempel et al., 2016). Interestingly, it was shown that gamma oscillations in human primary somatosensory cortex reflect pain perception (Gross et al., 2007; Zhang et al., 2012) and sensory gating (Cheng et al., 2016). The primary somatosensory cortex is seen “as a site for integration of input from different afferent sources leading to perceptual recognition of the presence, location, intensity, submodality and quality of touch and pain” (Vierck et al., 2013). It was shown in an animal model for central pain syndrome that neurons in the somatosensory cortex exhibited higher spontaneous activity as well increased responses evoked by innocuous and noxious

stimuli (Quiton et al., 2010). Given the fact that SSI is more prominent in occurrence as well as in amplitude in PC in somatosensory cortex compared to CA3, it is conceivable that activation of CB₂Rs might also modulate oscillatory activity in this brain area. In addition, the expression of SSI in both, PCs as well as in RSNPCs might suggest an even stronger significance for network modulation. Thus, activation of CB₂Rs might possibly be a way to decrease cortical excitation having beneficial effects on pain sensation in central pain syndrome.

In conclusion, it is important for future research to identify the precise cellular identity of RSNPCs by using specific interneuron reporter lines (Reelin-Cre x Ai9, VIP-Cre x Ai9 or 5HT_{3A}-BAC-GFP) as well as more detailed immunohistochemical stainings to understand the role of SSI in the specific cell types. Further, it will be interesting to see the effects of SSI on the network level: How does CB₂R activation affect the transmission and processing of the information in layer 2/3? Do the network effects induced by SSI differ between layer 2/3 and layer 5 of the somatosensory cortex? Are neuronal oscillations such as up-down states affected?

4.3 Neuroprotective role of CB₂Rs

Due to the low CB₂R expression levels in neuronal cells under physiological conditions, it has been a challenging task to study CNS effects of CB₂Rs. Unspecific CB₁R-pharmacology (Stempel et al., 2016) and CB₂R antibodies of insufficient specificity (Cecyre et al., 2014; Marchalant et al., 2014; Zhang et al., 2019) have previously impeded a convincing discrimination between CB₁R- and CB₂R-mediated effects in the CNS. However, in recent years, evidence accumulated suggesting that both CB₁- and CB₂Rs serve divergent physiological effects. Stempel et al. and Chen et al. proposed that CB₁Rs seem to be mainly involved in modulation of synaptic functions while CB₂R activation results in postsynaptic inhibition (Chen et al., 2017; Stempel et al., 2016). A plethora of studies showed the involvement of microglial and neuronal CB₂Rs in various pathological conditions (chapter 1.2.3). For example, manipulation of CB₂R expression in CA1 PC or microglia was shown to induce distinct behavioral phenotypes in mice: while microglial CB₂Rs were involved in contextual fear memory, overexpression or disruption of CB₂Rs in PC lowered anxiety levels or enhanced spatial working memory, respectively (Li and Kim, 2017). Moreover, constitutive deletion of CB₂Rs induces a schizophrenic phenotype in mice (Ortega-Alvaro et al., 2011), increases aggressive behavior (Rodriguez-Arias et al., 2015) and modulates drug-seeking behavior for ethanol (Ortega-Alvaro et al., 2015) and nicotine (Navarrete et al., 2013). CB₂R expression was also increased after *status epilepticus* in hippocampal regions assumingly as a protection against neuronal loss (Wu and Wang, 2018).

In line with the protective role assigned to CB₂R signaling (Pacher and Mechoulam, 2011), the CB₂R mediated self-inhibition described here may represent a cell-autonomous feedback loop preventing neurons from damage due to excessive excitability. SSI-induced hyperpolarization is indiscriminately observed in different types of regular spiking cells (cortical PCs, RSNPCs, CA3 PCs). In contrast, FSs do not show this phenomenon, which argues in favor of a protective role against intolerable amounts of excitation. It is well-known that different cell types show different properties in Ca²⁺ buffering (Matthews and Dietrich, 2015). Thus it is conceivable that some cell types are more sensitive to excessive intracellular Ca²⁺ increase due to the absence of fast and effective buffering mechanisms. Depending on the excitatory inputs under physiological conditions, some cell types may require mechanisms to prevent over-excitability due to Ca²⁺ influx. For example, FSs express the Ca²⁺ buffer parvalbumin that is not present in regular spiking neurons, possibly rendering these cells more tolerable to excitability. In addition, we showed that SSI induction is sensitive to intracellular Ca²⁺ handling, since both BAPTA and K-gluconate based intracellular solution interfered with the induction of SSI (Figure 11; Stempel et al., 2016). One possibility is that introducing additional Ca²⁺ buffering mechanisms to the cells (intracellular BAPTA or gluconate) results in an increased Ca²⁺ tolerance of the recorded cell. Hence, the threshold for activation of a potential protection mechanism, to support the cell coping with elevated intracellular Ca²⁺ would be increased and thus SSI induction prevented. In addition, the different AP half widths in responding and non-responding RSNPCs might argue in favor of the involvement of Ca²⁺ handling for SSI induction, since larger AP half widths lead to increased Ca²⁺ entry into the cell.

Interestingly, SSI is present in both, hippocampal and cortical neurons, suggesting a general role for CB₂R-mediated self-inhibition. Trains of APs induce a long-lasting hyperpolarization in regular spiking cells in both regions (Figure 7; Figure 13). However, the underlying mechanism of SSI differs between hippocampus and the somatosensory cortex: while hippocampal SSI represents an input resistance-independent mechanism which is established via activation of NBCs (Figure 10), cortical SSI is accompanied with a change in input resistance due to GIRK activation (Figure 20). Next to the decrease in cell-excitability through hyperpolarization, both mechanisms can further support the inhibitory manner of SSI: Change of extracellular pH might suppress excessive excitation without preventing information transmission, while GIRK activation could lead to shunting of the incoming excitation and thus result in a separation of the cell from the network. On a speculative note, SSI that reduces the input resistance might be more effective as a protective mechanism: It can change the dendritic integration and can lead to the exclusion of a cortical cell from the network in episodes of excessive excitation to prevent cellular damage. On the other hand, changes in extracellular pH by NBC might serve as a modulatory mechanism to inhibit excessive excitation while remaining the

network intact. Interestingly, the amplitudes of hyperpolarization were larger in input resistance-altering SSI in cortical neurons compared to SSI in the hippocampus in which the input resistance did not change. Thus, the putative CB₂R-mediated protective system might utilize a different pathway and be less effective in hippocampal cells in order to preserve the network.

Further experimental work is necessary to directly address the question of whether SSI is linked to the neuroprotective effects described for CB₂Rs. *In vitro* experiments should be performed to test the beneficial effects of neuronal CB₂R activation for example in slice models of epilepsy and whether CB₂R activation affects epileptic seizures or increases neuronal survival rates.

Under physiological conditions, CB₂R expression is very low in the CNS. However, in pathological conditions neuronal as well as microglial CB₂R expression up-regulates quickly and profoundly proposing CB₂Rs as a disease-associated target. CB₂R expression is much higher in peripheral tissue, including immune cells and in spleen, compared to the CNS and its activation results in anti-inflammatory and anti-nociceptive effects in these organs. Thus, systemic administration of CB₂R-targeting agents would activate both, central as well as peripheral CB₂Rs. This dual activation might be beneficial in pathological conditions, since the neuroprotective properties of neuronal CB₂R activation will be supported by central and peripheral immune mechanisms (Chen et al., 2017).

Together with the lack of psychoactive effects upon CB₂R activation and other CB₁R activation-related side effects (Pertwee, 2012), these findings highlight that CB₂Rs represent an excellent target for drug-discovery research for multiple pathological conditions. The description of the crystal structure for both CB₁Rs and CB₂Rs will enable structure-guided drug discovery to develop more selective compounds specifically targeting either CB₂Rs alone or polypharmacologically both cannabinoid receptors to modulate the endocannabinoid system for therapeutic purposes. However, deeper understanding of the role of CB₂Rs under physiological and pathological conditions is crucial to utilize the cannabinoid system for therapeutic approaches.

5. References

- Adams, R., Hunt, M., Clark, J. H., 1940. Structure of Cannabidiol, a Product Isolated from the Marihuana Extract of Minnesota Wild hemp. *J Am Chem Soc* 62, 196-200.
- Ando, H., Kawai, K., Mikoshiba, K., 2014. IRBIT: a regulator of ion channels and ion transporters. *Biochim Biophys Acta* 1843, 2195-2204.
- Ando, H., Mizutani, A., Matsu-ura, T., Mikoshiba, K., 2003. IRBIT, a novel inositol 1,4,5-trisphosphate (IP3) receptor-binding protein, is released from the IP3 receptor upon IP3 binding to the receptor. *J Biol Chem* 278, 10602-10612.
- Araque, A., Castillo, P. E., Manzoni, O. J., Tonini, R., 2017. Synaptic functions of endocannabinoid signaling in health and disease. *Neuropharmacology* 124, 13-24.
- Araque, A., Parpura, V., Sanzgiri, R. P., Haydon, P. G., 1999. Tripartite synapses: glia, the unacknowledged partner. *Trends in Neurosciences* 22, 208-215.
- Arey, B. J., 2014. An Historical Introduction to Biased Signaling. *Biased Signaling in Physiology, Pharmacology and Therapeutics*, pp. 1-39.
- Atwood, B. K., Straiker, A., Mackie, K., 2012a. CB(2) cannabinoid receptors inhibit synaptic transmission when expressed in cultured autaptic neurons. *Neuropharmacology* 63, 514-523.
- Atwood, B. K., Wager-Miller, J., Haskins, C., Straiker, A., Mackie, K., 2012b. Functional selectivity in CB(2) cannabinoid receptor signaling and regulation: implications for the therapeutic potential of CB(2) ligands. *Mol Pharmacol* 81, 250-263.
- Bacci, A., Huguenard, J. R., Prince, D. A., 2003. Functional Autaptic Neurotransmission in Fast-Spiking Interneurons: A Novel Form of Feedback Inhibition in the Neocortex. *J Neurosci* 23, 859-866.
- Bacci, A., Huguenard, J. R., Prince, D. A., 2004. Long-lasting self-inhibition of neocortical interneurons mediated by endocannabinoids. *Nature* 431, 312-316.
- Bari, M., Paradisi, A., Pasquariello, N., Maccarrone, M., 2005. Cholesterol-dependent modulation of type 1 cannabinoid receptors in nerve cells. *J Neurosci Res* 81, 275-283.
- Barry, P.H., 1994. JPCalc, a software package for calculating liquid junction potential corrections in patch-clamp, intracellular, epithelial and bilayer measurements and for correcting junction potential measurements. *J Neurosci Meth* 51, 107-116.
- Basavarajappa, B. S., Shivakumar, M., Joshi, V., Subbanna, S., 2017. Endocannabinoid system in neurodegenerative disorders. *J Neurochem* 142, 624-648.
- Beierlein, M., Regehr, W. G., 2006. Local interneurons regulate synaptic strength by retrograde release of endocannabinoids. *J Neurosci* 26, 9935-9943.
- Benard, G., Massa, F., Puente, N., Lourenco, J., Bellocchio, L., Soria-Gomez, E., Matias, I., Delamarre, A., Metna-Laurent, M., Cannich, A., Hebert-Chatelain, E., Mulle, C., Ortega-Gutierrez, S., Martin-

- Fontecha, M., Klugmann, M., Guggenhuber, S., Lutz, B., Gertsch, J., Chaouloff, F., Lopez-Rodriguez, M. L., Grandes, P., Rossignol, R., Marsicano, G., 2012. Mitochondrial CB(1) receptors regulate neuronal energy metabolism. *Nat Neurosci* 15, 558-564.
- Benito, C., Nunez, E., Romero, J., 2003. Cannabinoid CB2 Receptors and Fatty Acid Amide Hydrolase Are Selectively Overexpressed in Neuritic Plaque-Associated Glia in Alzheimer's Disease Brains. *J Neurosci* 23, 11136 - 11141.
- Bilkei-Gorzo, A., Albayram, O., Draffehn, A., Michel, K., Piyanova, A., Oppenheimer, H., Dvir-Ginzberg, M., Racz, I., Ulas, T., Imbeault, S., Bab, I., Schultze, J. L., Zimmer, A., 2017. A chronic low dose of Delta(9)-tetrahydrocannabinol (THC) restores cognitive function in old mice. *Nat Med* 23, 782-787.
- Billakota, S., Devinsky, O., Marsh, E., 2019. Cannabinoid therapy in epilepsy. *Current Opinion in Neurology* 32, 220-226.
- Bisogno, T., Bobrov, M. Y., Gretskays, N. M., Bezuglov, V. V., De Petrocellis, L., Di Marzo, V., 2000. N-acyl-dopamines: novel synthetic CB1 cannabinoid-receptor ligands and inhibitors of anandamide inactivation with cannabimimetic activity in vitro and in vivo. *Biochem J* 351, 817-824.
- Blankman, J. L., Simon, G. M., Cravatt, B. F., 2007. A comprehensive profile of brain enzymes that hydrolyze the endocannabinoid 2-arachidonoylglycerol. *Chem Biol* 14, 1347-1356.
- Bock, A., Bermudez, M., 2018. A panoramic view on GPCRs: the 1st Berlin Symposium for Interdisciplinary GPCR research. *Naunyn Schmiedebergs Arch Pharmacol* 391, 769-771.
- Bouaboula, M., Bianchini, L., McKenzie, F. R., Pouyssegur, J., Casellas, P., 1999. Cannabinoid receptor CB1 activates the Na⁺/H⁺ exchanger NHE-1 isoform via Gi-mediated mitogen activated protein kinase signalingtransduction pathways. *FEBS Lett* 499, 61-65.
- Bourne, J. N., Harris, K. M., 2012. Nanoscale analysis of structural synaptic plasticity. *Curr Opin Neurobiol* 22, 372-382.
- Broyd, S. J., van Hell, H. H., Beale, C., Yucel, M., Solowij, N., 2016. Acute and Chronic Effects of Cannabinoids on Human Cognition-A Systematic Review. *Biol Psychiatry* 79, 557-567.
- Buckley, N. E., McCoy, K.L., Mezey, E., Bonner, T., Zimmer, A. M., Felder, C.C., Glass, M., Zimmer, A., 2000. Immunomodulation by cannabinoids is absent in mice deficient for the cannabinoid CB2 Receptor *Eur J Pharmacol* 396, 141 - 149.
- Busquets-Garcia, A., Puighermanal, E., Pastor, A., de la Torre, R., Maldonado, R., Ozaita, A., 2011. Differential role of anandamide and 2-arachidonoylglycerol in memory and anxiety-like responses. *Biol Psychiatry* 70, 479-486.
- Cahn, R. S., 1933. Cannabis Indica Resin. Part IV. The Synthesis of Some 2:2-Dimethyldibenzopyrans, and Confirmation of the Structure of Cannabinol. *J Chem Soc*, 1400 - 1405.
- Callen, L., Moreno, E., Barroso-Chinea, P., Moreno-Delgado, D., Cortes, A., Mallol, J., Casado, V., Lanciego, J. L., Franco, R., Lluís, C., Canela, E. I., McCormick, P. J., 2012. Cannabinoid receptors CB1 and CB2 form functional heteromers in brain. *J Biol Chem* 287, 20851-20865.

Campos, A. C., Moreira, F. A., Gomes, F. V., Del Bel, E. A., Guimaraes, F. S., 2012. Multiple mechanisms involved in the large-spectrum therapeutic potential of cannabidiol in psychiatric disorders. *Philos Trans R Soc Lond B Biol Sci* 367, 3364-3378.

Carter, E., Wang, X. J., 2007. Cannabinoid-mediated disinhibition and working memory: dynamical interplay of multiple feedback mechanisms in a continuous attractor model of prefrontal cortex. *Cereb Cortex* 17 Suppl 1, i16-26.

Caslisle, S. J., Marciano-Cabral, F., Staab, A., Ludwick, C., Cabral, G. A., 2002. Differential expression of the CB2 cannabinoid receptor by rodent macrophages and macrophage-like cells in relation to cell activation. *Internat Immunopharmacol* 2, 69-82.

Castillo, P. E., Younts, T. J., Chavez, A. E., Hashimoto, Y., 2012. Endocannabinoid signaling and synaptic function. *Neuron* 76, 70-81.

Cecyre, B., Thomas, S., Pfitzner, M., Casanova, C., Bouchard, J. F., 2014. Evaluation of the specificity of antibodies raised against cannabinoid receptor type 2 in the mouse retina. *Naunyn Schmiedeberg Arch Pharmacol* 387, 175-184.

Chakrabarti, A., Onaivi, E. S., Chaudhuri, G., 1995. Cloning and sequencing of a cDNA encoding the mouse brain-type cannabinoid receptor protein. *DNA Sequence* 5, 385-388.

Chaveleyre, V., Castillo, P. E., 2003. Heterosynaptic LTD of Hippocampal GABAergic Synapses: A Novel Role of Endocannabinoids in Regulating Excitability. *Neuron* 38, 461-472.

Chen, D. J., Gao, M., Gao, F. F., Su, Q. X., Wu, J., 2017. Brain cannabinoid receptor 2: expression, function and modulation. *Acta Pharmacol Sin* 38, 312-316.

Cheng, C. H., Chan, P. Y., Niddam, D. M., Tsai, S. Y., Hsu, S. C., Liu, C. Y., 2016. Sensory gating, inhibition control and gamma oscillations in the human somatosensory cortex. *Sci Rep* 6, 20437.

Chesler, M., 2003. Regulation and Modulation of pH in the Brain. *Physiol Rev* 83, 1183-1221.

Chevalyere, V., Heifets, B. D., Kaeser, P. S., Südhof, T. C., Castillo, P. E., 2007. Endocannabinoid-mediated long-term plasticity requires cAMP/PKA signaling and RIM1alpha. *Neuron* 54, 801-812.

Christensen, R., Kristensen, P. K., Bartels, E. M., Bliddal, H., Astrup, A., 2007. Efficacy and safety of the weight-loss drug rimonabant: a meta-analysis of randomised trials. *The Lancet* 370, 1706-1713.

Clarke, R. C., Merlin, M. D., 2017. Cannabis Domestication, Breeding History, Present-day Genetic Diversity, and Future Prospects. *Critical Reviews in Plant Sciences* 35, 293-327.

ClinicalTrials.gov [Internet]. Search for "cannabinoids" 2019 [cited 2019 March 22]. Available from <https://clinicaltrials.gov/>.

Coke, C. J., Scarlett, K. A., Chetram, M. A., Jones, K. J., Sandifer, B. J., Davis, A. S., Marcus, A. I., Hinton, C. V., 2016. Simultaneous Activation of Induced Heterodimerization between CXCR4 Chemokine Receptor and Cannabinoid Receptor 2 (CB2) Reveals a Mechanism for Regulation of Tumor Progression. *J Biol Chem* 291, 9991-10005.

Concannon, R. M., Okine, B. N., Finn, D. P., Dowd, E., 2015. Differential upregulation of the cannabinoid CB(2) receptor in neurotoxic and inflammation-driven rat models of Parkinson's disease. *Exp Neurol* 269, 133-141.

Concannon, R. M., Okine, B. N., Finn, D. P., Dowd, E., 2016. Upregulation of the cannabinoid CB2 receptor in environmental and viral inflammation-driven rat models of Parkinson's disease. *Exp Neurol* 283, 204-212.

Cui, Y., Perez, S., Venance, L., 2018. Endocannabinoid-LTP Mediated by CB1 and TRPV1 Receptors Encodes for Limited Occurrences of Coincident Activity in Neocortex. *Front Cell Neurosci* 12, 182.

Cui, Y., Prokin, I., Xu, H., Delord, B., Genet, S., Venance, L., Berry, H., 2016. Endocannabinoid dynamics gate spike-timing dependent depression and potentiation. *Elife* 5, e13185.

Danielsen, A.A., Parker, M.D., Lee, S., Boron, W.F., Aalkjaer, C., Boedtker, E., 2013. Splice cassette II of Na⁺HCO₃⁻ cotransporter NBCn1 (slc4a7) interacts with calcineurin A: implications for transporter activity and intracellular pH control during rat artery contractions. *J Biol Chem* 288, 8146-8155.

Database of Clinical Studies regarding cannabinoids [Internet]. Germany: International Association for Cannabinoid Medicines; 2019 [cited 2019 March 22]. Available from: <http://www.cannabis-med.org/studies/study.php>.

Deleuze, C., Pazienti, A., Bacci, A. 2014. Autaptic self-inhibition of cortical GABAergic neurons: synaptic narcissism or useful introspection? *Curr Opin Neurobiol* 26, 64-71.

den Boon, F. S., Chameau, P., Houthuijs, K., Bolijn, S., Mastrangelo, N., Kruse, C. G., Maccarrone, M., Wadman, W. J., Werkman, T. R., 2014. Endocannabinoids produced upon action potential firing evoke a Cl⁻ current via type-2 cannabinoid receptors in the medial prefrontal cortex. *Pflugers Arch* 466, 2257-2268.

den Boon, F. S., Chameau, P., Schaafsma-Zhao, Q., van Aken, W., Bari, M., Oddi, S., Kruse, C. G., Maccarrone, M., Wadman, W. J., Werkman, T. R., 2012. Excitability of prefrontal cortical pyramidal neurons is modulated by activation of intracellular type-2 cannabinoid receptors. *Proc Natl Acad Sci U S A* 109, 3534-3539.

Devane, W. A., Dysarz, F. A., Johnson, R., Melvin, L. S., Howlett, A. C., 1988. Determination and Characterization of a Cannabinoid Receptor in Rat Brain. *Mol Pharmacol* 34, 605-613.

Devane, W. A., Hanus, L., Breuer, A., Pertwee, R. G., Stevenson, L. A., Griffin, G., Gibson, D., Mandelbaum, A., Etinger, A., Mechoulam, R., 1992. Isolation and Structure of a Brain Constituent That Binds to a Cannabinoid Receptor. *Science* 258, 1946 - 1949.

DeVree, B. T., Mahoney, J. P., Velez-Ruiz, G. A., Rasmussen, S. G., Kuzak, A. J., Edwald, E., Fung, J. J., Manglik, A., Masureel, M., Du, Y., Matt, R. A., Pardon, E., Steyaert, J., Kobilka, B. K., Sunahara, R. K., 2016. Allosteric coupling from G protein to the agonist-binding pocket in GPCRs. *Nature* 535, 182-186.

Dhopeswarkar, A., Mackie, K., 2014. CB2 Cannabinoid Receptor as a Therapeutic Target - What Does the Future Hold? *Mol Pharmacol* 86, 430-437.

- Dhopeswarkar, A., Mackie, K., 2016. Functional Selectivity of CB2 Cannabinoid Receptor Ligands at a Canonical and Noncanonical Pathway. *J Pharmacol Exp Ther* 358, 342-351.
- Di Marzo, V., De Petrocellis, L., 2012. Why do cannabinoid receptors have more than one endogenous ligand? *Philos Trans R Soc Lond B Biol Sci* 367, 3216-3228.
- Di Marzo, V., Fontana, A., Cadas, H., Schinelli, S., Cimino, G., J.-C., S., Piomelli, D., 1994. Formation and inactivation of endogenous cannabinoid anandamide in central neurons. *Nature* 372, 686-691.
- Di Pasquale, E., Chahinian, H., Sanchez, P., Fantini, J., 2009. The insertion and transport of anandamide in synthetic lipid membranes are both cholesterol-dependent. *PLoS One* 4, e4989.
- Di, S., Boudaba, C., Popescu, I. R., Weng, F. J., Harris, C., Marcheselli, V. L., Bazan, N. G., Tasker, J. G., 2005. Activity-dependent release and actions of endocannabinoids in the rat hypothalamic supraoptic nucleus. *J Physiol* 569, 751-760.
- Di Scala, C., Fantini, J., Yahi, N., Barrantes, F. J., Chahinian, H., 2018. Anandamide Revisited: How Cholesterol and Ceramides Control Receptor-Dependent and Receptor-Independent Signal Transmission Pathways of a Lipid Neurotransmitter. *Biomolecules* 8.
- Duncan, M., Millns, P., Smart, D., Wright, J. E., Kendall, D. A., Ralevic, V., 2004. Noladin ether, a putative endocannabinoid, attenuates sensory neurotransmission in the rat isolated mesenteric arterial bed via a non-CB1/CB2 G(i/o) linked receptor. *Br J Pharmacol* 142, 509-518.
- Elphick, M. R., Egertova, M., 2001. The neurobiology and evolution of cannabinoid signalling. *Philos Trans R Soc Lond B Biol Sci* 356, 381-408.
- Fankhauser, M., 2008. Cannabis as medicine in Europe in the 19th century. A cannabis reader: global issues and local experiences. EMCDDA, Lisbon, PRT.
- Felder, C. C., Joyce, K. E., Briley, E. M., Glass, M., Mackie, K. P., Fahey, K. J., Cullinan, G. J., Hunden, D. C., Johnson, D. W., Chaney, M. O., Koppel, G. A., Brownstein, M., 1998. LY320135, a Novel Cannabinoid CB1 Receptor Antagonist, Unmasks Coupling of the CB1 Receptor to Stimulation of cAMP Accumulation. *J Pharmacol Exp Ther* 284, 291-297.
- Felder, C. C., Joyce, K. E., Briley, E. M., Mansouri, J., Mackie, K., Blond, O., Lai, Y., Ma, A. L., Mitchell, R. L., 1995. Comparison of the Pharmacology and Signal Transduction of the Human Cannabinoid CB1 and CB2 Receptors. *Mol Pharmacol* 48, 444-450.
- Feldmeyer, D., 2012. Excitatory neuronal connectivity in the barrel cortex. *Front Neuroanat* 6, 24.
- Feng, L., Zhao, T., Kim, J., 2015. neuTube 1.0: A New Design for Efficient Neuron Reconstruction Software Based on the SWC Format. *eNeuro* 2.
- Fernandez-Ruiz, J., Berrendero, F., Hernandez, M. L., Ramos, J. A., 2000. The endogenous cannabinoid system and brain development. *Trends in Neurosciences* 23, 14-20.
- Fernandez-Ruiz, J., Garcia, C., Sagredo, O., Gomez-Ruiz, M., de Lago, E., 2010. The endocannabinoid system as a target for the treatment of neuronal damage. *Expert Opin Ther Targets* 14, 387-404.

- Foldy, C., Neu, A., Jones, M. V., Soltesz, I., 2006. Presynaptic, activity-dependent modulation of cannabinoid type 1 receptor-mediated inhibition of GABA release. *J Neurosci* 26, 1465-1469.
- Forro, T., Valenti, O., Lasztocki, B., Klausberger, T., 2015. Temporal organization of GABAergic interneurons in the intermediate CA1 hippocampus during network oscillations. *Cereb Cortex* 25, 1228-1240.
- Fowler, C. J., 2013. Transport of endocannabinoids across the plasma membrane and within the cell. *FEBS J* 280, 1895-1904.
- Fraguas-Sanchez, A. I., Torres-Suarez, A. I., 2018. Medical Use of Cannabinoids. *Drugs* 78, 1665-1703.
- Fukaya, M., Uchigashima, M., Nomura, S., Hasegawa, Y., Kikuchi, H., Watanabe, M., 2008. Predominant expression of phospholipase C β 1 in telencephalic principal neurons and cerebellar interneurons, and its close association with related signaling molecules in somatodendritic neuronal elements. *Eur J Neurosci* 28, 1744-1759.
- Gantz, S. C., Bean, B. P., 2017. Cell-Autonomous Excitation of Midbrain Dopamine Neurons by Endocannabinoid-Dependent Lipid Signaling. *Neuron* 93, 1375-1387.
- Gaoni, Y., Mechoulam, R., 1964. Isolation, Structure and Partial Synthesis of an Active Constituent of Hashish. *J Am Chem Soc* 86, 1646-1647.
- Garcia-Gutierrez, M. S., Garcia-Bueno, B., Zoppi, S., Leza, J. C., Manzanares, J., 2012. Chronic blockade of cannabinoid CB2 receptors induces anxiolytic-like actions associated with alterations in GABA(A) receptors. *Br J Pharmacol* 165, 951-964.
- Garcia-Gutierrez, M. S., Manzanares, J., 2010. The cannabinoid CB1 receptor is involved in the anxiolytic, sedative and amnesic actions of benzodiazepines. *J Psychopharmacol* 24, 757-765.
- Garcia-Gutierrez, M. S., Navarrete, F., Navarro, G., Reyes-Resina, I., Franco, R., Lanciego, J. L., Giner, S., Manzanares, J., 2018. Alterations in Gene and Protein Expression of Cannabinoid CB2 and GPR55 Receptors in the Dorsolateral Prefrontal Cortex of Suicide Victims. *Neurotherapeutics* 15, 796-806.
- Garcia-Gutierrez, M. S., Ortega-Alvaro, A., Busquets-Garcia, A., Perez-Ortiz, J. M., Caltana, L., Ricatti, M. J., Brusco, A., Maldonado, R., Manzanares, J., 2013. Synaptic plasticity alterations associated with memory impairment induced by deletion of CB2 cannabinoid receptors. *Neuropharmacology* 73, 388-396.
- Gerard, C., Mollereau, C., Vassart, G., Parmentier, M., 1990. Nucleotide sequence of a human cannabinoid receptor cDNA. *Nucleic Acids Res* 18, 7142.
- Gerdeman, G. L., Ronesi, J., Lovinger, D. M., 2002. Postsynaptic endocannabinoid release is critical to long-term depression in the striatum. *Nat Neurosci* 5, 446-451.
- Gomez-Gonzalo, M., Navarrete, M., Perea, G., Covelo, A., Martin-Fernandez, M., Shigemoto, R., Lujan, R., Araque, A., 2015. Endocannabinoids Induce Lateral Long-Term Potentiation of Transmitter Release by Stimulation of Gliotransmission. *Cereb Cortex* 25, 3699-3712.
- Gong, J. P., Onaivi, E. S., Ishiguro, H., Liu, Q. R., Tagliaferro, P. A., Brusco, A., Uhl, G. R., 2006. Cannabinoid CB2 receptors: immunohistochemical localization in rat brain. *Brain Res* 1071, 10-23.

- Grabiec, U., Dehghani, F., 2017. N-Arachidonoyl Dopamine: A Novel Endocannabinoid and Endovanilloid with Widespread Physiological and Pharmacological Activities. *Cannabis Cannabinoid Res* 2, 183-196.
- Grimsey, N. L., Graham, E. S., Dragunow, M., Glass, M., 2010. Cannabinoid Receptor 1 trafficking and the role of the intracellular pool: implications for therapeutics. *Biochem Pharmacol* 80, 1050-1062.
- Gross, J., Schnitzler, A., Timmermann, L., Ploner, M., 2007. Gamma oscillations in human primary somatosensory cortex reflect pain perception. *PLoS Biol* 5, e133.
- Grueter, B. A., Brasnjo, G., Malenka, R. C., 2010. Postsynaptic TRPV1 triggers cell type-specific long-term depression in the nucleus accumbens. *Nat Neurosci* 13, 1519-1525.
- Guimarães-Ferreira, L., 2014. Role of the phosphocreatine system on energetic homeostasis in skeletal and cardiac muscles. *Einstein (São Paulo)* 12, 126-131.
- Guo, J., Ikeda, S. R., 2003. Endocannabinoids Modulate N-Type Calcium Channels and G protein-Coupled Inwardly Rectifying Potassium Channels via CB1 Cannabinoid Receptors Heterologously Expressed in Mammalian Neurons. *Mol Pharmacol* 65, 665-674.
- Gurevich, V. V., Gurevich, E. V., 2017. Molecular Mechanisms of GPCR Signaling: A Structural Perspective. *Int J Mol Sci* 18, 2519.
- Guzman, S. J., Schlögl, A., Frotscher, M., Jonas, P., 2016. Synaptic mechanisms of pattern completion in the hippocampal CA3 network. *Science* 353, 1117-1123.
- Haas, H. L., Schaerer, B., Vosmansky, M., 1979. A simple perfusion chamber for the study of nervous tissue slices in. *J Neurosci Meth* 1, 323-325.
- Han, J., Kesner, P., Metna-Laurent, M., Duan, T., Xu, L., Georges, F., Koehl, M., Abrous, D. N., Mendizabal-Zubiaga, J., Grandes, P., Liu, Q., Bai, G., Wang, W., Xiong, L., Ren, W., Marsicano, G., Zhang, X., 2012. Acute cannabinoids impair working memory through astroglial CB1 receptor modulation of hippocampal LTD. *Cell* 148, 1039-1050.
- Hanus, L., Abu-Lafi, S., Fride, E., Breuer, A., Vogel, Z., Shalev, D. E., Kustanovich, I., Mechoulam, R., 2001. 2-Arachidonoyl glyceryl ether, an endogenous agonist of the cannabinoid CB1 receptor. *Proc Natl Acad Sci U S A* 98, 3662-3665.
- Hanus, L., Breuer, A., Tchilibon, S., S., S., Goldenberg, D., Horowitz, M., Pertwee, R. G., Ross, R. A., Mechoulam, R., Fride, E., 1999. HU-308: A specific agonist for CB2, a peripheral cannabinoid receptor. *Proc Natl Acad Sci U S A* 96, 14228-14233.
- Hanus, L. O., Meyer, S. M., Munoz, E., Tagliatela-Scafati, O., Appendino, G., 2016. Phytocannabinoids: a unified critical inventory. *Nat Prod Rep* 33, 1357-1392.
- Hebert-Chatelain, E., Desprez, T., Serrat, R., Bellocchio, L., Soria-Gomez, E., Busquets-Garcia, A., Pagano Zottola, A. C., Delamarre, A., Cannich, A., Vincent, P., Varilh, M., Robin, L. M., Terral, G., Garcia-Fernandez, M. D., Colavita, M., Mazier, W., Drago, F., Puente, N., Reguero, L., Elezgarai, I., Dupuy, J. W., Cota, D., Lopez-Rodriguez, M. L., Barreda-Gomez, G., Massa, F., Grandes, P., Benard, G., Marsicano, G., 2016. A cannabinoid link between mitochondria and memory. *Nature* 539, 555-559.

Helmstaedter, M., Staiger, J. F., Sakmann, B., Feldmeyer, D., 2008. Efficient recruitment of layer 2/3 interneurons by layer 4 input in single columns of rat somatosensory cortex. *J Neurosci* 28, 8273-8284.

Herkenham, M., Lynn, A. B., Little, M. D., Johnson, M. R., Melvin, L. S., de Costa, B. R., Rice, K. C., 1990. Cannabinoid receptor localization in brain. *Proc Natl Acad Sci U S A* 87, 1932-1936.

Hilger, D., Masureel, M., Kobilka, B. K., 2018. Structure and dynamics of GPCR signaling complexes. *Nature Structural & Molecular Biology* 25, 4-12.

Hillard, C. J., Auchampach, J. A., 1994. In vitro activation of brain protein kinase C by the cannabinoids. *Biochim Biophys Acta* 1220, 163-170.

Hojo, M., Sudo, Y., Ando, Y., Minami, K., Takada, M., Matsubara, T., Kanaide, M., Taniyama, K., Sumikawa, K., Uezono, Y., 2008. μ -Opioid Receptor Forms a Functional Heterodimer With Cannabinoid CB1 Receptor: Electrophysiological and FRET Assay Analysis. *Journal of Pharmacological Sciences* 108, 308-319.

Hua, T., Vemuri, K., Nikas, S. P., Laprairie, R. B., Wu, Y., Qu, L., Pu, M., Korde, A., Jiang, S., Ho, J. H., Han, G. W., Ding, K., Li, X., Liu, H., Hanson, M. A., Zhao, S., Bohn, L. M., Makriyannis, A., Stevens, R. C., Liu, Z. J., 2017. Crystal structures of agonist-bound human cannabinoid receptor CB1. *Nature* 547, 468-471.

Hua, T., Vemuri, K., Pu, M., Qu, L., Han, G. W., Wu, Y., Zhao, S., Shui, W., Li, S., Korde, A., Laprairie, R. B., Stahl, E. L., Ho, J. H., Zvonok, N., Zhou, H., Kufareva, I., Wu, B., Zhao, Q., Hanson, M. A., Bohn, L. M., Makriyannis, A., Stevens, R. C., Liu, Z. J., 2016. Crystal Structure of the Human Cannabinoid Receptor CB1. *Cell* 167, 750-762.

Huang, S. M., Bisogno, T., Trevisani, M., Al-Hayani, A., De Petrocellis, L., Fezza, F., Tognetto, M., Petros, T. J., Krey, J. F., Chu, C. J., Miller, J. D., Davies, S. N., Geppetti, P., Walker, J. M., Di Marzo, V., 2002. An endogenous capsaicin-like substance with high potency at recombinant and native vanilloid VR1 receptors. *Proc Natl Acad Sci U S A* 99, 8400-8405.

Ibsen, M. S., Connor, M., Glass, M., 2017. Cannabinoid CB1 and CB2 Receptor Signaling and Bias. *Cannabis Cannabinoid Res* 2, 48-60.

Isaacson, J. S., Scanziani, M., 2011. How inhibition shapes cortical activity. *Neuron* 72, 231-243.

Ishiguro, H., Horiuchi, Y., Tabata, K., Liu, Q. R., Arinami, T., Onaivi, E. S., 2018. Cannabinoid CB2 Receptor Gene and Environmental Interaction in the Development of Psychiatric Disorders. *Molecules* 23.1836.

Ishiguro, H., Iwasaki, S., Teasenfitz, L., Higuchi, S., Horiuchi, Y., Saito, T., Arinami, T., Onaivi, E. S., 2007. Involvement of cannabinoid CB2 receptor in alcohol preference in mice and alcoholism in humans. *Pharmacogenomics J* 7, 380-385.

Jacob, A., Todd, A. R., 1940. Cannabidiol and Cannabiol, Constituents of Cannabis indica Resin. *Nature* 145, 350.

- Jenniches, I., Ternes, S., Albayram, O., Otte, D. M., Bach, K., Bindila, L., Michel, K., Lutz, B., Bilkei-Gorzo, A., Zimmer, A., 2016. Anxiety, Stress, and Fear Response in Mice With Reduced Endocannabinoid Levels. *Biol Psychiatry* 79, 858-868.
- Jiang, X., Shen, S., Cadwell, C. R., Berens, P., Sinz, F., Ecker, A. S., Patel, S., Tolias, A. S., 2015. Principles of connectivity among morphologically defined cell types in adult neocortex. *Science* 350, aac9462.
- Jordan, C. J., Xi, Z. X., 2019. Progress in brain cannabinoid CB2 receptor research: From genes to behavior. *Neurosci Biobehav Rev* 98, 208-220.
- Kano, M., Ohno-Shosaku, T., Hashimotodani, Y., Uchigashima, M., Watanabe, M., 2009. Endocannabinoid-mediated control of synaptic transmission. *Physiol Rev* 89, 309-380.
- Kargl, J., Balenga, N., Parzmair, G. P., Brown, A. J., Heinemann, A., Waldhoer, M., 2012. The cannabinoid receptor CB1 modulates the signaling properties of the lysophosphatidylinositol receptor GPR55. *J Biol Chem* 287, 44234-44248.
- Katona, I., Sperlagh, B., Freund, T. F., 1999. Presynaptically Located CB1 Cannabinoid Receptors Regulate GABA Release from Axon Terminals of Specific Hippocampal Interneurons. *J Neurosci* 19, 4544-4558.
- Katona, I., Urban, G. M., Wallace, M., Ledent, C., Jung, K. M., Piomelli, D., Mackie, K., Freund, T. F., 2006. Molecular composition of the endocannabinoid system at glutamatergic synapses. *J Neurosci* 26, 5628-5637.
- Kihara, Y., Maceyka, M., Spiegel, S., 2014. Lysophospholipid receptor nomenclature review: IUPHAR Review 8. *British Journal of Pharmacology* 171, 3575-3594.
- Kim, J., Isokawa, M., Ledent, C., Alger, B. E., 2002. Activation of Muscarinic Acetylcholine Receptors Enhances the Release of Endogenous Cannabinoids in the Hippocampus. *J Neurosci* 22, 10182-10191.
- Kinnischtzke, A. K., Sewall, A. M., Berkepile, J. M., Fanselow, E. E., 2012. Postnatal maturation of somatostatin-expressing inhibitory cells in the somatosensory cortex of GIN mice. *Front Neural Circuits* 6, 33.
- Kofalvi, A., Rodrigues, R. J., Ledent, C., Mackie, K., Vizi, E. S., Cunha, R. A., Sperlagh, B., 2005. Involvement of cannabinoid receptors in the regulation of neurotransmitter release in the rodent striatum: a combined immunochemical and pharmacological analysis. *J Neurosci* 25, 2874-2884.
- Kreitzer, A. C., Carter, A. G., Regehr, W. G., 2002. Inhibition of Interneuron Firing Extends the Spread of Endocannabinoid Signaling in the Cerebellum. *Neuron* 34, 787-796.
- Kreitzer, A. C., Regehr, W. G., 2001a. Cerebellar Depolarization-Induced Suppression of Inhibition Is Mediated by Endogenous Cannabinoids. *J Neurosci* 21, 1-5.
- Kreitzer, A. C., Regehr, W. G., 2001b. Retrograde Inhibition of Presynaptic Calcium Influx by Endogenous Cannabinoids at Excitatory Synapses onto Purkinje Cells. *Neuron* 29, 717-727.

- Kruk-Slomka, M., Dzik, A., Budzynska, B., Biala, G., 2017. Endocannabinoid System: the Direct and Indirect Involvement in the Memory and Learning Processes-a Short Review. *Mol Neurobiol* 54, 8332-8347.
- Ledent, C., Valverde, O., Cossu, G., Petitet, F., Aubert, J.-F., Beslot, F., Böhme, G. A., Imperato, A., Pedrazzini, T., Roques, B. P., Vassart, G., Fratta, W., Parmentier, M., 1999. Unresponsiveness to Cannabinoids and Reduced Addictive Effects of Opiates in CB1 Receptor Knockout Mice. *Science* 283, 401-404.
- Lee, S., Kruglikov, I., Huang, Z. J., Fishell, G., Rudy, B., 2013. A disinhibitory circuit mediates motor integration in the somatosensory cortex. *Nat Neurosci* 16, 1662-1670.
- Lemtiri-Chlieh, F., Levine, E. S., 2007. Lack of depolarization-induced suppression of inhibition (DSI) in layer 2/3 interneurons that receive cannabinoid-sensitive inhibitory inputs. *J Neurophysiol* 98, 2517-2524.
- Lenz, R. A., Wagner, J. J., Alger, B. E., 1998. N- and L_type calcium channel involvement in depolarization-induced suppression of inhibition in rat hippocampal CA1 cells. *J Physiol* 512, 61—73.
- Leung, D., Saghatelian, A., Simon, G. M., Cravatt, B. F., 2006. Inactivation of N-Acyl Phosphatidylethanolamine Phospholipase D Reveals Multiple Mechanisms for the Biosynthesis of Endocannabinoids. *Biochemistry* 45, 4720-4726.
- Lewerenz, J., Maher, P., 2015. Chronic Glutamate Toxicity in Neurodegenerative Diseases-What is the Evidence? *Front Neurosci* 9, 469.
- Li, X., Hua, T., Vemuri, K., Ho, J. H., Wu, Y., Wu, L., Popov, P., Benchama, O., Zvonok, N., Locke, K., Qu, L., Han, G. W., Iyer, M. R., Cinar, R., Coffey, N. J., Wang, J., Wu, M., Katritch, V., Zhao, S., Kunos, G., Bohn, L. M., Makriyannis, A., Stevens, R. C., Liu, Z. J., 2019. Crystal Structure of the Human Cannabinoid Receptor CB2. *Cell* 176, 459-467.
- Li, Y., Kim, J., 2015. Neuronal expression of CB2 cannabinoid receptor mRNAs in the mouse hippocampus. *Neuroscience* 311, 253-267.
- Li, Y., Kim, J., 2016. Deletion of CB2 cannabinoid receptors reduces synaptic transmission and long-term potentiation in the mouse hippocampus. *Hippocampus* 26, 275-281.
- Li, Y., Kim, J., 2017. Distinct roles of neuronal and microglial CB2 cannabinoid receptors in the mouse hippocampus. *Neuroscience* 363, 11-25.
- Liu, Q. R., Canseco-Alba, A., Zhang, H. Y., Tagliaferro, P., Chung, M., Dennis, E., Sanabria, B., Schanz, N., Escosteguy-Neto, J. C., Ishiguro, H., Lin, Z., Sgro, S., Leonard, C. M., Santos-Junior, J. G., Gardner, E. L., Egan, J. M., Lee, J. W., Xi, Z. X., Onaivi, E. S., 2017. Cannabinoid type 2 receptors in dopamine neurons inhibits psychomotor behaviors, alters anxiety, depression and alcohol preference. *Sci Rep* 7, 17410.
- Lograno, M. D., Romano, M. R., 2004. Cannabinoid agonists induce contractile responses through Gi/o-dependent activation of phospholipase C in the bovine ciliary muscle. *Eur J Pharmacol* 494, 55-62.

- Lu, H. C., Mackie, K., 2016. An Introduction to the Endogenous Cannabinoid System. *Biol Psychiatry* 79, 516-525.
- Ma, Z., Gao, F., Larsen, B., Gao, M., Chen, D., Ma, X.K., Qiu, S., Zhou, Y., Xie, J.X., Xi, Z.X., Wu, J., 2019. Mechanisms of CB2 receptor-induced reduction of dopamine neuronal excitability in mouse ventral tegmental area. Preprint available at SSRN: <https://ssrn.com/abstract=3314420>
- Madisen, L., Zwingman, T. A., Sunkin, S. M., Oh, S. W., Zariwala, H. A., Gu, H., Ng, L. L., Palmiter, R. D., Hawrylycz, M. J., Jones, A. R., Lein, E. S., Zeng, H., 2010. A robust and high-throughput Cre reporting and characterization system for the whole mouse brain. *Nat Neurosci* 13, 133-140.
- Maejima, T., Hashimoto, K., Yoshida, T., Aiba, A., Kano, M., 2001. Presynaptic inhibition caused by Retrograde Signaling from Metabotropic Glutamate to Cannabinoid Receptors. *Neuron* 31, 463-475.
- Maglio, L. E., Noriega-Prieto, J. A., Maraver, M. J., Fernandez de Sevilla, D., 2018. Endocannabinoid-Dependent Long-Term Potentiation of Synaptic Transmission at Rat Barrel Cortex. *Cereb Cortex* 28, 1568-1581.
- Maier, N., Morris, G., Jochenning, F. W., Schmitz, D., 2009. An approach for reliably investigating hippocampal sharp wave-ripples in vitro. *PLoS One* 4, e6925.
- Mailleux, P., Vanderhaeghen, J.-J., 1992. Distribution of the neuronal cannabinoid receptor in the adult rat brain: a comparative receptor binding radioautography and in situ hybridization histochemistry. *Neuroscience* 48, 655-668.
- Majumdar, D., Maunsbach, A. B., Shacka, J. J., Williams, J. B., Berger, U. V., Schultz, K. P., Harkins, L. E., Boron, W. F., Roth, K. A., Bevensee, M. O., 2008. Localization of electrogenic Na/bicarbonate cotransporter NBCe1 variants in rat brain. *Neuroscience* 155, 818-832.
- Marchalant, Y., Brownjohn, P. W., Bonnet, A., Kleffmann, T., Ashton, J. C., 2014. Validating Antibodies to the Cannabinoid CB2 Receptor: Antibody Sensitivity Is Not Evidence of Antibody Specificity. *J Histochem Cytochem* 62, 395-404.
- Marinelli, S., Di Marzo, V., Florenzano, F., Fezza, F., Viscomi, M. T., van der Stelt, M., Bernardi, G., Molinari, M., Maccarrone, M., Mercuri, N. B., 2007. N-arachidonoyl-dopamine tunes synaptic transmission onto dopaminergic neurons by activating both cannabinoid and vanilloid receptors. *Neuropsychopharmacology* 32, 298-308.
- Marinelli, S., Pacioni, S., Bisogno, T., Di Marzo, V., Prince, D. A., Huguenard, J. R., Bacci, A., 2008. The endocannabinoid 2-arachidonoylglycerol is responsible for the slow self-inhibition in neocortical interneurons. *J Neurosci* 28, 13532-13541.
- Marinelli, S., Pacioni, S., Cannich, A., Marsicano, G., Bacci, A., 2009. Self-modulation of neocortical pyramidal neurons by endocannabinoids. *Nat Neurosci* 12, 1488-1490.
- Maroso, M., Szabo, G. G., Kim, H. K., Alexander, A., Bui, A. D., Lee, S. H., Lutz, B., Soltesz, I., 2016. Cannabinoid Control of Learning and Memory through HCN Channels. *Neuron* 89, 1059-1073.

- Martin, B. R., Compton, D. R., Thomas, B. F., Prescott, W. R., Little, P. J., Razdan, R. K., Johnson, M. R., Melvin, L. S., Mechoulam, R., Ward, S. J., 1991. Behavioral, Biochemical, and Molecular Modeling Evaluations of Cannabinoid Analogs *Pharmacol Biochem Behav* 40, 471-478.
- Martin, M., Ledent, C., Parmentier, M., Maldonado, R., Valverde, O., 2002. Involvement of CB1 cannabinoid receptors in emotional behaviour. *Psychopharmacology (Berl)* 159, 379-387.
- Matsuda, L. A., Bonner, T. I., Lolait, S. J., 1993. Localization of Cannabinoid Receptor mRNA in Rat Brain. *J Comp Neurol* 327, 545-550.
- Matsuda, L. A., Lolait, S. J., Brownstein, M. J., Young, A. C., Bonner, T. I., 1990. Structure of a cannabinoid receptor and functional expression of the cloned cDNA. *Nature* 346, 561-564.
- Matthews, E. A., Dietrich, D., 2015. Buffer mobility and the regulation of neuronal calcium domains. *Front Cell Neurosci* 9, 48.
- McFarland, M. J., Bardell, T. K., Yates, M. L., Placzek, E. A., Barker, E. L., 2008. RNA interference-mediated knockdown of dynamin 2 reduces endocannabinoid uptake into neuronal dCAD cells. *Mol Pharmacol* 74, 101-108.
- McHugh, D., 2012. GPR18 in microglia: implications for the CNS and endocannabinoid system signaling. *British Journal of Pharmacology* 167, 1575-1582.
- McPartland, J. M., Agraval, J., Gleeson, D., Heasman, K., Glass, M., 2006. Cannabinoid receptors in invertebrates. *J Evol Biol* 19, 366-373.
- McPartland, J. M., Di Marzo, V., Mercer, A., De Petrocellis, L., Glass, M., 2001. Cannabinoid Receptors are absent in insects. *J Comp Neurol* 436, 423-429.
- McPartland, J. M., Glass, M., Pertwee, R. G., 2007. Meta-analysis of cannabinoid ligand binding affinity and receptor distribution: interspecies differences. *Br J Pharmacol* 152, 583-593.
- Mechoulam, R., Ben-Shabat, S., Hanus, L., Ligumsky, M., Kaminski, N. E., Schatz, A. R., Gopher, A., Almog, S., Martin, B. R., Compton, D. R., Pertwee, R. G., Griffin, G., Bayewitch, M., Barg, J., Vogel, Z., 1995. Identification of an endogenous 2-Monoglyceride, present in canine gut, that binds to cannabinoid receptors. *Biochem Pharmacol* 50, 83-90.
- Mechoulam, R., Hanus, L., 2001. The cannabinoids: An overview. Therapeutic implications in vomiting and nausea after cancer chemotherapy, in appetite promotion, in multiple sclerosis and in neuroprotection. *pain res manage* 6, 67-73.
- Mechoulam, R., Parker, L. A., 2013. The endocannabinoid system and the brain. *Annu Rev Psychol* 64, 21-47.
- Mechoulam, R., Shvo, Y., 1963. Hashish. I. The structure of cannabidiol. *Tetrahedron* 19, 2073-2078.
- Mendiguren, A., Aostri, E., Pineda, J., 2018. Regulation of noradrenergic and serotonergic systems by cannabinoids: relevance to cannabinoid-induced effects. *Life Sci* 192, 115-127.
- Min, R., Nevian, T., 2012. Astrocyte signaling controls spike timing-dependent depression at neocortical synapses. *Nat Neurosci* 15, 746-753.

Morales, P., Reggio, P. H., 2017. An Update on Non-CB1, Non-CB2 Cannabinoid Related G protein-Coupled Receptors. *Cannabis Cannabinoid Res* 2, 265-273.

Moreau de Tours, J., 1845. *Du hachisch et de l'aliénation mentale*. Masson, Paris.

Munro, S., Thomas, K. L., Abu-Shaar, M., 1993. Molecular characterization of a peripheral receptor for cannabinoids. *Nature* 365, 61-65.

Navarrete, F., Rodriguez-Arias, M., Martin-Garcia, E., Navarro, D., Garcia-Gutierrez, M. S., Aguilar, M. A., Aracil-Fernandez, A., Berbel, P., Minarro, J., Maldonado, R., Manzanares, J., 2013. Role of CB2 cannabinoid receptors in the rewarding, reinforcing, and physical effects of nicotine. *Neuropsychopharmacology* 38, 2515-2524.

Navarrete, M., Araque, A., 2008. Endocannabinoids mediate neuron-astrocyte communication. *Neuron* 57, 883-893.

Navarrete, M., Araque, A., 2010. Endocannabinoids potentiate synaptic transmission through stimulation of astrocytes. *Neuron* 68, 113-126.

Navarro, G., Reyes-Resina, I., Rivas-Santisteban, R., Sanchez de Medina, V., Morales, P., Casano, S., Ferreira-Vera, C., Lillo, A., Aguinaga, D., Jagerovic, N., Nadal, X., Franco, R., 2018. Cannabidiol skews biased agonism at cannabinoid CB1 and CB2 receptors with smaller effect in CB1-CB2 heteroreceptor complexes. *Biochem Pharmacol* 157, 148-158.

Oehlke, O., Speer, J. M., Roussa, E., 2013. Variants of the electrogenic sodium bicarbonate cotransporter 1 (NBCe1) in mouse hippocampal neurons are regulated by extracellular pH changes: evidence for a Rab8a-dependent mechanism. *Int J Biochem Cell Biol* 45, 1427-1438.

Ohno-Shosaku, T., Hashimoto-dani, Y., Ano, M., Takeda, S., Tsubokawa, H., Kano, M., 2007. Endocannabinoid signalling triggered by NMDA receptor-mediated calcium entry into rat hippocampal neurons. *J Physiol* 584, 407-418.

Ohno-Shosaku, T., Maejima, T., Kano, M., 2001. Endogenous Cannabinoids Mediate Retrograde Signals from Depolarized Postsynaptic Neurons to Presynaptic Terminals. *Neuron* 29, 729-738.

Ohno-Shosaku, T., Matsui, M., Fukudome, Y., Shosaku, J., Tsubokawa, H., Taketo, M. M., Manabe, T., Kano, M., 2003. Postsynaptic M1 and M3 receptors are responsible for the muscarinic enhancement of retrograde endocannabinoid signalling in the hippocampus. *European Journal of Neuroscience* 18, 109-116.

Ohno-Shosaku, T., Sawada, S., Kano, M., 2000. Heterosynaptic expression of depolarization-induced suppression of inhibition (DSI) in rat hippocampal cultures. *Neuroscience Research* 36, 67-71.

Ohno-Shosaku, T., Shosaku, J., Tsubokawa, H., Kano, M., 2002a. Cooperative endocannabinoid production by neuronal depolarization and group I metabotropic glutamate receptor activation. *Eur J Neurosci* 15, 953-961.

Ohno-Shosaku, T., Tsubokawa, H., Mizushima, I., Yoneda, N., Zimmer, A., Kano, M., 2002b. Presynaptic Cannabinoid Sensitivity Is a Major Determinant of Depolarization-Induced Retrograde Suppression at Hippocampal Synapses. *The Journal of Neuroscience* 22, 3864-3872.

Oka, S., Nakajima, K., Yamashita, A., Kishimoto, S., Sugiura, T., 2007. Identification of GPR55 as a lysophosphatidylinositol receptor. *Biochem Biophys Res Commun* 362, 928-934.

Oliveira da Cruz, J. F., Robin, L. M., Drago, F., Marsicano, G., Metna-Laurent, M., 2016. Astroglial type-1 cannabinoid receptor (CB1): A new player in the tripartite synapse. *Neuroscience* 323, 35-42.

Onaivi, E. S., 2006. Neuropsychobiological evidence for the functional presence and expression of cannabinoid CB2 receptors in the brain. *Neuropsychobiology* 54, 231-246.

Onaivi, E. S., Ishiguro, H., Gong, J. P., Patel, S., Meozzi, P. A., Myers, L., Perchuk, A., Mora, Z., Tagliaferro, P. A., Gardner, E., Brusco, A., Akinshola, B. E., Liu, Q. R., Chirwa, S. S., Hope, B., Lujilde, J., Inada, T., Iwasaki, S., Macharia, D., Teasentfitz, L., Arinami, T., Uhl, G. R., 2008. Functional expression of brain neuronal CB2 cannabinoid receptors are involved in the effects of drugs of abuse and in depression. *Ann N Y Acad Sci* 1139, 434-449.

Ortega-Alvaro, A., Aracil-Fernandez, A., Garcia-Gutierrez, M. S., Navarrete, F., Manzanares, J., 2011. Deletion of CB2 cannabinoid receptor induces schizophrenia-related behaviors in mice. *Neuropsychopharmacology* 36, 1489-1504.

Ortega-Alvaro, A., Ternianov, A., Aracil-Fernandez, A., Navarrete, F., Garcia-Gutierrez, M. S., Manzanares, J., 2015. Role of cannabinoid CB2 receptor in the reinforcing actions of ethanol. *Addict Biol* 20, 43-55.

Pacher, P., Mechoulam, R., 2011. Is lipid signaling through cannabinoid 2 receptors part of a protective system? *Prog Lipid Res* 50, 193-211.

Pain, S., 2015. A potted history. *Nature* 525, S10-11.

Palazuelos, J., Aguado, T., Pazos, M. R., Julien, B., Carrasco, C., Resel, E., Sagredo, O., Benito, C., Romero, J., Azcoitia, I., Fernandez-Ruiz, J., Guzman, M., Galve-Roperh, I., 2009. Microglial CB2 cannabinoid receptors are neuroprotective in Huntington's disease excitotoxicity. *Brain* 132, 3152-3164.

Pandey, P., Chaurasiya, N. D., Tekwani, B. L., Doerksen, R. J., 2018. Interactions of endocannabinoid virodhamine and related analogs with human monoamine oxidase-A and -B. *Biochem Pharmacol* 155, 82-91.

Pangalos, M., Donoso, J. R., Winterer, J., Zivkovic, A. R., Kempter, R., Maier, N., Schmitz, D., 2013. Recruitment of oriens-lacunosum-moleculare interneurons during hippocampal ripples. *Proc Natl Acad Sci U S A* 110, 4398-4403.

Pertwee, R. G., 2012. Targeting the endocannabinoid system with cannabinoid receptor agonists: pharmacological strategies and therapeutic possibilities. *Philos Trans R Soc Lond B Biol Sci* 367, 3353-3363.

Pertwee, R. G., 2015. *Endocannabinoids*. Springer Nature, Berlin.

Pertwee, R. G., Howlett, A. C., Abood, M. E., Alexander, S. P., Di Marzo, V., Elphick, M. R., Greasley, P. J., Hansen, H. S., Kunos, G., Mackie, K., Mechoulam, R., Ross, R. A., 2010. International Union of Basic

and Clinical Pharmacology. LXXIX. Cannabinoid receptors and their ligands: beyond CB(1) and CB(2). *Pharmacol Rev* 62, 588-631.

Pfeffer, C. K., Xue, M., He, M., Huang, Z. J., Scanziani, M., 2013. Inhibition of inhibition in visual cortex: the logic of connections between molecularly distinct interneurons. *Nat Neurosci* 16, 1068-1076.

Pi, H. J., Hangya, B., Kvitsiani, D., Sanders, J. I., Huang, Z. J., Kepecs, A., 2013. Cortical interneurons that specialize in disinhibitory control. *Nature* 503, 521-524.

Pitler, T. A., Alger, B. E., 1992. Postsynaptic Spike Firing Reduces Synaptic GABA_A Responses in Hippocampal Pyramidal Cells. *J Neurosci* 12, 4122-4132.

Porter, A. C., Sauer, J.-M., Knierman, M. D., Becker, G. W., Berna, M. J., Bao, J., Nomikos, G. G., Carter, P., Bymaster, F. P., Baker Leese, A., Felder, C. C., 2002. Characterization of a Novel Endocannabinoid, Virodhamine, with Antagonist Activity at the CB1 Receptor. *J Pharmacol Exp Ther* 301, 1020-1024.

Puighermanal, E., Marsicano, G., Busquets-Garcia, A., Lutz, B., Maldonado, R., Ozaita, A., 2009. Cannabinoid modulation of hippocampal long-term memory is mediated by mTOR signaling. *Nat Neurosci* 12, 1152-1158.

Quiton, R. L., Masri, R., Thompson, S. M., Keller, A., 2010. Abnormal activity of primary somatosensory cortex in central pain syndrome. *J Neurophysiol* 104, 1717-1725.

Rasooli-Nejad, S., Palygin, O., Lalo, U., Pankratov, Y., 2014. Cannabinoid receptors contribute to astroglial Ca²⁺(+)-signalling and control of synaptic plasticity in the neocortex. *Philos Trans R Soc Lond B Biol Sci* 369, 20140077.

Rinaldi-Carmona, M., Barth, F., Millan, J., Derocq, J. M., Casellas, P., Congy, C., Oustric, D., Sarran, M., M., B., Calandra, B., Portier, M., D., S., C., B. J., Le Fur, G., 1998. SR 144528, the First Potent and Selective Antagonist of the CB2 Cannabinoid Receptor. *J Pharmacol Exp Ther* 248, 644-650.

Robbe, D., Kopf, M., Remaury, A., Bockaert, J., Manzoni, O. J., 2002. Endogenous cannabinoids mediate long-term synaptic depression in the nucleus accumbens. *Proc Natl Acad Sci U S A* 99, 8384-8388.

Robertson, J. M., Achua, J. K., Smith, J. P., Prince, M. A., Staton, C. D., Ronan, P. J., Summers, T. R., Summers, C. H., 2017. Anxious behavior induces elevated hippocampal Cb2 receptor gene expression. *Neuroscience* 352, 273-284.

Rodriguez-Arias, M., Navarrete, F., Blanco-Gandia, M. C., Arenas, M. C., Aguilar, M. A., Bartoll-Andres, A., Valverde, O., Minarro, J., Manzanares, J., 2015. Role of CB2 receptors in social and aggressive behavior in male mice. *Psychopharmacology (Berl)* 232, 3019-3031.

Rudy, B., Fishell, G., Lee, S., Hjerling-Leffler, J., 2011. Three groups of interneurons account for nearly 100% of neocortical GABAergic neurons. *Dev Neurobiol* 71, 45-61.

Russo, E.B., Grotenhermen, F., 2013. *Cannabis and Cannabinoids: Pharmacology, Toxicology, and Therapeutic Potential*. Routledge, London, UK.

- Ryberg, E., Vu, H. K., Larsson, N., Groblewski, T., Hjorth, S., Elebring, T., Sjogren, S., Greasley, P. J., 2005. Identification and characterisation of a novel splice variant of the human CB1 receptor. *FEBS Lett* 579, 259-264.
- Ryberg, E., Larsson, N., Sjogren, S., Hjorth, S., Hermansson, N. O., Leonova, J., Elebring, T., Nilsson, K., Drmota, T., Greasley, P. J., 2007. The orphan receptor GPR55 is a novel cannabinoid receptor. *Br J Pharmacol* 152, 1092-1101.
- Saleh, N., Hucke, O., Kramer, G., Schmidt, E., Montel, F., Lipinski, R., Ferger, B., Clark, T., Hildebrand, P. W., Tautermann, C. S., 2018. Multiple Binding Sites Contribute to the Mechanism of Mixed Agonistic and Positive Allosteric Modulators of the Cannabinoid CB1 Receptor. *Angew Chem Int Ed Engl* 57, 2580-2585.
- Sang, N., Zhang, J., Chen, C., 2006. PGE2 glycerol ester, a COX-2 oxidative metabolite of 2-arachidonoyl glycerol, modulates inhibitory synaptic transmission in mouse hippocampal neurons. *J Physiol* 572, 735-745.
- Schindelin, J., Arganda-Carreras, I., Frise, E., Kaynig, V., Longair, M., Pietzsch, T., Preibisch, S., Rueden, C., Saalfeld, S., Schmid, B., Tinevez, J. Y., White, D. J., Hartenstein, V., Eliceiri, K., Tomancak, P., Cardona, A., 2012. Fiji: an open-source platform for biological-image analysis. *Nat Methods* 9, 676-682.
- Schmole, A. C., Lundt, R., Gennequin, B., Schrage, H., Beins, E., Kramer, A., Zimmer, T., Limmer, A., Zimmer, A., Otte, D. M., 2015. Expression Analysis of CB2-GFP BAC Transgenic Mice. *PLoS One* 10, e0138986.
- Seillier, A., Giuffrida, A., 2018. The cannabinoid transporter inhibitor OMDM-2 reduces social interaction: Further evidence for transporter-mediated endocannabinoid release. *Neuropharmacology* 130, 1-9.
- Sekar, K., Pack, A., 2019. Epidiolex as adjunct therapy for treatment of refractory epilepsy: a comprehensive review with a focus on adverse effects. *F1000Res* 8.
- Shao, Z., Yin, J., Chapman, K., Grzemska, M., Clark, L., Wang, J., Rosenbaum, D. M., 2016. High-resolution crystal structure of the human CB1 cannabinoid receptor. *Nature* 540, 602-606.
- Shirakabe, K., Priori, G., Yamada, H., Ando, H., Horita, S., Fujita, T., Fujimoto, I., Mizutani, A., Seki, G., Mikoshiba, K., 2006. IRBIT, an inositol 1,4,5-trisphosphate receptor-binding protein, specifically binds to and activates pancreas-type Na/HCO₃ cotransporter (pNBC1). *Proc Natl Acad Sci U S A* 103, 9542-9547.
- Shire, D., Carillon, C., Kaghad, M., Calandra, B., Rinaldi-Carmona, M., Le Fur, G., Caput, D., Ferrara, P., 1995. An Amino-terminal Variant of the Central Cannabinoid Receptor Resulting from Alternative Splicing. *J Biol Chem* 270, 3726-3731.
- Sierra, S., Luquin, N., Rico, A. J., Gomez-Bautista, V., Roda, E., Dopeso-Reyes, I. G., Vazquez, A., Martinez-Pinilla, E., Labandeira-Garcia, J. L., Franco, R., Lanciego, J. L., 2015. Detection of cannabinoid receptors CB1 and CB2 within basal ganglia output neurons in macaques: changes following experimental parkinsonism. *Brain Struct Funct* 220, 2721-2738.

- Sinning, A., Hübner, C.A., 2013. Minireview: pH and synaptic transmission. *FEBS Lett* 587, 1923-1928.
- Sjöström, P. J., Turrigiano, G. G., Nelson, S. B., 2003. Neocortical LTD via Coincident Activation of Presynaptic NMDA and Cannabinoid Receptors. *Neuron* 39, 641-654.
- Smith, J. S., Rajagopal, S., 2016. The beta-Arrestins: Multifunctional Regulators of G Protein-coupled Receptors. *J Biol Chem* 291, 8969-8977.
- Soethoudt, M., Grether, U., Fingerle, J., Grim, T. W., Fezza, F., de Petrocellis, L., Ullmer, C., Rothenhausler, B., Perret, C., van Gils, N., Finlay, D., MacDonald, C., Chicca, A., Gens, M. D., Stuart, J., de Vries, H., Mastrangelo, N., Xia, L., Alachouzos, G., Baggelaar, M. P., Martella, A., Mock, E. D., Deng, H., Heitman, L. H., Connor, M., Di Marzo, V., Gertsch, J., Lichtman, A. H., Maccarrone, M., Pacher, P., Glass, M., van der Stelt, M., 2017. Cannabinoid CB2 receptor ligand profiling reveals biased signalling and off-target activity. *Nat Commun* 8, 13958.
- Song, Z.-H., Bonner, T. I., 1996a. A Lysine Residue of the Cannabinoid Receptor Is Critical for Receptor Recognition by Several Agonists but not WIN55212-2. *Mol Pharmacol* 49, 891-896.
- Song, Z.-H., Bonner, T. I., 1996b. A Lysine Residue of the Cannabinoid receptor is Critical for Receptor Recognition by Several Agonists but not WIN55212-2. *Mol Pharmacol* 49, 891-896.
- Stempel, A. V., 2015. Cannabinoid type 2 receptors mediate a cell type-specific plasticity in the hippocampus. PhD diss, Freie Universität, Berlin. Refubium (12258).
- Stempel, A. V., Stumpf, A., Zhang, H. Y., Ozdogan, T., Pannasch, U., Theis, A. K., Otte, D. M., Wojtalla, A., Racz, I., Ponomarenko, A., Xi, Z. X., Zimmer, A., Schmitz, D., 2016. Cannabinoid Type 2 Receptors Mediate a Cell Type-Specific Plasticity in the Hippocampus. *Neuron* 90, 795-809.
- Stockings, E., Zagic, D., Campbell, G., Weier, M., Hall, W. D., Nielsen, S., Herkes, G. K., Farrell, M., Degenhardt, L., 2018. Evidence for cannabis and cannabinoids for epilepsy: a systematic review of controlled and observational evidence. *J Neurol Neurosurg Psychiatry* 89, 741-753.
- Sugaya, Y., Yamazaki, M., Uchigashima, M., Kobayashi, K., Watanabe, M., Sakimura, K., Kano, M., 2016. Crucial Roles of the Endocannabinoid 2-Arachidonoylglycerol in the Suppression of Epileptic Seizures. *Cell Rep* 16, 1405-1415.
- Sugiura, T., Kodaka, T., Kondo, S., Nakane, S., Kondo, H., Waku, K., Ishima, Y., Watanabe, K., Yamamoto, I., 1997. Is the Cannabinoid CB1 Receptor a 2-Arachidonoylglycerol Receptor? Structural Requirements for Triggering a Ca²⁺ Transient in NG108-15 Cells. *J Biochem* 122, 890-895.
- Sugiura, T., Kondo, S., Sukagawa, A., Nakane, S., Shinoda, A., Itoh, K., Yamashita, A., Waku, K., 1995. 2-Arachidonoylglycerol: a possible endogenous cannabinoid receptor ligand in brain. *Biochem Biophys Res Com* 215, 89-97.
- Svichar, N., Esquenazi, S., Chen, H. Y., Chesler, M., 2011. Preemptive regulation of intracellular pH in hippocampal neurons by a dual mechanism of depolarization-induced alkalinization. *J Neurosci* 31, 6997-7004.

- Svizenska, I. H., Brazda, V., Klusakova, I., Dubovy, P., 2013. Bilateral changes of cannabinoid receptor type 2 protein and mRNA in the dorsal root ganglia of a rat neuropathic pain model. *J Histochem Cytochem* 61, 529-547.
- Taniguchi, H., He, M., Wu, P., Kim, S., Paik, R., Sugino, K., Kvitsiani, D., Fu, Y., Lu, J., Lin, Y., Miyoshi, G., Shima, Y., Fishell, G., Nelson, S. B., Huang, Z. J., 2011. A resource of Cre driver lines for genetic targeting of GABAergic neurons in cerebral cortex. *Neuron* 71, 995-1013.
- Tanimura, A., Yamazaki, M., Hashimotodani, Y., Uchigashima, M., Kawata, S., Abe, M., Kita, Y., Hashimoto, K., Shimizu, T., Watanabe, M., Sakimura, K., Kano, M., 2010. The endocannabinoid 2-arachidonoylglycerol produced by diacylglycerol lipase alpha mediates retrograde suppression of synaptic transmission. *Neuron* 65, 320-327.
- Thomas, A., Baillie, G. L., Phillips, A. M., Razdan, R. K., Ross, R. A., Pertwee, R. G., 2007. Cannabidiol displays unexpectedly high potency as an antagonist of CB1 and CB2 receptor agonists in vitro. *Br J Pharmacol* 150, 613-623.
- Thornell, I. M., Bevensee, M. O., 2015. Phosphatidylinositol 4,5-bisphosphate degradation inhibits the Na⁺/bicarbonate cotransporter NBCe1-B and -C variants expressed in *Xenopus* oocytes. *J Physiol* 593, 541-558.
- Thornell, I. M., Wu, J., Liu, X., Bevensee, M. O., 2012. PIP2 hydrolysis stimulates the electrogenic Na⁺-bicarbonate cotransporter NBCe1-B and -C variants expressed in *Xenopus laevis* oocytes. *J Physiol* 590, 5993-6011.
- Torrecilla, I., Spragg, E. J., Poulin, B., McWilliams, P. J., Mistry, S. C., Blaukat, A., Tobin, A. B., 2007. Phosphorylation and regulation of a G protein-coupled receptor by protein kinase CK2. *J Cell Biol* 177, 127-137.
- Tremblay, R., Lee, S., Rudy, B., 2016. GABAergic Interneurons in the Neocortex: From Cellular Properties to Circuits. *Neuron* 91, 260-292.
- Tsou, K., Brown, S., Sanudo-Pena, M. C., Mackie, K., Walker, J. M., 1998. Immunohistochemical Distribution of cannabinoid CB1 Receptors in the rat central nervous system. *Neuroscience* 83, 391-411.
- Tsou, K., Mackie, K., Sanudo-Pena, M. C., Walker, J. M., 1999. Cannabinoid CB1 Receptors are Located Primarily on Cholecystinin-Containing GABAergic Interneurons in the Rat Hippocampal Formation. *Neuroscience* 93, 969-975.
- Tsuboi, K., Ikematsu, N., Uyama, T., Deutsch, D. G., Tokumura, A., Ueda, N., 2013. Biosynthetic Pathways of Bioactive N-acylethanolamines in Brain. *CNS Neurolog Drug Targets* 12, 7-16.
- Uriguen, L., Perez-Rial, S., Ledent, C., Palomo, T., Manzanares, J., 2004. Impaired action of anxiolytic drugs in mice deficient in cannabinoid CB1 receptors. *Neuropharmacology* 46, 966-973.
- Varma, N., Carlson, G. C., Ledent, C., Alger, B. E., 2001. Metabotropic Glutamate Receptors drive the Endocannabinoid system in Hippocampus. *J Neurosci* 21, 1-5.

Viader, A., Blankman, J. L., Zhong, P., Liu, X., Schlosburg, J. E., Joslyn, C. M., Liu, Q. S., Tomarchio, A. J., Lichtman, A. H., Selley, D. E., Sim-Selley, L. J., Cravatt, B. F., 2015. Metabolic Interplay between Astrocytes and Neurons Regulates Endocannabinoid Action. *Cell Rep* 12, 798-808.

Vierck, C. J., Whitsel, B. L., Favorov, O. V., Brown, A. W., Tommerdahl, M., 2013. Role of primary somatosensory cortex in the coding of pain. *Pain* 154, 334-344.

Vincent, P., Marty, A., 1993. Neighboring Cerebellar Purkinje Cells Communicate via Retrograde Inhibition of Common Presynaptic Interneurons *Neuron* 11, 885-893.

Wang, W., Trieu, B. H., Palmer, L. C., Jia, Y., Pham, D. T., Jung, K. M., Karsten, C. A., Merrill, C. B., Mackie, K., Gall, C. M., Piomelli, D., Lynch, G., 2016. A Primary Cortical Input to Hippocampus Expresses a Pathway-Specific and Endocannabinoid-Dependent Form of Long-Term Potentiation. *eNeuro* 3, e0160.

Wettschureck, N., Offermanns, S., 2005. Mammalian G proteins and their cell type specific functions. *Physiol Rev* 85, 1159-1204.

Wilson, R. I., Nicoll, R. A., 2001. Endogenous cannabinoids mediate retrograde signalling at hippocampal synapses. *Nature* 410, 588-592.

Woehler, A., Lin, K. H., Neher, E., 2014. Calcium-buffering effects of gluconate and nucleotides, as determined by a novel fluorimetric titration method. *J Physiol* 592, 4863-4875.

Wood, T. B., Newton Spivey, W. T., Easterfield, T. H., 1896. Charas. The resin of Indian hemp. *J Chem Soc Trans* 69, 539-546.

Wu, J., Hocevar, M., Foss, J. F., Bie, B., Naguib, M., 2017. Activation of CB2 receptor system restores cognitive capacity and hippocampal Sox2 expression in a transgenic mouse model of Alzheimer's disease. *Eur J Pharmacol* 811, 12-20.

Wu, Q., Wang, H., 2018. The spatiotemporal expression changes of CB2R in the hippocampus of rats following pilocarpine-induced status epilepticus. *Epilepsy Res* 148, 8-16.

Yoshida, T., Fukaya, M., Uchigashima, M., Miura, E., Kamiya, H., Kano, M., Watanabe, M., 2006. Localization of diacylglycerol lipase- α around postsynaptic spine suggests close proximity between production site of an endocannabinoid, 2-arachidonoyl-glycerol, and presynaptic cannabinoid CB1 receptor. *J Neurosci* 26, 4740-4751.

Yu, S. J., Reiner, D., Shen, H., Wu, K. J., Liu, Q. R., Wang, Y., 2015. Time-Dependent Protection of CB2 Receptor Agonist in Stroke. *PLoS One* 10, e0132487.

Zarruk, J. G., Fernandez-Lopez, D., Garcia-Yebenes, I., Garcia-Gutierrez, M. S., Vivancos, J., Nombela, F., Torres, M., Burguete, M. C., Manzanares, J., Lizasoain, I., Moro, M. A., 2012. Cannabinoid type 2 receptor activation downregulates stroke-induced classic and alternative brain macrophage/microglial activation concomitant to neuroprotection. *Stroke* 43, 211-219.

Zhang, H. Y., Bi, G. H., Li, X., Li, J., Qu, H., Zhang, S. J., Li, C. Y., Onaivi, E. S., Gardner, E. L., Xi, Z. X., Liu, Q. R., 2015. Species differences in cannabinoid receptor 2 and receptor responses to cocaine self-administration in mice and rats. *Neuropsychopharmacology* 40, 1037-1051.

- Zhang, H. Y., Gao, M., Liu, Q. R., Bi, G. H., Li, X., Yang, H. J., Gardner, E. L., Wu, J., Xi, Z. X., 2014. Cannabinoid CB2 receptors modulate midbrain dopamine neuronal activity and dopamine-related behavior in mice. *Proc Natl Acad Sci U S A* 111, E5007-5015.
- Zhang, H. Y., Gao, M., Shen, H., Bi, G. H., Yang, H. J., Liu, Q. R., Wu, J., Gardner, E. L., Bonci, A., Xi, Z. X., 2017. Expression of functional cannabinoid CB2 receptor in VTA dopamine neurons in rats. *Addict Biol* 22, 752-765.
- Zhang, H. Y., Shen, H., Jordan, C. J., Liu, Q. R., Gardner, E. L., Bonci, A., Xi, Z. X., 2019. CB2 receptor antibody signal specificity: correlations with the use of partial CB2-knockout mice and anti-rat CB2 receptor antibodies. *Acta Pharmacol Sin* 40, 398-409.
- Zhang, Z. G., Hu, L., Hung, Y. S., Mouraux, A., Iannetti, G. D., 2012. Gamma-band oscillations in the primary somatosensory cortex- a direct and obligatory correlate of subjective pain intensity. *J Neurosci* 32, 7429-7438.
- Zimmer, A., Zimmer, A. M., Hohmann A. G., Herkenham, M., Bonner, T.I., 1999. Increased mortality, hypoactivity, and hypoalgesia in cannabinoid CB1 receptor knockout mice. *Proc Natl Acad Sci U S A* 96, 5780-5785.
- Zoppi, S., Madrigal, J. L., Caso, J. R., Garcia-Gutierrez, M. S., Manzanares, J., Leza, J. C., Garcia-Bueno, B., 2014. Regulatory role of the cannabinoid CB2 receptor in stress-induced neuroinflammation in mice. *Br J Pharmacol* 171, 2814-2826.
- Zoratti, C., Kipmen-Korgun, D., Osibow, K., Malli, R., Graier, W. F., 2003. Anandamide initiates Ca(2+) signaling via CB2 receptor linked to phospholipase C in calf pulmonary endothelial cells. *Br J Pharmacol* 140, 1351-1362.
- Zuardi, A. W., 2006. History of cannabis as a medicine: a review. *Rev Bras Psiquiatr* 28, 153-157.

6. Appendix

6.1. Glossary

2-AG	2-arachnidonyl glycerol
2-ALPI	2-arachidonoyl lysophosphatidyl inositol
5-HT	5-hydroxytryptamine, serotonin
AA	Arachidonic acid
ABHD	α/β -Hydrolase domain containing enzyme
AC	Adenylyl cyclase
ACSF	Artificial cerebrospinal fluid
ADP/ATP	Adenosine di/triphosphate
AEA	Anandamide, N-arachidonylethanolamine
AHP	Afterhyperpolarization
AM-251	Inverse agonist at the CB ₁ R
AM-404	Cannabinoid reuptake inhibitor
AMPAR	α -amino-3-hydroxy-5-methyl-4-isoxazolepropionic acid receptor
AP	Action potential
ATPase	Adenosinetriphosphatase
BAC-GFP	Baculovirus vector based expression of green fluorescent protein
BAPTA	1,2-bis(o-aminophenoxy)ethane-tetraacetic acid; Calcium chelator
Bumetanide	Inhibitor of the Na-K-Cl cotransporter (NKCC)
CA1/3	Cornu Ammonis area 1/3 in the hippocampus
cAMP	Cyclic adenosine monophosphate
Cariporide	NA/H exchange inhibitor
CB_{1/2}R	Cannabinoid receptor type 1/2
cGMP	Cyclic Guanosine monophosphate
CGP55845	GABA _B receptor antagonist
CNR1/2	Gene encoding cannabinoid receptor type 1/2
CNS	Central nervous system
Cox-2	Cyclooxygenase-2
CP55,940	Synthetic CB ₁ R and CB ₂ R agonist
CPA	Cyclopiazonic acid, inhibitor of SERCA ATPase
DAG	Diacylglycerol
DAGL	Diacylglycerol lipase
DIA	Depolarization-induced alkalization
DNDS	Dinitro-disulfonic stilbene, Cl ⁻ channel inhibitor
DSE/DSI	Depolarization induced suppression of excitation/inhibition
ER	Endoplasmatic reticulum
ERK	Extracellular signal-regulated kinase
FAAH	Fatty acid amide hydrolase
FS	Fast spiking interneuron
GABA	γ -aminobutyric acid
Gabazine	SR-95531, GABA _A receptor antagonist

GAD67	Glutamic acid decarboxylase; marker for GABAergic interneurons
GDP/GTP	Guanosine di/triphosphate
GIRK	G protein-coupled inwardly-rectifying K ⁺ channel
GP-AEA	Glycerophospho-anandamide
GPCR	G protein-coupled receptor
HU-308	CB ₂ R selective agonist
IP₃	Inositol triphosphate
IRBIT	Inositol triphosphate receptor-binding protein
JWH133	CB ₂ R selective agonist
KCC2	K ⁺ /Cl ⁻ transporter
KO	Knockout
LPI	Lysophosphatidylinositol
LTD/LTP	Long term depression/ potentiation
LTS	Low-threshold spiking interneurons
Ly320135	CB ₁ R inverse agonist
Lyso-PI	Lyso-phosphatidylinositol
Lyso-PLC/D	Lyso-phospholipase C/D
mACh	Muscarinic acetylcholine receptor
MAGL	Monoacylglycerol lipase
MAO	Monoamine oxidase
MAPK	Mitogen-activated protein kinase
mGluR	Metabotropic glutamate receptor
MSE/MSI	Metabotropic suppression of excitation/inhibition
NAAA	N-acylethanolamine-hydrolysing acid amidase
NADA	N-arachidonoyl dopamine
NAPE	N-arachidonoyl phosphatidylethanolamines
NAPE-PLC/PLD	N-arachidonoyl phosphatidylethanolamines specific phospholipase C/D
NAT	N-acyltransferase
NBC	Na ⁺ /bicarbonate
NGS	Normal goat serum
NKCC	Na ⁺ /K ⁺ /Cl ⁻ transporter
NMDA	N-methyl-D-aspartate
NMDG	N-methyl-D-glucamin
OLM	Oriens-lacunosum moleculare
OMDM-2	Cannabinoid reuptake inhibitor
Ouabaine	Na ⁺ /K ⁺ -ATPase inhibitor
PBS	Phosphate-buffered saline
PC	Pyramidal cell
PGE2-GE	Prostaglandin 2 glycerol ester
PE	Phosphatidyl-ethanolamines
PI	Phosphatidylinositol
PIP_{2/3}	Phosphatidylinositol bi/triphosphate
PKA/PKC	Protein kinase A/C
PLA/PLC	Phospholipase A/C
PTX	Pertussis toxin, blocks G _{α_{i/o}} subunit signaling

RhoGEF	Rho-guanine nucleotide exchange factors)
R_{in}	Input resistance
Rotenone	Inhibits complex I of the mitochondrial electron transport chain
RSNPC	Regular spiking non-pyramidal cells
S0859	NBC blocker
sACSF	Sucrose based artificial cerebrospinal fluid
SCH23390	GIRK channel blocker
SERCA	Sarcoplasmic/endoplasmic reticulum Ca ²⁺ ATPase
SR144258	CB ₂ R inverse agonist
SSI	Slow self-inhibition
THC	(-)- <i>trans</i> - Δ^9 -tetrahydrocannabinol
TRPV / TRPM	Transient receptor potential ion channel; type vanilloid/melastatin
VGCC	Voltage-gated Ca ²⁺ channel
VIP	Vasoactive intestinal peptide
V_m	Membrane potential
VU0240551	KCC2 inhibitor
WIN55,212-2	Synthetic cannabinoid receptor agonist
WT	Wild type
ΔV_m	Membrane potential difference

6.2. Statement of contributions

All experiments in this thesis were conceived and designed by my PhD supervisors, Prof. Dietmar Schmitz, Dr. A. Vanessa Stempel, Dr. Benjamin R. Rost, Dr. Jörg M. Breustedt and me. Some of the data presented was acquired with the kind help of other people. All data analysis was performed by me. In the following I state the contribution of other people to the data presented:

Dr. A. Vanessa Stempel who was my PhD supervisor in the beginning of my PhD, contributed 23/491 recordings – especially for control experiments in hippocampal SSI.

Dr. Ulrike Pannasch contributed 17/491 recordings for disentangling the molecular mechanism of hippocampal SSI.

Daniel Parthier and **Dr. Rosanna Sammons** contributed 24/491 and 12/491 recordings in cortical neurons of transgenic animals, respectively.

Susanne Rieckmann and **Anke Schönherr** performed breeding and genotyping of transgenic animals.

6.3. List of Publications

6.3.1 Related to this dissertation

Stumpf A., Parthier D., Sammons R.P., Stempel A.V., Breustedt J., Rost B.R., Schmitz D. 2018. Cannabinoid type 2 receptors mediate a cell type-specific self-inhibition in cortical neurons. *Neuropharmacology* 139, 217-225.

Stempel A.V., **Stumpf A.**, Zhang H.Y., Özdogan T., Pannasch U., Theis A.K., Otte D.M., Wojtalla A., Rácz I., Ponomarenko A., Xi Z.X., Zimmer A., Schmitz D. 2016. Cannabinoid Type 2 Receptors Mediate a Cell Type-Specific Plasticity in the Hippocampus. *Neuron* 90, 795-809.

6.3.2. Non-related to this dissertation

Neagoie, I.*, Liu C.* , **Stumpf, A.**, Lu, Y., He, D., Francis, R., Chen, J., Reynen, P., Alaoui-Ismail, M. H., Fukui, H. 2018. The GluN2B subunit represents a major functional determinant of NMDA receptors in human induced pluripotent stem cell-derived cortical neurons. *Stem Cell Res* 28, 102-114.

Subkhangulova, A., Malik, A. R., Hermey, G., Popp, O., Dittmar, G., Rathjen, T., Poy, M. N., **Stumpf, A.**, Beed, P. S., Schmitz, D., Breiderhoff, T., Willnow, T. E. 2018. SORCS1 and SORCS3 control energy balance and orexigenic peptide production. *EMBO Rep* 19, pii: e44810.

Grael, M. K.* , Maglione, M.* , Reddy-Alla, S.* , Willmes, C. G., Brockmann, M. M., Trimbuch, T., Rosenmund, T., Pangalos, M., Vardar, G., **Stumpf, A.**, Walter, A.M., Rost, B. R., Eickholt, B. J., Haucke, V., Schmitz, D., Sigrist, S. J., Rosenmund, C., 2016. RIM-binding protein 2 regulates release probability by fine-tuning calcium channel localization at murine hippocampal synapses. *Proc Natl Acad Sci U S A* 113, 11615-11620.

Kreye, J.* , Wenke, N. K.* , Chayka, M., Leubner, J., Murugan, R., Maier, N., Jurek, B., Ly, L. T., Brandl, D., Rost, B. R., **Stumpf, A.**, Schulz, P., Radbruch, H., Hauser, A. E., Pache, F., Meisel, A., Harms, L., Paul, F., Dirnagl, U., Garner, C., Schmitz, D., Wardemann, H., Prüss, H., 2016. Human cerebrospinal fluid monoclonal N-methyl-D-aspartate receptor autoantibodies are sufficient for encephalitis pathogenesis. *Brain* 139, 2641-2652.

* These authors contributed equally to this publication

6.3.3. In revision or preparation

Brockmann, M. M.*, Maglione, M.*, Willmes, C. G.*, **Stumpf, A.**, Bouazza, B. A., Moreno-Velasquez, L. M., Grauel, K., Beed, P., Sigrist, S. J., Schmitz, D., 2019. RIM-BP2 primes synaptic vesicles via recruitment of Munc13-1 at hippocampal mossy fiber synapses. (Under revision in ELife in Jan. 2019)

Sammons, R. P., Parthier, D., **Stumpf, A.**, Schmitz, D., 2019. Electrophysiological and molecular characterization of the mouse parasubiculum. (Submitted to J Neuroscience in Mar. 2019)

Kornau, H., C., Kreye, J., **Stumpf, A.**, Parthier, D., Kurpjuweit, S., Fukata, Y., Fukata, M., Prüss, H., Schmitz, D., 2019. Human CSF monoclonal LGI1 autoantibodies cause elevated intrinsic neuronal excitability. (Submitted to Brain in Jan. 2019)

Beed, P.*, Ray, S.*, **Stumpf A.**, Moreno-Velasquez, L., Parthier, D., Breustedt, J., Las, L., Brecht, M., Schmitz, D., 2019. Species difference in synaptotagmin 7 expression correlate with differences in hippocampal short-term plasticity. (Manuscript in preparation)

* These authors contributed equally to this publication

6.4. Presentations

FENS Conference. Berlin, Germany **2018**

Cannabinoid type 2 receptors mediate a cell type-specific self-inhibition in cortical neurons
Poster Presentation

Berlin Symposium for Young GPCR Researchers, (Bock and Bermudez, 2018) **2018**

Berlin, Germany.

CB2 receptors mediate cell type-specific self-inhibition in cortical neurons.
Oral presentation

Göttingen Meeting of the German Neuroscience Society. Göttingen, Germany **2017**

Autocrine endocannabinoid signaling in cortical neurons
Poster presentation

6.5. Erklärung an Eides statt

Ich, Alexander Stumpf, geboren am 23. Juli 1989 in Wladiwostok (Russland), versichere an Eides statt durch meine eigenhändige Unterschrift, dass ich die vorgelegte Dissertation mit dem Thema: „Cannabinoid type 2 receptor-mediated cell type-specific self-inhibition in hippocampal and cortical neurons“ selbstständig und ohne nicht offengelegte Hilfe Dritter verfasst und keine anderen als die angegebenen Quellen und Hilfsmittel genutzt habe. Die Bedeutung dieser eidesstattlichen Versicherung und die strafrechtlichen Folgen einer unwahren eidesstattlichen Versicherung (§156, 161 des Strafgesetzbuches) sind mir bekannt und bewusst.

Berlin, den

Alexander Stumpf